Aus dem Institut für Tierpathologie des Fachbereichs Veterinärmedizin der Freien Universität Berlin sowie der Klinik für Dermatologie, Venerologie und Allergologie der Charité - Universitätsmedizin Berlin

Follicular penetration of nano-sized particulate FA-PLGA and the dye RhBITC in dorsal dog and rat skin, and porcine ear skin as an in vitro model for the human integument

Inaugural-Dissertation
zur Erlangung des Grades eines Doktors
der Veterinärmedizin an der Freien Universität Berlin

vorgelegt von
Fanny Esther Knorr
Tierärztin aus Wilmington (USA)

Berlin 2010

Journal-Nr.: 3400

Gedruckt mit Genehmigung des Fachbereichs Veterinärmedizin

der Freien Universität Berlin

Dekan:	Univ.-Prof. Dr. L. Brunnberg
Erster Gutachter:	Univ.-Prof. Dr. R. Rudolph
Zweiter Gutachter:	Prof. Dr. Dr.-Ing. J. Lademann
Dritter Gutachter:	Univ.-Prof. Dr. K. Müller

Deskriptoren (nach CAB-Thesaurus):
Hair follicles, skin, penetration, particles, size, extraction, pigs, dogs, rats

Tag der Promotion: 16.12.2010

Bibliografische Information der *Deutschen Nationalbibliothek*

Die Deutsche Nationalbibliothek verzeichnet diese Publikation in der Deutschen Nationalbibliografie; detaillierte bibliografische Daten sind im Internet über <http://dnb.ddb.de> abrufbar.

ISBN: 978-3-86664-961-3
Zugl.: Berlin, Freie Univ., Diss., 2010
Dissertation, Freie Universität Berlin
D 188

Dieses Werk ist urheberrechtlich geschützt.
Alle Rechte, auch die der Übersetzung, des Nachdruckes und der Vervielfältigung des Buches, oder Teilen daraus, vorbehalten. Kein Teil des Werkes darf ohne schriftliche Genehmigung des Verlages in irgendeiner Form reproduziert oder unter Verwendung elektronischer Systeme verarbeitet, vervielfältigt oder verbreitet werden.

Die Wiedergabe von Gebrauchsnamen, Warenbezeichnungen, usw. in diesem Werk berechtigt auch ohne besondere Kennzeichnung nicht zu der Annahme, dass solche Namen im Sinne der Warenzeichen- und Markenschutz-Gesetzgebung als frei zu betrachten wären und daher von jedermann benutzt werden dürfen.

This document is protected by copyright law.
No part of this document may be reproduced in any form by any means without prior written authorization of the publisher.

Alle Rechte vorbehalten | all rights reserved
© Mensch und Buch Verlag 2011
Choriner Str. 85 - 10119 Berlin
verlag@menschundbuch.de – www.menschundbuch.de

Table of contents

Abbreviations and acronyms

cm, cm²	Centimeter, centimeter squared
et al.	And others (*latin* et alii)
FA-PLGA	5-fluoresceinamine-labelled poly(lactide-*co*-glycolide)
Fig(s).	Figure(s)
g	Grams
kg	Kilograms
LSM	Laser scanning microscope
max	Maximum
min	Minimum
ml	Milliliter
µm	Micrometer
mm	Millimeter
N	Sample size
N.N.	Not known
nm	Nanometer
PGA	Poly(glycolic acid)
PLA	Poly(lactic acid)
PLGA	Poly(lactic acid-co-glycolic acid)
RhBITC	Rhodamine B isothiocyanate

Abbreviations and acronyms

RPM	Revolutions per minute
SD	Standard deviation
Tab(s).	Table(s)
$\overline{x}$	Mean

1. Introduction and research aims

1.1. Introduction

The skin is the outer covering of the body. It provides protection against environmental insults, maintains water homeostasis, and regulates body temperature as well as waste excretion. The skin is comprised of the epidermis as the protective barrier, the dermis forming the bulk of the skin, and the hypodermis, which regulates energy storage and metabolism, and provides thermal insulation (Schäfer & Redelmeier, 1996). It is well established that pharmaceutical agents applied to the surface penetrate into the skin by diffusing into the lipid matrix of the stratum corneum and spreading into the upper corneocyte layers (Bouwstra et al., 2001; Choi et al., 1999; Essa et al., 2002; Hadgraft, 2001). Continuous sloughing off of corneocytes through desquamation however results in rapid depletion of drugs dispersed in the horny layer. The pilosebaceous units, consisting of the integrated structures of the hair follicles, the hair shaft, the adjoining arrector pili muscle and the associated sebaceous glands, were previously not considered to participate in transdermal penetration. Recent in vitro and in vivo studies have now provided substantial evidence for their roles as shunt routes to deeper skin layers in a number of laboratory animals and humans (Dokka et al., 2005; Jung et al., 2006; Meidan et al., 1998; Ogiso et al., 2002; Otberg et al., 2007; Teichmann et al., 2006). The success and efficacy of penetration into the hair follicles is determined by the numbers, distributions, morphometries and activities of the pilosebaceous units found in the skin, the constitution of the skin (Feldmann & Maibach, 1967; Hueber et al, 1992; Lademann et al., 2001; Lauer et al., 1996; Maibach et al., 1971; Mangelsdorf, 2007; Otberg et al., 2004a; Rivière & Papich, 2001; Singh et al., 2000; Walters & Roberts, 1993), the properties of the applied agent (Langer, 1990), as well as the method of application (Lademann et al., 2007). Substance retention and storage in the hair follicles is long-term in comparison to that in the stratum corneum, as their contents are depleted only through the slow processes of sebum retention and hair growth (Ossadnik et al., 2006).

Interest in the pilosebaceous units as target structures is aimed at their use as depots for localized therapy, particularly for the treatment of skin diseases, follicle-related disorders (Meidan et al., 2005) and hair growth abnormalities. The sebaceous glands of humans are implicated in the etiology of acne (Thiboutot, 2004), androgenetic alopecia (Meidan & Touitou, 2001) and other sebaceous gland dysfunctions, and are thus obvious targets for locally active therapeutic agents. Considerable effort has been directed towards maximizing the accumulation of drugs in the hair follicles and sebaceous glands including adapalene (Rolland et al., 1993), isotretinoin (Tschan et al., 1997), and anti-androgen RU58841 (Bernard et al., 1997; Münster et al., 2005). Substantial attention has also been focused on exploiting the hair follicles for systemic drug delivery (Meidan et al., 2005). Topically applied substances that reach the dense network of capillaries surrounding the hair follicles (Ryan, 1983) can permeate into the central circulatory system, resulting in rapid dilution (Schäfer &

Redelmeier, 1996) and dispersion (Lauer et al., 1996) of the drugs throughout the body. Langerhans cells found in abundance along the hair follicles and other immune cells (Vogt et al., 2005) can be targeted by topical immunization to enable needle-free delivery (Fan et al., 1999; Gupta et al., 2005). The multipotent and highly proliferative hair follicle bulge cells (Ohyama, 2007a) have attracted attention for applications in human cutaneous regenerative medicine (Cotsarelis, 2006; Stenn & Cotsarelis, 2005), and may provide alternatives to embryonic stem cells (Hoffman, 2007).

The concept of targeted drug delivery was first proposed by Paul Ehrlich at the beginning of the 20th century with the idea of a 'magic bullet' that can selectively bind to specific types of cells without causing toxic side-effects at non-therapeutic sites (Yokoyama, 2005). In recent years, the development of particulate systems for drug delivery has tremendously impacted nearly every branch of medicine (Alvarez-Román et al., 2004a, 2004b; Brigger et al., 2002; Koziara et al., 2004; Lamprecht et al., 2001; Langer, 1998; Salata, 2004). Nanotechnology in particular offers a suitable means for delivering small molecular weight drugs, as well as macromolecules such as proteins, peptides or genes, by either localized or targeted delivery to the tissue or organ of interest. It focuses on formulating therapeutic agents in biocompatible nanocomposites including nano-sized particulates and capsules, micellar systems, and conjugates. Nano-sized particulates are solid colloidal particles sized 10 to 1000 nm with pharmaceutical agents encapsulated within their matrix or adsorbed or conjugated onto their surface (Kreuter, 2004). Since these systems are submicron in size, they have multifaceted advantages in drug delivery. They can be used to sustain a drug or gene effect in the target structure, to improve the stability of therapeutic agents against enzymatic degradation, especially of drugs pertaining to proteins, peptides and nucleic acids (Moghimi et al., 2001), and to reduce adverse side effects (Lamprecht et al., 2001; Langer, 1998). Nano-sized particulates have been reported to successfully target specific anatomical sites such as the eye (Cavalli et al., 2002; Calvo et al., 1994), nose (Fernandez-Urrusuno et al., 1999; Ghirardelli et al., 1999) brain (Ramge et al., 2000; Schröder et al., 1998), intestine (Pan et al., 2002; Zara et al., 2002) and skin (Alvarez-Román et al., 2001; de Vringer & de Ronde, 1995; Jenning et al., 2000; Müller et al., 1995; Müller et al., 1998; Schütt et al., 1998).

1.2. Research aims

The therapeutic use of topically administered nano-sized drug delivery systems customized to target follicular structures is a novel and highly promising prospect. In the follicular canal, the particulates are shielded from abrasion, enabling drug retention (Baroli et al., 2007; Lademann et al., 2007; Otberg et al., 2008; Shim et al., 2004). To date, only very few studies have been conducted on the penetration of nano-sized particulates into the hair follicles of

animal species relevant for veterinary practitioners. The comparatively high density of hair follicles found in most companion and farm animals offers an obvious abundance of follicular target structures. In veterinary practice, patient and patient owner compliance plays a crucial and often limiting role in the success of a treatment regimen. Particulate drug delivery systems that can be administered topically instead of orally or by needle, and in fewer dosages, would therefore greatly facilitate ministration of patients, in particular when treating uncooperative pets or wild animals. Similarly, the potential reduction in animal handling, resulting in decreased animal stress and economic savings, would be of significant benefit in the treatment of farm animals. These factors will be major driving forces in the development of such topically applicable drug delivery systems for veterinary practice in the near future.

The quantification of therapeutic agents located in the hair follicles is of substantial pharmacological relevance for questions regarding administration, concentrations and dosages. The method of differential stripping developed by Teichmann et al. (2005) is widely used to selectively and differentially quantify drugs dispersed throughout the upper layers of the stratum corneum and within the appendageal structures in in vivo studies with human subjects (Lademann et al., 2006; Ossadnik et al., 2007; Patzelt et al., 2008). Differential stripping does not however provide valid results for in vitro studies using porcine skin as a model for human skin, as it is not possible to remove the complete follicular casts from porcine skin without producing tears in the cyanoacrylate. This is presumably due to the fact that although there is not a high density of hair follicles on the porcine ear, the bristles are relatively thick and penetrate deeply into the skin (Meyer, 1986), and are thus much more difficult to remove. Testing of substances with unknown or potentially harmful effects on in vitro models such as porcine skin prior to the administration to human subjects is necessary to ensure product safety for humans, generating a high demand for alternative procedures applicable to porcine skin.

The research aims of this study can be divided into two sections as specified below:

1) To examine the follicular penetration of 5-fluoresceinamine-labelled poly(lactide-co-glycolide) (FA-PLGA) particulates sized 256 nm and 430 nm suspended in cellulose gels in excised dog, rat and porcine skin; interindividual and interspecial variations in follicular morphometries and skin constitutions as well as characteristics of the particulates will be discussed as factors of influence;

2) To develop a novel procedure that enables the selective quantification of drugs located in the follicular canals of porcine skin subsequent to topical application using the dye Rhodamine B Isothiocyanate (RhBITC) a model drug.

2. Literature review

2.1. Skin

The skin is the body's largest organ, with a surface of 1.8 to 2 m^2 and a weight of almost 9 kg in humans (Degim, 2006). Its complex structure reflects a myriad of biological functions (Rivière & Papich, 2001). It represents the outer boundary and protective barrier of the body, as well as a large surface for contact with the environment. The skin provides protection against mechanical, thermal, chemical and biological insults (Liebich, 1993). It effectively mounts immune responses to small amounts of antigen (Fan et al., 1999) and functions as a sensory organ for mechanical and thermal stimuli, as well as pain (Leonhardt, 1990). It is flexible enough to resist permanent distortion from movement, and thin enough to allow stimulation (Degim, 2006). Skin glands and blood vessels regulate body temperature and water homeostasis (Leonhardt, 1990), and control the expulsion of waste products (Barry, 1983; Scheuplein & Blank, 1971). Finally, the skin plays a regulatory role in the excretion of stress hormones (Künzel, 1990).

The skin is a highly organized structure consisting of three main layers, the epidermis, the dermis and the hypodermis, as well as a number of distinct appendages. The superficial layer, the epidermis, consists of multilayered, squamous epithelium (Fritsch, 1998). The second layer is the dermis, which is a dense, 1 to 4 mm thick layer of fibroelastic connective tissue (Odland, 1991), forming the bulk of the skin. The third layer, the hypodermis, is composed of loose fatty connective tissue (Schäfer & Redelmeier, 1996). The thickness and staunchness of the skin varies depending on the species, breed, age and body region. Skin on the back is generally thicker than the skin on the stomach, as is mechanically strained skin (Habermehl, 1996) and skin covered by hair (Liebich, 1993).

2.1.1. Epidermis

The epidermis mainly consists of epidermal keratinocytes, which proliferate and divide in the epidermal basal layer and move upwards through the skin as they mature to form cornified cells (Fritsch, 1998). Other cell types present in the epidermis are melanocytes for skin pigmentation (Jimbow et al., 1993), Langerhans cells for antigen presentation and immune responses (Stingl et al., 1993), as well as Merkel cells for sensory reception (Kim & Holbrook, 1995).

The basal cell layer is a single layer consisting of cubic to columnar shaped basal cells, including the epidermal stem cell population. It is responsible for the regeneration of the keratinocytes, and balances cell loss (Fritsch, 1998). The basal cells have a basophilic cytoplasm, desmosomes for cell attachments, gap junctions for cell communication and

hemidesmosomes in order to connect with the extracellular matrix and the underlying basal membrane. Keratin filaments and tonofilaments are distributed in bundles at the periphery of the nucleus in the cytoplasm of the keratinocytes, from where they connect with hemidesmosomes and desmosomes to form a rigid cellular cytoskeleton (Shimizu, 2007). The suprabasal layer consists of 2 to 5 layers of larger polygonal keratinocytes that are connected via desmosomes despite large intercellular clefts (Leonhardt, 1990). The cells are polygonal in the lower layer and flattened in the upper layers (Shimizu, 2007). Characteristic Odland bodies are cell organelles found containing lipids and enzymes. The onset of terminal differentiation in this layer causes cells to lose the ability for cell division. At the transition into the granular cell layer, keratinocytes flatten and are characterized by basophilic keratohyalin granules. Dehydration occurs, and cell nuclei and organelles are lost. The exocytosis of Odland bodies induces the production of an impermeable intercellular cement, which fixates the cells (Fritsch, 1998). The stratum lucidum is thickest on the palms of the hands and the soles of the feet. The cells are eosinophil and contain densely packed filaments and degraded cell organelles. This layer could be identified in various regions of mouse, rat, guinea pig and dog skin (Zirra, 1976).

Most of the cells in the stratum corneum are terminally differentiated, flat, polyhedral shaped corneocytes that are tightly packed in stacks which run perpendicular to the skin surface (Cevc, 2004; Schäfer & Redelmeier, 1996). Mammalian corneocytes are approximately 0.3 µm thick, although higher values have been reported (Schätzlein & Cevc, 1998; Plewig et al., 1983). The cells are thicker and smaller in the deeper epidermis (Iizuka, 1994). The stratum corneum consists of approximately 15 corneocyte layers, with a total thickness of 6 to 8 µm in humans (Cevc, 2004). It can be up to 10 times thicker at body sites of increased pressure, such as the palms of the hands and the soles of the feet (Stevens & Lowe, 1992).

The corneocytes are cell remnants of terminally differentiated keratinocytes found in the viable epidermis, whose cellular organelles and cytoplasms vanished during the process of cornification (Schäfer & Redelmeier, 1996). They are composed primarily of bundled keratins (Eckert, 1989; Steinert, 1993), which provide them with structural stability, tensile strength and elasticity (Schäfer & Redelemeier, 1996). The bundled keratins are surrounded by a chemically highly resistant cell envelope, which is stabilized by cross-linked proteins (Reichert et al., 1993). Covalently bound lipids are grafted onto the cornified envelopes (Wertz et al., 1989). The corneocytes are interconnected by polar structures such as corneodesmosomes that contribute to the cohesion of the stratum corneum (Caputo & Peluchette, 1976). The intercellular region consists of lipids that accumulate in small organelles known as lamellar granules as epidermal keratinocytes differentiate (Grayson et al., 1985; Landmann, 1986; Menon et al., 1992). The lipids are extruded into the intercellular spaces where they undergo enzymatic processing to produce a mixture of ceramides,

cholesterol and fatty acids. They are organized into a multilamellar complex that fills most of the intercellular space of the horny layer (Schäfer & Redelmeier, 1996). The ceramides are considered to function as emollients, which render the skin soft while conferring water-retention properties on the stratum corneum (Imokawa, 1989; Kerscher & Korting, 1991; Landmann, 1986; Schurer & Elias, 1991). The corneocytes are 'cemented' to adjacent cell layers via the intercellular lipid matrix (Rivière & Papich, 2001), forming a 'brick and mortar' structure (Elias, 1983) which has been used to conceptualize the barrier properties of the skin. This unique morphology of the stratum corneum results in a highly convoluted and tortuous lipid pathway for water diffusion, causing the water molecules to migrate over much greater distances than the stratum corneum thickness. This renders the water permeability about 1000 times lower than that of most other biomembranes (Potts & Francoeur, 1991).

On the skin surface, the upper layers of the stratum corneum are continually sloughed off to the external environment by friction and replaced by the migration of differentiated cells from the layers below. In humans, this cycle takes approximately four weeks (Rivière & Papich, 2001). The process of desquamation requires the controlled destruction of cell-cell adhesive structures such as desmosomes through enzymatic proteolysis (Houben et al., 2007). Topically applied substances stored in the uppermost layers are consequently lost along with the desquamated cells (Lademann et al., 2006). Epidermal structures such as claws, hooves, horn, the cortex and cuticula of hair, as well as feathers, with the exception of the interior of the quill, are developed through cornification. This process is cyclical and can take weeks or months such as in hair, or can be continuous such as in hooves (Künzel, 1990).

2.1.2. Dermis

The dermis forms the bulk of the skin and contributes to 15 to 20% of the total body weight. Its thickness determines the total thickness of the skin. The dermis consists of two compartments, the papillary dermis and the reticular dermis. The papillary dermis is the thinner outermost portion of the dermis, constituting approximately 10% of the thickness of the dermis. It contains smaller and more loosely distributed elastic and collagen fibrils than the underlying reticular dermis, and has a larger amount of ground substance (Hendriks, 2005). The papillary layer is separated from the epidermis by the dermo-epidermal junction, a physical barrier formed by ridges in the papillary layer, which interdigitate with epidermal invaginations (Odland, 1991; Ebling et al., 1992). The papillae at the dermal side contain capillary loops that provide nutrients for the avascular epidermis (Liebich, 1993), as well as small fenestrated lymphatic vessels (Cevc, 2004). Encapsulated nerve endings called Meissner's corpuscles can also be found. The underlying reticular dermis constitutes the larger bulk of the dermis (Hendriks, 2005).

Fibrous, filamentous and amorphous connective tissue of the dermis determines the tensile strength and elasticity, and provides support for extensive nerve and vascular networks (Schäfer & Redelmeier, 1996). Finlay (1969) showed that collagen fiber bundles, which comprise about 75% of the fat free dry weight and 18 to 30% of the volume of the dermis, form an irregular network that runs almost parallel to the epidermal surface. A network of elastin is interwoven among the bundles of collagen, which restores the normal fibrous array following deformation through external mechanical forces. The elastic fibers account for 4% of the fat free dry weight and 1% of the volume of the dermis (Ebling et al., 1992), and are associated with the hair follicles and vascular networks (Schäfer & Redelmeier, 1996). According to Oxlund et al. (1988), direct connections between elastin and collagen fibres have not been shown, but collagen fibrils appear to be wound around the elastin cores. The amorphous ground substance is composed of glycosaminoglycans and proteoglycans (Holbrook & Wolff, 1993). These compounds bind large amounts of water and are therefore primarily responsible for the water-retaining capacity of the dermis. Cells in this region include fibroblasts, endothelial cells and mast cells. Fibroblasts produce the connective tissue components collagen, laminin, fibronectin and vitronectin. Mast cells are important for tissue regeneration after trauma and in defense against parasites. Macrophages, lymphocytes and leukocytes, which are involved in cellular defense and immune responses, infiltrate during pathological processes (Schäfer & Redelmeier, 1996).

The dermis has an extensive vascular network, which participates in several processes such as nutrition, heat exchange repair, immune responses and thermal regulation (Ryan, 1983). Blood flows through the dermis and epidermis in arterioles, arterial precapillaries and arterial loops. In turn, the blood is drained from the skin via venous loops, postcapillaries and venules, which end in the skin veins (Braverman, 1989). The system of capillary beds reaches the upper dermis so that capillary loops line the papillae (60 to 70 per mm^2) which contact the epidermis, but do not penetrate it (Ryan, 1983). Studies indicate that the blood flow in the skin can be increased up to 100-fold in response to the environment, hormones or xenobiotics. In skin areas that are exposed to high pressure, such as the palms of the hands and the soles of the feet, up to 60% of the blood flow can be directly shunted from the arteries to the venules, avoiding the capillary network (Ryan, 1983; Stüttgen & Forssmann, 1981). The lymphatics also play a role in skin circulation by regulating the pressure of the interstitial fluid in the dermis. The lymph vessels lie under the epidermis and organize into lymphatic systems that drain into lymph nodes. Most of the lymph flow occurs passively, and valves located within the system contribute to the flow direction (Ryan, 1983). Schäfer and Redelmeier (1996) suggested that the lymph circulatory system is the principle pathway for the removal of extracellular proteins from the dermis.

2.1.3. Hypodermis

The hypodermis underlies the dermal layer and consists of a network of adipocytes arranged in lobules. The adipocytes are made up of fat droplets containing triglycerides, which are composed of olein acid and palmitin acid. Fiber bundles produced in the dermis connect with the fascia and the periostea through the hypodermis to strengthen the connection between the dermis and deeper tissues (Shimizu, 2007). The hypodermis plays an important role in energy storage and metabolism, provides thermal insulation, absorbs shocks, and contributes to the toughness of the skin (Schäfer & Redelmeier, 1996). The thickness of the hypodermis varies according to body site, race, sex, age, as well as the nutritional and endocrine status of the individual (Hendriks, 2005).

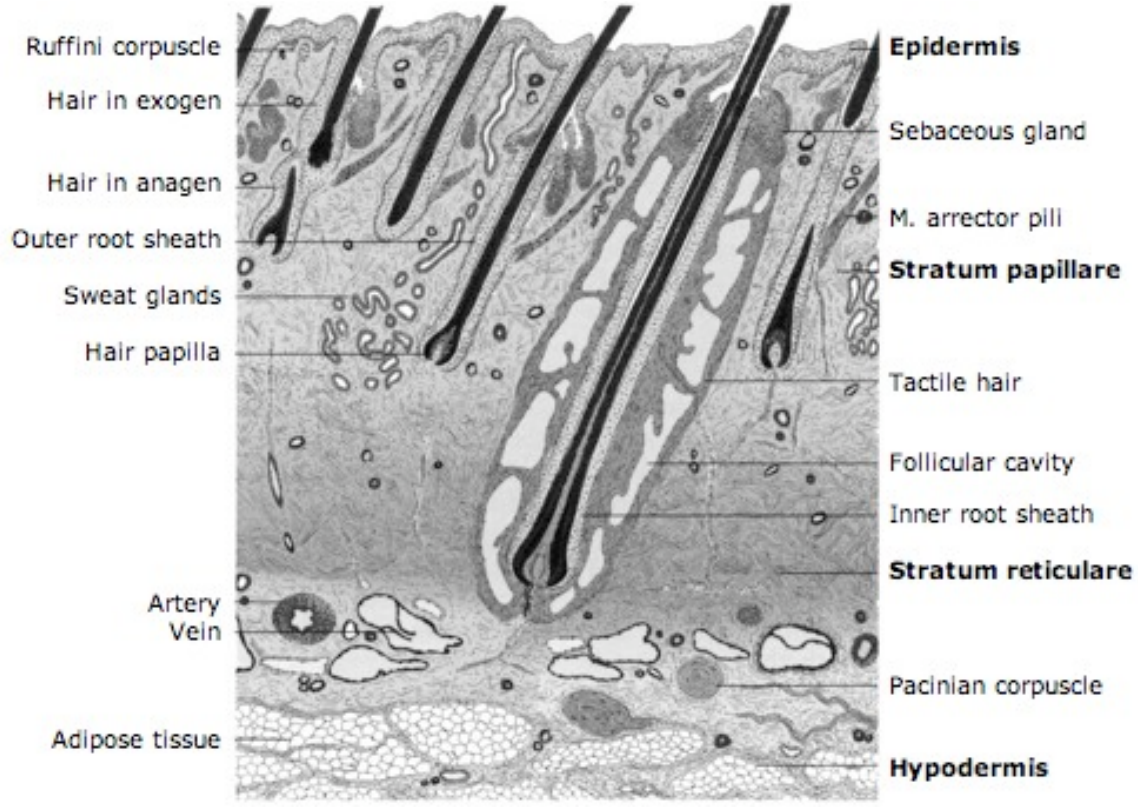

Fig. 1: Structure of the skin (from Liebich, 2004)

2.1.4. Appendages

Hair follicles

Animal hair constitutes a more or less dense coat, which shows characteristics dependent on species and breed. The hair coat covers the animal body, providing heat insulation that is adaptable to climatic conditions, protection against UV radiation, mechanical protection of

the skin, touch sense, dispersion of glandular secretions, social communication and camouflage. The hair coat consists of strong primary hairs (guard hairs), and thin, often curled secondary hairs (wool hairs), which form the insulating wool hair coat (Meyer et al., 2002a). Their density strongly increases during the winter months, providing more sufficient insulation. Hair protrudes from the skin from the hair follicles, which extend from the surface of the epidermis to the deep dermis in humans (Rogers, 2004). It has four distinct structural components. These include the cuticle (outside covering), the cortex (inner sheath) with its strongly keratinized cells that are arranged longitudinally, the medulla (central core) consisting of keratinized and often shrunk cell groups with intercellular spaces, and pigment granules, which can be found scattered throughout the cortex and the medulla (Meyer et al., 2002b). Fine animal hairs such as merino wool consist only of the cuticle and the cortex (Robbins, 2002). The hair cuticle bundles up, supports and protects the cortex parts of the hair shaft as the outer part of the hair that extends beyond the surface (Meyer et al., 2002a). It consists of a large number of overlapping transparent scales of keratin. Along the hair shaft, the scales have a specific contour and are arranged in a typical pattern according to mammalian groups and species (Meyer et al., 2002b). The basal parts of the scales are attached to the hair cortex by an intercellular substance, the distal parts point apically. The apically pointing cells anchor the hair into the inner root sheath cuticle, as the cells belonging to the root sheath run in the opposite direction. It has been suggested that the unattached edges of the hair cuticle scales may help to transport cell debris and glandular secretion to the skin surface during hair growth (Meyer et al., 2002a), and lock the hair in its follicle.

In most mammalian species, three types of hair follicles can be distinguished. Central primary hair follicles emerge first during ontogenesis, followed by lateral primary hair follicles, producing heavy and light guard hairs, respectively. The primary hair follicles are equipped with, besides sebaceous glands, an apocrine tubular gland. Secondary hair follicles emerge last during ontogenesis, and produce secondary wool hairs. While sebaceous glands can be found in these follicles, apocrine tubular glands are not present. The primary hair follicles are commonly arranged in groups of three, where the central primary hair follicle is flanked by two lateral primary hair follicles on each side of the group. This formation is phylogenetically characteristic of the mammalian integument, and is still present in most species. In densely haired species such as rodents, the group arrangement is completed by varying numbers of secondary hair follicles, whereas they are found as individual follicles between the primary hair follicles in large mammals. (Meyer, 2009). Other types of hair found in animals are eyelashes (cilia), tactile hairs (vibrissa) used for sensory functions, the spines of the Western hedgehog, the bristle hairs of the domestic pig, and the tail and mane hair of the horse (Mangelsdorf, 2007, Meyer et al., 2002a; Teerink, 1991). Structurally and functionally similar to the tactile hairs of the head are the tylotrich hairs, which have been found in mice, rats, guinea pigs, rabbits (Straile, 1960), dogs (Habermehl, 1996) and humans (Straile, 1960).

Pressure applied on a tylotrich hair compresses an epidermal thickening that surrounds the tylotrich follicle, which is associated with neurovascular tissue. This tylotrich pad represents a highly sensitive touch receptor (Smith, 1977). Hair is generally absent on the nasal plane, anus, labia, as well as on the digital organs of animals. Guinea pigs have an additional hairless region behind the ears (Mangelsdorf, 2007).

In humans, the palms of the hands, the soles of the feet and the lips are devoid of hair follicles (Meidan et al., 2005). Structural and functional differentiations can be made between laguno, vellus and terminal hair, which differ regarding hair diameter, hair length, pigmentation and development of the inner and outer root sheath as well as the glassy membrane (Vogt & Blume-Peytavi, 2003). Lugano hair is produced in utero and is generally shed before or shortly after birth. Vellus hair follicles of different size and density cover most of the skin surface area in adults. Vellus hair fibres are usually thin with a diameter < 30 µm and a length of < 2 mm (Meidan et al., 2005, Vogt et al., 2008). They are barely pigmented or not pigmented, and have no medulla (Blume et al., 1991). Terminal hair is characterized by pigmented hair fibers > 60 µm diameter and > 2 mm length, often reaching into the subcutis. It is mainly found on the scalp as well as in hormone-dependent body regions such as the beard, axilla and the pubic region (Blume et al., 1991, Meidan et al., 2005, Vogt et al., 2008).

The integrated structures of the hair follicle, the hair shaft, the sebaceous glands, the associated stem cells and the adjoining arrector pili muscle represent the hair follicle complex (Meidan et al., 2005; Rogers, 2004), which in humans is termed the pilosebaceous unit. Hair follicles are composed of several concentric cylinders of epithelial cells, the root sheaths, which surround the hair shaft (Sperling, 1991). The hair shaft is enveloped in an inner root sheath ending about halfway up the hair follicle, an outer root sheath, and an outermost acellular basement membrane termed the glassy membrane. The outer root sheath is a keratinised layer that is continuous with the epidermis (Meidan et al., 2005) and thereby of greatest importance with regard to drug delivery, as it increases the skin surface area susceptible to penetration. The function of the outer root sheath is the protection and moulding of the inner layers (Lauer et al., 1996). Each hair follicle is associated with one or more flask-like sebaceous glands, which are outgrowths of epithelial cells. Ducts join these glands to the upper part of the follicular canal (Meidan et al., 2005), from which they release sebum (Lauer et al., 1996). The region between the orifice of the hair follicle on the skin surface, and the opening of the sebaceous gland in the follicular canal, is marked as the infundibulum. The superficial part of the infundibulum is lined by epidermis including a well-developed stratum corneum and a stratum granulosum. In the lower infundibulum, a continuous loss of epidermal differentiation occurs, creating a major entry point for applied substances (Schäfer & Lademann, 2001). It extends to the isthmus, the region between the sebaceous gland opening and the bulge region (Sperling, 1991). The isthmus lacks distinctive

features, as it provides a border zone, in which the hair follicle becomes noticeably thinner and the outer root sheath merges with the skin epithelium. As part of the outer root sheath, the bulge region harbors stem cells and immature populations of immune cells, and marks the end of the permanent portion of the hair follicle, above which no significant cyclic changes are observed. The suprabulbar region lies below the isthmus and comprises various layers of differentiating follicles (Wosicka & Cal, 2010). A cluster of specialized dermal cells, the dermal papilla, can be found at the base of the follicular canal. These cells play an important role in the regulation of hair growth cycles. It is believed that signals from the dermal papilla instruct stem cells residing in the bulge region of the hair follicle to divide transiently (Paus & Cotsarelis, 1999). Stem cell progeny migrate to the base of the follicle, where they surround the dermal papilla, and form the hair matrix (Oshima et al., 2001; Taylor et al., 2000). During this actively growing phase or anagen, matrix cells proliferate in response to further signals from the dermal papilla, and begin the process of terminal differentiation, moving upward in the follicle to form the hair shaft and the inner root sheath (Cotsarelis, 2006). Pigmentation of the hair results from the activity of melanocytes, which reside in the hair follicle bulb and deposit pigment granules into the hair shaft while it forms (Millar, 2002). Eventually, matrix cells stop proliferating, hair shaft and inner root sheath differentiation slow, and the lower part of the follicle enters a destructive phase known as catagen, reducing the follicle to an epithelial strand. This drags the dermal papilla upward to rest just below the permanent, non-cycling upper follicle (Fuchs, 2007). The follicle then enters a resting period termed telogen, in which it lies dormant, prior to the hair being shed in exogen (Milner et al., 2002). Anagen subsequently reoccurs as the hair matrix cells start dividing and the lower follicle redevelops (Meidan et al., 2005). Cyclical hair growth continues throughout postnatal life, enabling remodeling of the follicle (Millar, 2002). With the exception of humans and guinea pigs, in which each hair follicle has an individual hair growth cycle, the hairs of most species grow in synchronized cycles (Harkey, 1993). In human scalp hairs, the cycle lasts approximately 4 years, whereby the follicles spend about 90% of the time in anagen (Kligman, 1961). Vellus hair anagen is much shorter in contrast. In the human thigh for example, anagen only lasts about 54 days in males and less than half of that time in females (Seago & Ebling, 1985).

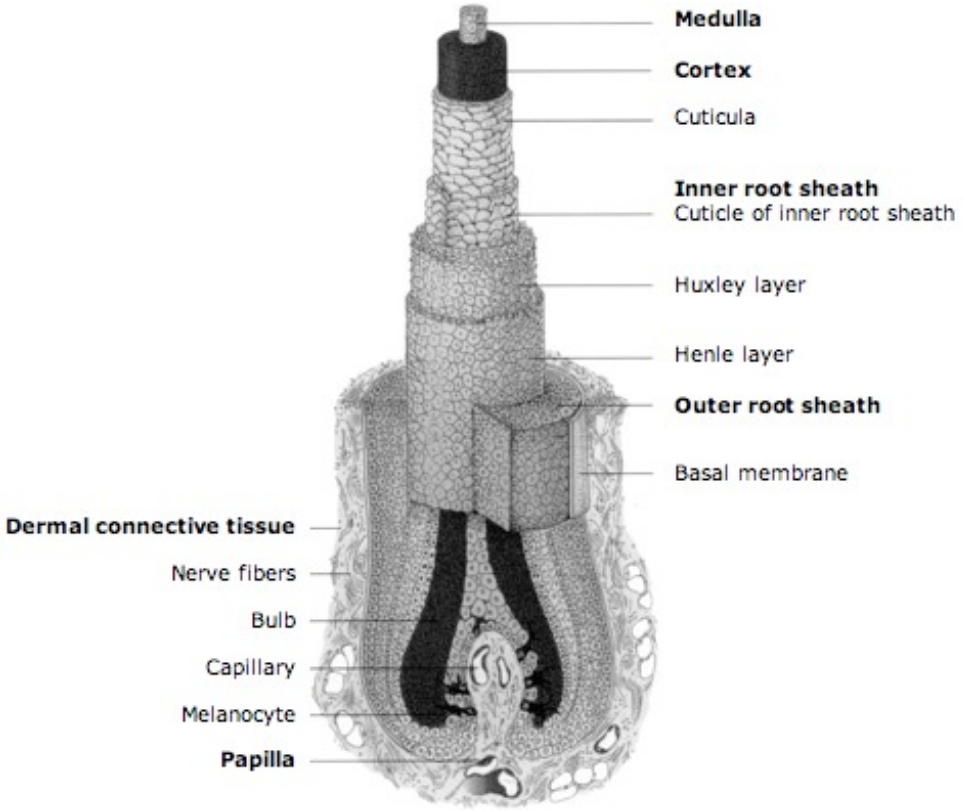

Fig. 2: Structure of a hair follicle (from Liebich, 2004)

Sebaceous glands

The sebaceous glands are connected to the hair follicle via the sebaceous duct, which opens into the follicular duct in the lower infundibulum (Vogt et al., 2005). However, they also exist individually, such as the meibomian glands in the eyelid or the ceruminous glands in the external acoustic meatus (Liebich et al., 1999). No sebaceous glands can be found on the palms of the hands, the soles of the feet, and in some mucous membranes in humans (Schäfer & Redelmeier, 1996). High densities of sebaceous glands can be found near mucocutaneous junctions, in interdigital regions, as well as on the dorsal neck, rump, chin and tail area (Kahn & Line, 2005). The function of these glands is the synthesis and release of sebum, a fungistatic and bacteriostatic mixture of short chain fatty acids. Human sebum consists of a high triglyceride content (57%), wax esters (26%), squalene (12%), cholesterol esters (2%) and cholesterol (1.5%) (Strauss et al., 1976). Animal sebum does not contain squalene or triglycerides. In contrast, large amounts of diesters and only small amounts of monoesters can be found. According to Nicolaides et al. (1968), the composition of porcine sebum is relatively similar to that of human sebum.

The sebum secretion is formed by the total disintegration of the glandular cells. It is discharged via the ducts into the upper third of the follicular canal (Clarys & Barel, 1995),

creating an environment rich in neutral, non-polar lipids in this region of the follicle (Meidan et al., 2005). The hair shaft is thus surrounded with sebum before the secretion reaches the skin surface via the follicular openings. On the skin surface, sebum coats the epidermis with a thin lipid layer (Liebich et al., 1999). This plays a role in maintaining skin hydration (Schäfer & Redelmeier, 1996), and provides animal hair coats with sheen. Sebum secretion may be associated with scent marking in some species (Kahn & Line, 2005). Based on the observation that sebum continues to be secreted in human skin under a film of heavy paraffin oil, Kligman and Shelley (1958) concluded that the synthesis and excretion of sebum continues at a steady rate regardless of any physical changes on the skin surface, including the accumulation of sebum itself. Sebaceous cells are relatively inactive during the first few days after their production in the germinative layer. They then slowly begin sebum synthesis, produce the bulk of the sebaceous lipids between 5 and 11 days before excretion, and then rapidly decline in lipid synthesis during the final days in the lives of the cells (Downing et al., 1981). In a study to determine the delay between sebum production and excretion, Downing et al. (1975) injected [1-^{14}C]acetate into the skin of three human males and subsequently measured the radioactivity in the skin lipids at the injection site. The results suggested that the average time elapsing between synthesis and excretion of sebum is 8 days in humans. Unpublished data indicates that this time-period is 5 days in rats and 14 days in horses (Downing et al., 1981). In a similar experiment, Colton et al. (1985) detected a peak of radioactivity in the equolides and cholesterol esters on the skin surface of horses 15 to 21 days and 10 to 16 days after injection of [1-^{14}C]acetate, respectively.

Secretion is almost completely absent in infants, is increased during puberty, reaches the highest values in acne patients, and is reduced in old age (Piérard et al., 1987). Androgens stimulate and maintain the amount, size and activity of the sebaceous glands. Sexually immature or neutered animals produce less sebum (Steward & Downing, 1999). Interestingly, the rate of sebum production is not proportional to the density of the follicles (Pagnoni et al., 1994), but rather dependent on age and body site (Ebling, 1974; Blume et al., 1991), as well as nutrition (Pochi et al., 1970)

Sweat glands

According to Schäfer and Redelmeier (1996), sweat glands are the most numerous of all appendages, and are distributed over the human body at a density of approximately 400 glands per cm². Human sweat glands are either eccrine, distributed throughout most of the body, or apocrine, found only on specific body sites. The glands consist of a coiled duct that is connected to the skin surface via a secretory tube and a spiral channel, which permeates the epidermis. Secretory, mucoid and myoepithelial cells line the lumen of the gland. Human sweat glands respond to increased skin temperatures by secreting an almost isotonic solution

that corresponds approximately to the low-molecular weight portion of plasma. In addition to water and salt, high concentrations of urea, ammonium, amino acids and low-molecular-weight proteins are present in the secretion. The glands actively recycle the secreted sodium chloride, which accounts for the hypotonicity of the sweat.

In domestic animals, apocrine sweat glands are found to be associated with hair follicles throughout the body, although they may be more numerous in some body sites. In most mammals, these glands produce an odoriferous, oily compound that is a sexual attractant, a territorial marker, as well as a warning signal. Eccrine glands are sweat glands present on the footpads of carnivores, the frog of ungulates, the carpus of pigs, as well as the nasolabial region of ruminants. The evaporation of sweat from the skin is the primary cooling mechanism for horses, cattle and primates, as well as to a lesser degree for pigs, sheep and goats. Some clinical evidence exists that limited sweating occurs in dogs and cats, although these animals are thought to thermoregulate primarily by panting, drooling and the spreading of saliva on their coats (Kahn & Line, 2005). The secretion of the glands (pH 4 to 6) is believed to inhibit the growth of bacteria and fungi on the skin surface (Nickel et al., 1996).

Arrector pili muscle

The arrector pili muscle is a smooth muscle bundle between the outer root sheath and the dermal upper layer that is 10 to 140 µm thick, depending on the size of the hair follicles, and stimulated by sympathetic nerve fibers (Meyer, 2009). As a result, the hair associated with the muscle stands perpendicular to the skin surface, which slightly elevates peripheral hair follicles (Shimizu, 2007), leading to piloerection. Piloerection is a defense mechanism in many species. Porcupines for example erect their quills when threatened (Cutts et al., 2002). In humans, piloerection is a sensation that occurs in response to sensations such as the cold or fear (Roze et al., 2000).

2.2. Penetration pathways into the skin

The skin provides a painless and compliant interface for drug administration (Prausnitz et al., 2004). In spite of its barrier function, small drugs can cross the skin at low flux rates, providing a means for delivering therapeutic agents that are destroyed by the liver when taken orally (Langer, 1998), and for avoiding pulsed entry into the systemic circulation which can cause undesirable side effects (Wiechers, 1989). The stratum corneum is considered to be the greatest barrier to the transport of drugs. The corneocytes, which are held together by corneodesmosomes, confer structural stability to the horny layer. Its lipids, composed primarily of ceramides, cholesterol and fatty acids, are assembled into multilamellar bilayers.

The layer of lipids immediately adjacent to each corneocyte is covalently bound to the corneocyte and is important in maintaining its barrier function (Prausnitz et al., 2004). Its permeability depends on the thickness, hydration, cell density and intracellular structures, as well as the lipid content and molar composition of the skin. Age, wounds or scars and skin disorders also influence penetrability. The structure, size, lipo- or hydrophilicity and the presence of functional groups of a topically administered substance affect its transport through the horny layer (Loth, 1987).

2.2.1. Intercellular and transcellular penetration

During intercellular penetration, substances passively diffuse from the skin surface into the skin along the tortuous lipid matrix of the stratum corneum and spread into the upper corneocyte layers (Bouwstra et al., 2001; Choi et al., 1999; Essa et al., 2002; Hadgraft, 2001). The composition of the skin limits the number of suitable drugs for penetration to small, moderately lipophilic, and highly potent molecules (Alvarez-Román et al., 2004a). Experimental extraction of the stratum corneum lipids (Abrams et al., 1993; Alvarez-Román et al., 2003; Hadgraft et al., 1992) and alterations of the lipid composition through genetic modifications (Schäfer & Redelmeier, 1996) led to increased water permeability of the horny layer and changes in penetration rates (Flynn, 1990). Hydrophilic solutes exhibit comparatively low permeabilities that are often difficult to measure, and in many cases necessitate the aid of penetration enhancers (Prausnitz et al., 2004). Potts and Franceour (1991) reported that the corneocyte ‘flakes’ incorporated into the lipid matrix mechanically impede diffusion. The presence of the transcellular penetration pathway, in which substances permeate through the keratinocytes and lipid lamellae, has thus far not been established (Mangelsdorf, 2007).

2.2.2. Follicular penetration

Skin appendages such as hair follicles or sweat glands constitute a break in the continuity of the stratum corneum and can act as conduits for drugs to reach deeper skin layers as well as its vasculature. Earliest reports of the participation of follicles in percutaneous absorption were based primarily on qualitative histological studies of dye and stain localization in the hair follicle (Borelli & Metzger, 1957; MacKee et al., 1945; Montagna, 1954; Rutherford & Black, 1969; Scheuplein, 1967; Scheuplein et al., 1969). Later studies led to increasingly quantitative data. Feldmann and Maibach (1967) and Maibach et al. (1971) found regional variations of percutaneous absorption in different body sites, and assumed that the density and size of the hair follicles contribute to differences in penetration rates. Absorption was

increased in areas of higher follicular density such as the forehead and the scalp. Wahlberg (1968) demonstrated that, over a period of 24 hours, the absorption of $HgCl_2$ and NaCl was greater in hairy guinea pig skin in vitro than in the non-hairy region behind the ears. The penetration of corticosteroids was considerably lower in scarred skin free of appendages, as compared to normal skin (Hueber et al., 1992; Tenjarla et al., 1999). Similar observations have been made in engineered skin tissue, as the insertion of hair follicles significantly increased the penetration rate of hydrocortisone (Michel et al., 1999). Kao et al. (1988) found that percutaneous permeation of benzo[a]pyrene was higher in in vitro skin cultured from haired mice than from hairless mice. Photomicrographs of hairy skin showed benzo[a]pyrene fluoresce deep in the dermis, which the authors correlated to follicular and sebaceous ducts. No fluorescence was observed in the hairless skin. Rodents that are genetically altered to a hairless phenotype possess hair follicles with sparse, fuzzy hair, which are underdeveloped and less dense compared to hairy rodent skin (Lauer et al., 1995). Illel et al. (1991) used skin areas of rats with and without follicles to compare the penetration of [^{3}H]hydrocortisone, niflumic acid, caffeine and p-aminobenzoic acid applied in acetone, in a diffusion cell. For these compounds, the steady-state flux and the amounts diffusing during 24 or 48 hours were 2 to 4 times higher in appendaged rat skin (follicular density 10-200/cm²) than in the absence of appendages. These results were confirmed by a second model, in which diffusion of [^{3}H]hydrocortisone was studied in skin samples taken one day after birth, when the rat skin was still devoid of follicles, and compared to five-day postnatal skin samples, in which follicles were fully developed. Results indicated that the steady-state flux and the total diffusion during 24 hours were fivefold lower in the follicle-free skin. Meidan et al. (1998) extended these findings to mannitol, hydrocortisone, 5-fluorouracil and aminopyrine. Hisoire and Bucks (1997) compared the percutaneous absorption of retinoic acid in haired and hairless guinea pig skin. Shelley and Melton (1949) noted the appearance of tiny multiperifollicular wheals on haired in vivo human skin after the topical application of epinephrine and histamine phosphate in propylene glycol, whereas no responses occurred in regions with less hair density. Turner and Guy (1998) found significant iontophoric drug delivery across the skin via follicular structures. Using autoradiography, Rutherford and Black (1969) determined that a considerable amount of germicides penetrated via the pilosebaceous apparatus. Bidmon et al. (1990) also used autoradiography to detect ^{3}H-estradiol-17β in hairy rat skin in vivo. Radioactivity was at the highest concentration in the follicular papillae and the sebaceous glands for at least 24 hours, suggesting a drug depot effect. Essa et al. (2002) performed an in vitro Franz cell experiment for iontophoric drug delivery, in which follicular orifices were blocked, leading to an absorption rate that was five times lower than when the orifices were not blocked. Raufast and Mavon (2006) found that linoleic acid, implicated in the treatment of follicular diseases, preferentially accumulated in the hair follicles of the human scalp after topical application. Application of commercially available dyes to human

skin resulted in penetration into the hair follicles to depths of 1200 µm from the skin surface (Genina et al., 2002).

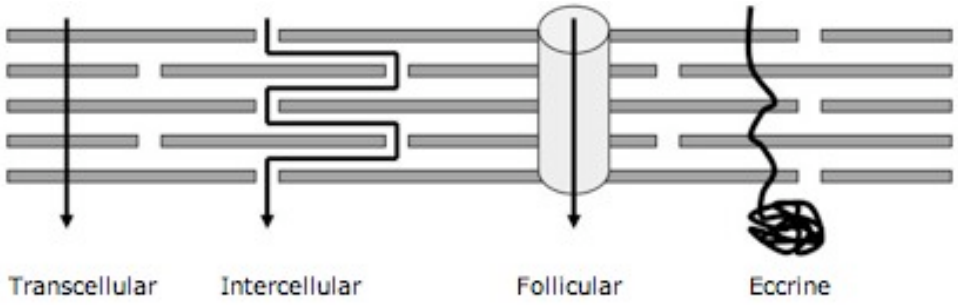

Fig. 3: Penetration pathways through the skin (modified from Hadgraft, 2001)

2.2.3. Methods for analyzing intercellular and follicular penetration

Tape stripping

The method of tape stripping first described by Pinkus (1951) is a minimally invasive technique used to examine the penetration and distribution of topically applied substances within the stratum corneum. After the topical application of a substance, a strip of adhesive tape is pressed onto the treated skin area with standardized pressure (Bashir et al., 2001), so that the upper layers of the stratum corneum attach to the strip, and is then removed. This process is repeated until all components of the horny layer, the corneocyte aggregates, the endogenous components of the horny layer and the topically applied substances are transferred completely from the skin to the adhesive tape strips (Weigmann et al., 1999a, 1999b). The number of tape strips taken is not proportional to the depth of the stratum corneum (Dreher et al., 1998; Marttin et al., 1996). Common sources of variation include the adhesive quality of the tape (Bashir et al., 2001), the vehicle parameters (Jacobi et al., 2003), the pressure applied, the time of application as well as the removal of the strips (Löffler et al., 2004). Because of an increased cohesiveness of the stratum cornuem in the deeper layers, the mass removed with each strip decreases as the stratum corneum is progressively stripped (Bashir et al., 2001). By using a roller to press the strips onto the skin, substance residues located in the furrows and wrinkles of the skin can be taken up (van der Molen et al., 1997; Lademann et al., 2002). Teichmann et al. (2005) confirmed these results by examining histological sections of porcine skin after tape stripping. Penetration profiles can be established by correlating the amount of test substance found on each strip to the number of cell layers removed from the skin (Dreher et al., 1998; Lindemann et al., 2003; Marttin et al., 1996; Weigmann et al., 1999a).

Cyanoacrylate follicular biopsy

In 1971, Marks and Dawber first described the cyanoacrylate skin surface biopsy as a method for studying the desquamated portion of the stratum corneum. By placing a drop of cyanoacrylate glue onto degreased skin, and covering it with a slightly moist glass slide, upper horn layers were removed from the skin as they attached to the slide during cyanoacrylate polymerization. The slides were then examined using histochemical techniques or electron microscopy. In addition to removing several layers of corneocytes, the samples also showed the orifices of follicles and sweat glands (Pagnoni et al., 2004). Mills and Kligman (1983) used this technique to extract the contents of the follicular infundibulum, consisting of a mixture of keratinized material, cell detritus, lipids and bacteria (Thielitz et al., 2001), which were then studied under light or electron microscopy. The modification was termed cyanoacrylate follicular biopsy, and is now widely used for the quantification of microcomedones and their changes under acne therapy (Lavker et al., 1992), the assessment of follicular density at different body sites (Pagnoni et al., 1994), microbial colonization (Holland et al., 1974), mite populations, enzyme location and the penetration of topical agents (Thielitz et al., 2001).

Differential stripping

In the method of differential stripping developed by Teichmann et al. (2005), the stratum corneum was removed using the method of tape stripping, and the amounts of test substance found on the strips were determined. Follicular casts were subsequently obtained with the technique described by Mills and Kligman (1983). Test substance located in the casts were then extracted with ethanol and quantified spectroscopically. This combined method of tape stripping and cyanoacrylate follicular biopsy enables the selective quantification of test substance found in the hair follicles after the topical administration to human subjects (Lademann et al., 2006; Ossadnik et al., 2007; Patzelt et al., 2008). The result is a depth profile for the administered substance. Differential stripping does not however provide valid results for studies using the surrogate porcine ear skin. Follicular casts can not be obtained without producing tears in the cyanoacrylate as the bristles are rooted firmly in the subcutaneous fat at a depth of up to 5 mm (Meyer, 1986), and are thus difficult to extract.

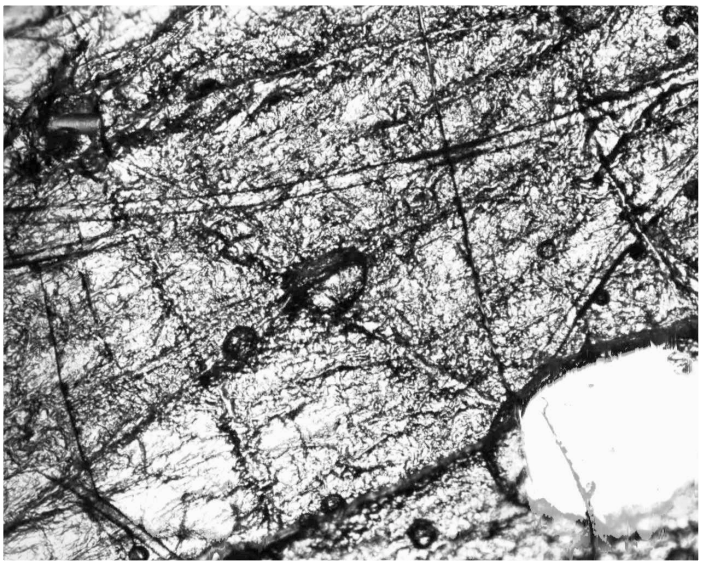

Fig. 4: Cyanoacrylate follicular biopsy taken from porcine skin with a follicular cast visible in the upper left-hand corner and a large tear in the lower right-hand corner (4x)

2.3. Follicular penetration of nano-sized particulates

Nano-sized particles are smaller than 1 μm with active substances encapsulated within their polymeric matrix or adsorbed or conjugated onto their surface (Labhasetwar, 1997). As particles become smaller, the proportion of atoms found at the surface increases relative to the proportion inside their volume, resulting in increased surface reactivity. Nano-sized particles therefore show greater biological activity per given mass compared with larger particles when taken up by living organisms. This can be either desirable, as in antioxidant activity, carrier capacity for therapeutics, and penetration for drug delivery, or undesirable, as in toxicity, induction of oxidative stress or cellular dysfunction (Oberdörster et al., 2005). They have been extensively investigated for sustained and targeted delivery of different agents including plasmid DNA, proteins and peptides, and low molecular weight compounds (Panyam & Labhasetwar, 2003). Drugs can be delivered from these particles by diffusion of the drug from or through the system, by chemical or enzymatic reactions leading to degradation or cleavage of the drug from the system, as well as by solvent activation, either through osmosis or swelling of the system (Langer, 1998). Encapsulation protects the therapeutic agent from harmful environmental influences (Daniels, 2006; Volodkin et al., 2004) and enables higher drug-carrying capacities (Langer, 1998). Modulation of the polymer characteristics can ensure optimal therapeutic efficacy (Song et al., 1998) through extended activity or enhanced uptake of the drug (Alvarez-Romàn et al., 2004b) and the reduction of adverse effects (Lamprecht et al., 2001). Functional coatings can facilitate the targeted accumulation and release at therapeutic sites (Dinauer et al., 2005; Kotrotsiou et al., 2005; Wartlick et al., 2004).

Lademann et al. (2007) demonstrated that subsequent to massage application, particulate formulations penetrated more deeply into the hair follicles of human subjects and porcine ear skin than non-particulate formulations (approximately 1500 μm vs. 300 μm, respectively, in porcine ear skin). Nano-sized particles labelled with fluorescein were detected in the hair follicles for up to 10 days after administration. Rolland et al. (1993) reported that PLGA-fluorescent microspheres dispersed in an aqueous gel were clearly visualized within the pilosebaceous structures of hairless rats and human skin after 35 minutes of passive permeation, while penetration through the stratum corneum was not observed. Baroli et al. (2007) showed that metallic particles smaller than 10 nm were able to penetrate the skin through the lipid matrix of the stratum corneum and hair follicle orifices, reaching the deepest layers of the stratum corneum and in a few cases, the uppermost strata of the viable epidermis. Lekki et al. (2007) reported the visualization of the penetration of sunscreen formulations containing TiO_2 particles sized about 20 nm in hair follicles of both human and porcine skin. Particles were found as deep as 400 μm in the hair follicles, and were assumed to be introduced mechanically. No particles were observed in vital tissue or in sebaceous glands. An in vivo penetration experiment, caffeine was detected in the blood 5 minutes subsequent to its topical application. When the hair follicles were blocked with a varnish-wax mixture, caffeine was found in the blood after a delay of 20 minutes (Otberg et al., 2008).

2.3.1. Nano-sized particulate PLGA

Different synthetic and natural polymers have been utilized in formulating biodegradable nano-sized particles (Moghimi et al., 2001). Synthetic polymers have the advantage of sustaining the release of the encapsulated drug over a time period of days to weeks compared to natural polymers, which have a short duration of drug release (Anderson & Shive, 1997), and are limited by the use of organic solvents and harsher formulation conditions (Panyam & Labhasetwar, 2003). Of the polymers used for nanoparticle formulation, the aliphatic poly(esters) poly(lactide) (PLA), poly(glycolide) (PGA) and their copolymer poly(lactide-co-glycolide) (PLGA) have been the most extensively studied for drug delivery (Jain, 2000; Langer, 1997). Due to their excellent biocompatibility and biodegradability, lactic and glycolic acid polymers are frequently utilized in controlled release systems, as well as in bioresorbable sutures, tracheal replacements, vascular grafts, and in dental and fracture repair (Jain, 2000). PLGA particles were administered into the systemic circulation without particle aggregation or blockage of blood capillaries. They have been tested extensively for toxicity and safety in animal studies (Panyam & Labhasetwar, 2003). The reported tissue response of PLGA was a minimal localized inflammation and foreign body reaction, which decreased with time. D,L-lactide and glycolide possessed low acute toxicity, presumably as a result of their rapid metabolism, and did not lead to any long-term effects (Bala et al., 2004). PLGA

can be synthesized directly from monomers, although it is also commercially available in different molar ratios of glycolic and lactic acid, and in varying molecular weights of the polymer chains. The physicochemical properties are therefore strongly dependent on the nature of the monomers. As lactic acid is more hydrophobic than glycolic acid, polymer features such as mechanical strength, crystallinity, swelling, polymer degradation rate and hydrolysis can be controlled by variation of the glycolic acid/lactic acid ratio (Bala et al., 2004; Jain, 2000). Drugs encapsulated within the PLGA matrix are released at a sustained rate by diffusion of the drug through the polymer barrier, by erosion of the polymer material (Anderson & Shive, 1997), or by a combination of both (Wu, 1995). In vitro and in vivo PLGA undergoes degradation in aqueous environments through scission of the backbone ester linkages (Göpferich, 1996). The most commonly used PLGA copolymer composition of 50:50 is reported to have the fastest degradation rate of the D,L-lactic acid and glycolic acid materials at approximately 50 to 60 days (Bala et al., 2004). Bulk erosion appears to be the main degradation mechanism for PLGA devices (von Burkersroda et al., 2002). Polymer chains are cleaved throughout the polymer matrix (Panyam et al., 2003), resulting in a decrease in molecular weight of the polymer without any significant weight loss. This is accompanied by a rapid loss of mass due to the formation of soluble degradation products. Finally, soluble monomer products are formed from soluble oligomeric fragments, leading to complete polymer solubilization (Jain, 2000). These degradation products are eventually metabolized in the body via the citric acid cycle, and subsequently eliminated from the body as carbon dioxide and water (Panyam et al., 2003).

2.3.2. Fluorescent markers

The dye fluorescein, which is commonly implemented to label nano-sized particles, is a relatively non-toxic, yellow, vital hydroxyxanthene dye that produces an intense green fluorescence in slightly acid to alkaline solutions. It is used to detect ophthalmic lesions and as a tracer in clinical studies. Fluorescein exhibits a high degree of ionization at physiologic pH and therefore does not penetrate intact epithelium or form a firm bond with vital tissue. When there is a break in the epithelial barrier, it can rapidly penetrate (Noga & Udomkusonsri, 2002). The dye absorbs light in the blue range of the visible spectrum, with absorption peaking at 480 to 500 nm, and it emits light from 500 to 600 nm (Cheng & Dovichi, 1988). Fluorescent dyes such as fluorescein are commonly used to determine cellular viability, endo- and exocytosis, membrane fluidity, protein trafficking, signal transduction and enzyme activity (Claxton et al., 200-). Fluorescence was first described by the British scientist Sir G. G. Stokes in 1852, who observed that the mineral fluorite emitted red light when it was illuminated by ultraviolet excitation (Spring & Davidson, 2009). He noted that fluorescence emission always occurred at a longer wavelength than that of the excitation light, a

phenomenon known as the Stokes shift (Lichtman & Conchello, 2005). Early investigations revealed that many specimens, including minerals, crystals, resins, crude drugs, chlorophyll, vitamins and inorganic compounds, exhibit autofluorescence when irradiated with ultraviolet light. The study of animal tissue or pathogens is often complicated with very faint or bright non-specific autofluorescence. It was not until the 1930s that the technique of secondary fluorescence, which employs fluorophore stains to label specific tissues, bacteria and other pathogens, was initiated in biological investigations. Fluorophores are excited by specific wavelengths or irradiating light and emit light of a defined intensity (Spring & Davidson, 2009). They are designed to bind to biological macromolecules such as proteins or nucleic acid, or to localize within a specific structural region of the cell including the cytoskeleton, mitochondria, Golgi apparatus, endoplasmic reticulum or the nucleus. Specific fluorophores are implemented in genetic mapping and chromosome analysis, or monitor dynamic processes and environmental variables such as pH, relative oxygen species and membrane potential. The application of fluorophore arrays has made it possible to identify cells and sub-microscopic cellular components with a high degree of specificity using fluorescence microscopes. Through the implementation of multiple fluorescence labeling, different probes can identify target molecules simultaneously (Spring & Davidson, 2009).

2.3.3. Methods for detecting fluorescent markers in the skin

Skin molecules such as collagen, elastin, tryptophan and nicotinamide adenine dinucleotide fluoresce when irradiated by light of certain wavelengths. Each fluorophore has a characteristic excitation-emission spectrum, which overlaps with the spectra of the other fluorophores in the skin. In a study by Na et al. (2000), the human skin autofluorescence spectra, provoked by excitation wavelengths between 340 and 380 nm, consisted of three component bands with centre wavelengths at 450, 520 and 625 nm. The 450 nm band contributed approximately 75% to the intensity of the overall spectrum, the 520 nm band contributed 25%, and the 625 nm band contributed about 2%. These values varied according to body sites. To avoid falsifications, the autofluorescence of the skin must be taken into account when detecting fluorescent markers or dyes by measuring fluorescence emission at according wavelengths.

Fluorescence microscopy

The basic function of the fluorescence microscope is to irradiate a specimen with a specific band of wavelengths, and then to separate the much weaker emitted fluorescence from the excitation light. Ideally, only the emission light should reach the detector, so that the resulting fluorescent structures are superimposed with high contrast against a dark background. The

limits of detection are governed by the darkness of the background, and the excitation light is commonly several hundred thousand to a million times brighter than the emitted fluorescence (Spring & Davidson, 2009). In a fluorescence microscope, the objective images and magnifies the specimen, and serves as the condenser that illuminates it. Only the small portion of the exciting light that is reflected off the sample must be blocked in the return light path. Since the exciting light and fluorescence emission overlap in the light path, a special beam splitter such as a dichroic mirror is necessary to separate the excitation from the emission. It is designed to be used in light paths in 45º angles. The dichroic mirror reflects shorter wavelength light coming from the light source and transmits the longer wavelengths of the emitted fluorescence. Each dichroic is designed to have a transition from reflection to transmission that resides between the excitation and emission peaks of the fluorophore it is used with. An excitation filter that preselects the exciting wavelengths and a barrier filter that only allows passage of the longer wavelength light back to the detector are implemented in addition to the dichroic. These filters are typically interference filters, which have highly specific wavelength selectivity. The exciter, the beamsplitting dichroic mirror and the barrier effectively separate the excitation light from the emitted light. In many fluorescence microscopes, filter cubes composed of the exciter, the dichroic mirror and the barrier filter, select the precise wavelength bands needed for excitation and emission. For fluorescence illumination, xenon arc lamps provide relatively even coverage of wavelengths. The image of the arc is focused sharply on the back aperture of the objective to avoid uneven illumination (Lichtman & Conchello, 2005).

Confocal laser scanning microscopy

Confocal laser scanning microscopy is an optical microscopy technique which is based on conventional wide-field fluorescence microscopy. It enables the serial production of thin (0.5-1.5 μm) optical sections from specimens that have a thickness of up to 50 μm. A series of images is collected by coordinating incremental changes in the fine focus of the microscope with sequential image acquisition at each step. Spatial filtering techniques eliminate out-of-focus light in specimens whose thickness exceeds the immediate plane of focus. Due to the reduction of background fluorescence and improved signal-to-noise, contrast and definition are dramatically improved over conventional microscopy. Light emitted by a laser excitation source passes through a pinhole aperture that is situated on a conjugate confocal plane with one scanning point on the specimen (0.25-0.8 μm in diameter, 0.5-1.5 μm deep) and a second pinhole aperture positioned in front of the photomultiplier tube detector. The laser is reflected by a dichromatic mirror and scanned across the specimen in a defined focal plane in a raster pattern. This is controlled by two high-speed oscillating mirrors. While one of the mirrors moves the beam from left to right along the x lateral axis, the other translates the beam in the y direction. After each scan along the x axis, the beam is transported back to the starting point

and shifted along the y axis to start a new scan. Image information is not collected during this process. This way, the area of interest on the specimen in a single focal plane is excited by laser illumination from the scanning unit. When the objective is refocused, the excitation and emission points on the specimen are shifted to a new plane, which becomes confocal with the pinhole apertures of the light source and the detector. While each scan line passes along the specimen in the lateral focal plane, fluorescence emission is collected by the objective and passed back through the confocal optical system. Secondary fluorescence emitted from points on the specimen in the same focal plane passes back through the dichromatic mirror and is focused as a confocal point at the detector pinhole aperture. The considerable amount of fluorescence emission that occurs at points above and below the objective focal plane is not confocal with the pinhole, and is termed out-of-focus light. As only a small fraction of the out-of-focus fluorescence emission is delivered through the pinhole aperture, most of it is not detected by the photomultiplier tube and therefore does not contribute to the resulting image. Fluorescence emission stays in a steady position at the pinhole aperture, but fluctuates with respect to intensity over time as the illumination spot scans the specimen producing variations in excitation. Fluorescence that passes through the pinhole aperture is converted into an analogue electrical signal with a continuously varying voltage by the photomultiplier. This signal is periodically sampled and converted into pixels. Information on the image is stored on the computer and displayed on the monitor. While a real image that can be observed through the eyepiece never exists, the confocal image of a specimen is reconstructed, point by point, from emission photon signals by the photomultiplier and accompanying electronics. (Claxton et al., 200-). The brightness of the resulting image pixel corresponds to the relative intensity of detected fluorescent light (Pawley, 2006).

Fluorescence spectroscopy

Spectrofluorometers analyze the emission spectra emitted from fluorescing samples. Light from an excitation source such as a pulsed xenon discharge lamp passes through a filter and strikes the sample, which is placed normal to the incident beam. Such intense light sources produce high sensitivity, but may however be sufficient to decompose the sample, necessitating a shutter so that the solution is only irradiated during the short period of measurement. A cuvette containing the sample is placed in a sample holder. The solvent used must be free of traces of contaminants as any compound that is capable of absorbing a portion of the excitation or emission energy in the solution can reduce the intensity of fluorescence. Cuvettes must be constructed of a material that will transmit both the incident and the emitted light (PerkinElmer, 2006). The sample absorbs a portion of the incident light, causing some of its molecules to give off fluorescence equally in all directions. A second filter placed at 90º to the incident light beam, so as to minimize the effect of light scattering by the solution and the cell, then collects the emitted fluorescence. The fluorescence obtained from the 90º collection

falls rapidly as the absorbance of the solution increases, leading to a progressively distorted fluorescence emission. It is finally detected with photomultiplier tubes and quantified electronically. The material from which the photocathode is made determines the spectral range of the photomultiplier. Generally two tubes are required to cover the complete UV-visible range. Detector output is amplified and displayed digitally (Lakowicz, 2006; PerkinElmer, 2006).

3. Materials and methods

3.1. Experiments on the follicular penetration of nano-sized particulate FA-PLGA in dog, rat and porcine skin

Two formulations containing fluorescing particles sized 256 nm and 430 nm were applied to excised dog and rat skin, as well as porcine ear skin. Preparation of the skin samples was carried out in the laboratories of the Centre for Applied and Experimental Physiology (CCP) (Klinik für Dermatologie, Allergologie und Venerologie, Charité Berlin), at a room temperature of 22° ± 2° C and a humidity of 50 to 75%. The penetration depths of the particles into the hair follicles of the skin samples were determined by detection of their fluorescence in cryohistological cross-sections using a confocal laser scanning microscope (Institut für Chemie, Humboldt-Universität zu Berlin). Approval for these experiments was obtained from the Veterinary Board of Control (Veterinäramt Treptow-Köpenick, Berlin).

3.1.1. Material

Formulations containing nano-sized particulate FA-PLGA

The test formulations were based on 1.5% hydroxyethylcellulose gel and contained 5-fluoresceinamine-labelled poly(lactide-co-glycolide) (FA-PLGA) particles sized 256 nm (FA-PLGA$_{256}$) and 430 nm (FA-PLGA$_{430}$) in a concentration of 0.1% (Biopharmazie und Pharmazeutische Technologie, Universität des Saarlandes). The particles were assumed to be distributed homogeneously throughout the gel. 5-fluoresceinamine used to label PLGA is a fluorescein derivative (Weiss, 2007). FA-PLGA was prepared along the guidelines of a method described by Horisawa et al. (2002). Particles were prepared from the FA-PLGA polymer by nanoprecipitation, as described in Fessi et al. (1998). The particles were stored at 4° C prior to their use to avoid premature degradation and aggregation of the particles (De & Robinson, 2004) and applied to the skin samples within 10 days of their preparation.

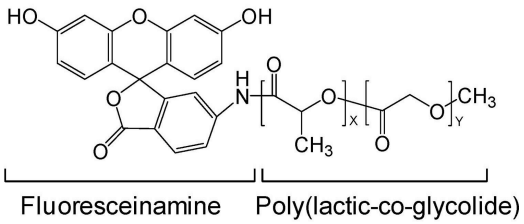

Fig. 5: Chemical composition of FA-PLGA (Xu et al., 2009)

Skin samples

Dog and rat skin samples were obtained from control groups belonging to the Bayer Schering Pharma AG (Berlin, Germany). While the dogs were euthanized with pentobarbital

(Narcoren®, Merial, Hallbergmoos), the rats were anesthetized with chloroform and exsanguinated with a cut to the throat. The samples were transported to the laboratories of the CCP and prepared for the experiments within 1 hour of the death of the animals. The Gut Hesterberg (Neuruppin-Lichtenberg) provided ears from freshly slaughtered crossbred pigs (Deutsches Edelschwein, Deutsches Hausschwein and Duroc). They were removed after the death of the animals and prior to steam sterilization of the bodies, and were delivered to the laboratory within 24 hours of slaughtering. Scarred, injured or diseased specimens were excluded from the study.

Tab. 1: Overview of the animals from which the skin samples were derived

Species	Breed	Gender/ Individuals	Age	Weight	Origin of the skin sample
Dog	Beagle	Male/5 Female/5	14 months	8-12 kg	Dorsum
Rat	Wistar	Male/8 Female/6	8-12 weeks	200-250 g	Dorsum
Pig	Crossbred	N.N./4	7-8 months	120 kg	Ear

3.1.2. Methods

Preparation of the skin samples

Upon arrival, the porcine ears were cleansed with cold running water and dabbed dry with paper towels. All skin samples were fixed on polystyrene boards using needles with the dorsal side facing upwards. The fur on the dog and rat skin samples and the bristles on the porcine ears were clipped to a length of 1 to 2 mm. Razors were not used to avoid damage of the skin. Two test areas of 4 by 4 cm were marked on each dog and porcine skin sample with a permanent marker (0.7 mm Black OHP Permanent Marker, SCHNEIDER Schreibgeräte GmbH & Co., Wernigerode). Due to the small size of the rat specimens, only one test area of 4 by 4 cm could be marked on each sample.

Application of the formulations containing nano-sized particulate FA-PLGA

For each test region, defined amounts of the test substance were weighed in plastic 1 ml sterile syringes using an analytical balance (Analysenwaage Kern® 770, KERN & Sohn GmbH, Balingen-Frommern). This was checked by weighing the syringes containing the test formulations before and after application, and calculating the difference. The formulations were applied homogeneously to the corresponding test areas, and massaged into the skin with a hand-held massage device (Petra® Electric PC60 Massagegerät, Elektrogerätefabrik,

Burgau) for 3 minutes using standardised pressure (60-80 g, Laborwaage Kern® 440-51, KERN & Sohn GmbH, Balingen-Frommern). The exposure time of 30 minutes allowed for penetration of the formulations into the skin subsequent to the massage application.

Skin biopsies

5 punch biopsies with a diameter of 8 mm were taken from each test region (STIEFEL® BIOPSY PUNCH, STIEFEL® Laboratorium GmbH, Offenbach am Main). The subcutaneous fat was excised along with the biopsies. The biopsies taken from the porcine ears were separated from the underlying cartilage using a scalpel. To facilitate the later preparation of the cross-sections, the samples were flattened between two glass slides and fixed with cryospray (Cryospray Instant Freezing Spray, Bio Optica®, Milano). They were then shock frozen in liquid nitrogen in freezing vials (Cryo.s™, Greiner Bio One, Solingen) and stored at - 20° C until further use. The freezing vials were labelled using random ciphers to encode the particle sizes applied to the samples to avoid the influence of an observer bias during sample analysis. The animal species corresponding to the samples were not encoded because the distinct species-specific morphologies made the sections clearly distinguishable from one another in the microscope.

Cryohistological cross-sections

For the preparation of the cryohistological cross-sections, the frozen biopsies were embedded in Neg - 50™ (Richard-Allan Scientific®, Kalamazoo, Michigan), a water-soluble frozen section medium. The sections were cut using a cryostat (Microm Cryo-Star HM 560, MICROM International® GmbH, Walldorf) and mounted on glass slides. By positioning of the frozen biopsies in the cyrostat, it was possible to cut vertically through the hair follicles. 10 µm thick sections were cut from the rat skin samples, while the dog and pig skin samples were cut into sections 14 to 16 µm thick. It was not possible to cut thinner sections because of the high density of the hair follicles in the specimens. The glass slides were stored at - 20° C after preparation.

Confocal laser scanning microscopy

A confocal laser scanning microscope (LSM) 410 (Zeiss, Berlin) was used to examine the cross-sections in transmission and fluorescence mode. Digital images and measurements of the penetration depths were obtained using the software LSM 410 Invert Basic, Version 3.98 (Zeiss, Berlin). The fluorescent probes were excited using an Argon laser with a wavelength of 488 nm. As porcine ear skin exhibits autofluorescence in a wavelength spectrum between

520 and 560 nm, emission signals were detected with the FT 580 dichroic beam splitter and long pass filter LP 590 to exclude any autofluorescence effects.

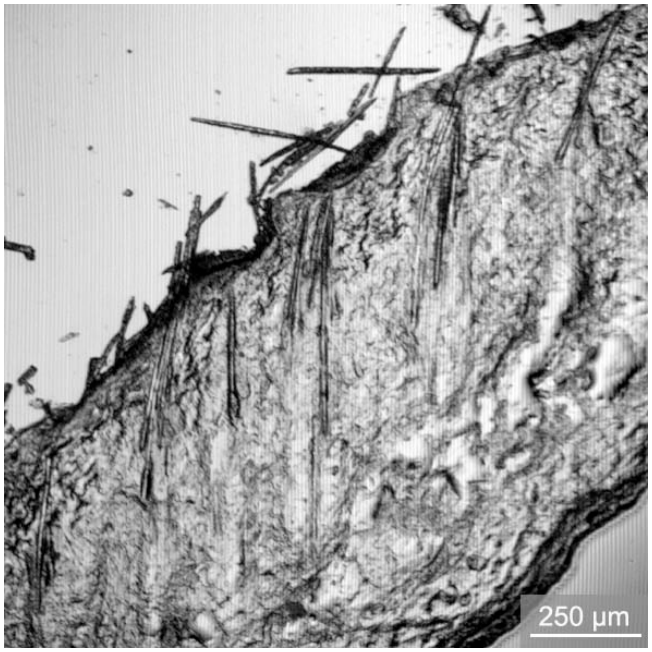

Fig. 6: Cross-section through rat skin treated with FA-PLGA$_{256}$ and examined in the transmission mode

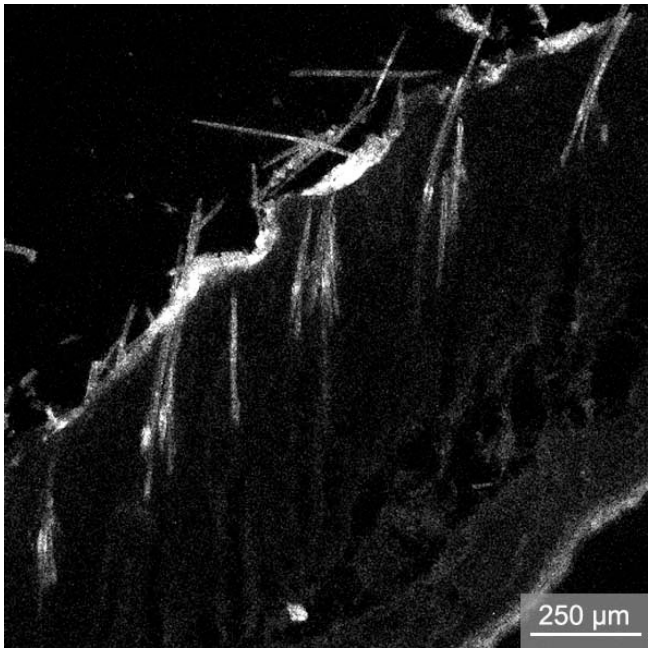

Fig. 7: Cross-section through rat skin treated with FA-PLGA$_{256}$ and examined in the fluorescence mode; fluorescence (white) is visible on the skin surface and in the hair follicles

3.2. Experiments on the selective quantification of follicular RhBITC in porcine skin

The method was developed in laboratories of the CCP (Klinik für Dermatologie, Allergologie und Venerologie, Charité Berlin). A gel formulation containing a red dye was topically applied to porcine ear skin. The stratum corneum was removed by tape stripping along with the dye that had diffused into the upper skin layers. The dye remaining in the hair follicles was extracted with ethanol and subsequently quantified using fluorescence spectrometry. All experiments were carried out at a room temperature of 22° ± 2° C and a humidity of 50 to 75%. Approval for these experiments was obtained from the Veterinary Board of Control (Veterinäramt Treptow-Köpenick, Berlin).

3.2.1. Material

Formulation containing RhBITC

Rhodamine B Isothiocyanate (RhBITC) ($C_{29}H_{30}ClN_3O_3S$) is a dye available as a red-brown powder that fluoresces in the red-orange range of the spectrum. Substance instability may be caused by contact with water or light, as well as with strong oxidizing agents. A formulation consisting of 0.1% RhBITC (Product 283924, Aldrich Chemie GmbH, Steinheim) and hydroxyethylcellulose gel 2.5% conserved with parabens (Apotheke Charité Campus Virchow Klinikum, Berlin) was used for this study. 5 mg RhBITC and 5 g hydroxyethylcellulose gel were weighed using an analytical balance (Analysenwaage Kern® 770, KERN & Sohn GmbH, Balingen-Frommern) and stirred together for 3 minutes, producing a dark red gel, in which RhBITC was assumed to be distributed homogeneously.

Skin samples

10 ears from healthy, freshly slaughtered crossbred pigs (Deutsches Edelschwein, Deutsches Hausschwein and Duroc) belonging to the Gut Hesterberg (Neuruppin-Lichtenberg) were used for this experiment. The ears were excised immediately after slaughtering and before the carcasses were scalded. At the time of their death, the animals were 7 to 8 months old and weighed approximately 120 kg. The genders corresponding to the excised ears were unknown. Scarred or injured ears were discarded.

3.2.2. Methods

Preparation of the skin samples

The porcine ears were prepared as described in section 4.1.2.

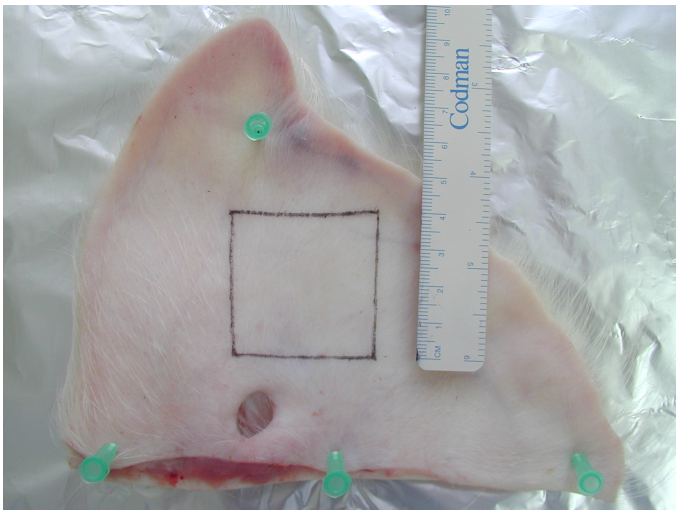

Fig. 8: Test area marked in the center of Specimen 1

Application of the formulation containing RhBITC

For each ear, defined amounts of the formulation were weighed in plastic 1 ml sterile syringes using an analytical balance (Analysenwaage Kern® 770, KERN & Sohn GmbH, Balingen-Frommern). The syringes were weighed before and after application of the formulation to the test areas to confirm the exact amount of substance applied. The formulation was applied to one test area on each ear and massaged into the skin for 3 minutes with standardized pressure (65-85 g, Präzisionswaage Kern® 440-51, KERN & Sohn GmbH, Balingen-Frommern) using a hand-held massage device (Petra® Electric PC60 Massagegerät, Elektrogerätefabrik, Burgau). This ensured homogenous distribution over the entire test areas. The exposure time for the formulation was 30 minutes to allow for penetration into the skin. The second test area on each ear was maintained as an experimental control, and therefore not treated with the RhBITC formulation.

Tape stripping

After the 30 minute exposure time, strips of adhesive tape (tesa® No. 5529, Beiersdorf, Hamburg) were pressed onto the treated and untreated skin areas so that the upper corneocyte layers of the stratum corneum attached to the strips. Small marks were made on the skin on both sides of the tapes to ensure that all strips were taken from precisely the same regions

with a permanent marker (Fig. 10). Prior to removal, each strip was positioned between the marks and covered with a piece of paper to avoid contaminations. A roller was rolled back and forth over each covered strip 5 times using standardized pressure (65-85 g, Präzisionswaage Kern® 440-51, KERN & Sohn GmbH, Balingen-Frommern). The strips were then removed with one swift movement and mounted on glass slides. This process was repeated 80 times for each test area (Figs. 11, 12). Macroscopically, the red dye corresponding to topically applied RhBITC was then visible only in the follicular pores. To verify the removal of the stratum corneum and the test formulation from the skin surface, the strips were subsequently examined using transmission and fluorescence microscopy.

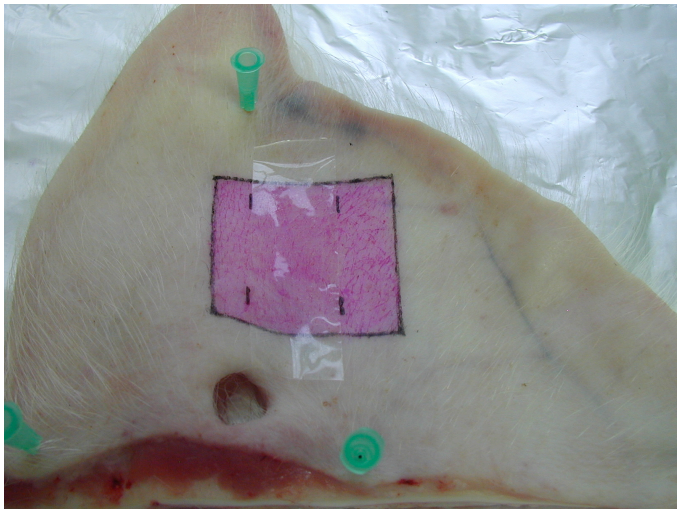

Fig. 9: Test area of Specimen 1 treated with the RhBITC formulation before the removal of the 1st strip

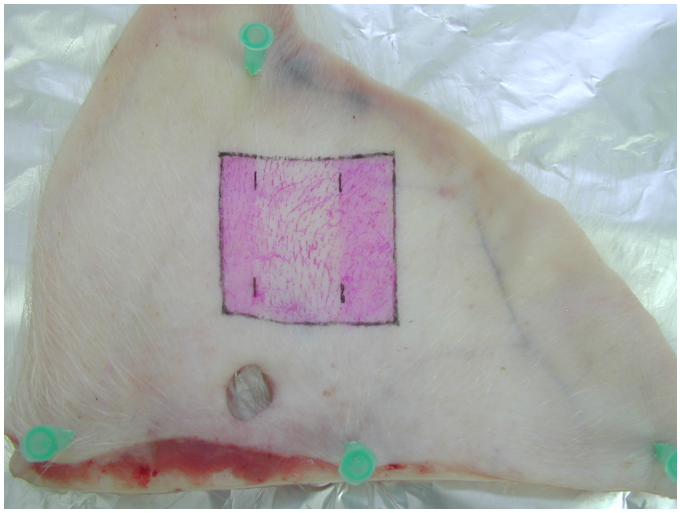

Fig. 10: Test area of Specimen 1 treated with the RhBITC formulation after the removal of the 25th strip

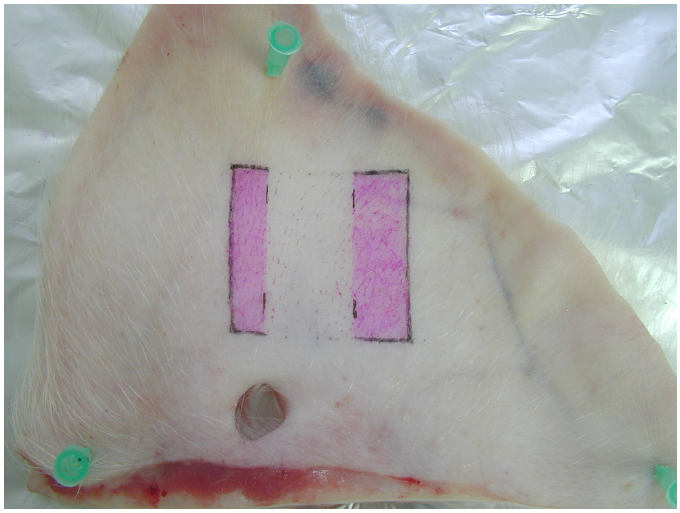

Fig. 11: Test area of Specimen 1 treated with the RhBITC formulation after the removal of the 80th strip

Fluorescence microscopy

A fluorescence microscope (BX 60, Olympus Optical Co. GmbH, Hamburg), operated through the imaging analysis software analySIS 3.1 (Olympus, Soft Imaging Solutions GmbH, Münster), was used to examine the 1st, 10th, 25th, 40th and 80th tape strips of each test region after their removal from the skin surface. Corneocytes and cell remnants attached to the tape strips were visualized using the transmission modus of the microscope. RhBITC located in the corneocyte matrix on the strips was envisaged with the red long pass WIY filter modus and an exposure time of 3 seconds. In this modus, the excitation wavelength was 545 to 580 nm, and the emission wavelength was > 610 nm, enabling the selective detection of red fluorescence.

Extraction of RhBITC

Once the stratum corneum was removed from the skin surface, 15 biopsies sized 5 mm, with a cumulative area of 2.95 cm^2 (STIEFEL® BIOPSY PUNCH, STIEFEL® Laboratorium GmbH, Offenbach am Main), were taken from the stripped regions in the demarcated areas of each ear. The biopsies were carefully detached from the underlying cartilage and submerged in 2.95 ml ethanol (Ethanol for Spectroscopy, Merck KGaA, Darmstadt) in test tubes for 24 hours under the exclusion of light. The areas of the biopsies of each sample were therefore analogous to the amount of ethanol in which the biopsies were immersed. The samples were treated with ultrasound in a non-heated ultrasonic bath (Sonorex Super RK 102 H, Bandelin Electronic GmbH & Co. KG, Berlin) for 60 minutes under the exclusion of light. They were subsequently centrifuged (MR 1812, Jouan, Unterhaching) at 4000 RPM for 10 minutes. After

centrifugation, 1 ml of the supernatant of each test tube was carefully decanted into 1 ml quartz cuvettes (Hellma GmbH & Co. KG, Müllheim), suitable for spectroscopic analysis. The biopsies were removed from the test tubes, and the remaining ethanol was discarded. They were subsequently resubmerged in 2.95 ml of fresh ethanol, and the extraction process was repeated a second time to extract any remaining RhBITC from the skin samples.

Fluorescence spectrometry

A fluorescence spectrometer (LS 50B, PerkinElmer, Waltham, Massachusetts), which was implemented using the software FL WinLab 4.00.01 (PerkinElmer, Waltham, Massachusetts), was used to measure fluorescence emitted by the extraction solutions. Fluorescence was induced with an excitation wavelength of 535 nm, and emission was measured at 570 nm. The quantification of RhBITC in the extraction solutions necessitated reference values by which the empirical relationship between the intensity of fluorescence emission and the concentrations of RhBITC could be established. Three dilution series of RhBITC in ethanol (Ethanol for Spectroscopy, Merck KGaA, Darmstadt) were therefore prepared in the concentrations 0.025 µg/ml, 0.05 µg/ml, 0.1 µg/ml, 0.15 µg/ml, 0.2 µg/ml and 0.25 µg/ml, and their fluorescence emissions measured. The mean fluorescence values of the three series for each dilution concentration were plotted against the known concentrations of RhBITC in the solutions in a calibration curve, providing the needed reference values. Linear regression analysis was conducted using Microsoft® Excel® 2004 for Mac, Version 11.5.5 (Microsoft Corporation, Redmond, Washington).

4. Results

4.1. The follicular penetration of nano-sized particulate FA-PLGA in dog, rat and porcine skin

The localization of fluorescence emitted by topically applied nano-sized FA-PLGA particles in the hair follicles of dog, rat and porcine skin was determined using confocal laser scanning microscopy. In cryohistological skin sections, fluorescence could be detected on the skin surface, as well as in the orifices and infundibula of approximately 60 to 70% of the hair follicles. The remaining follicles were devoid of fluorescence and therefore assumed to be inactive. The orifices of inactive follicles are occluded by cell debris and dried sebum, rendering them unreceptive to penetration (Otberg et al., 2004a). The exact number of inactive follicles could not be determined due to the high follicular densities and the thickness of the cross-sections, particularly in the dog and rat specimens. A more detailed examination of this phenomenon was not considered necessary for the purposes of this study. Using the digital images obtained by the laser scanning microscope, measurements were conducted of the follicular penetration depths of the fluorescing particles. In all specimens, measurements were only made for hair follicles which were sectioned vertically. The accepted level of significance for all statistical tests implemented was 5% ($p \leq 0.05$). For detailed results see Appendix a.

4.1.1. Follicular penetration of FA-PLGA$_{256}$ and FA-PLGA$_{430}$ in dog skin

For each specimen and test area, approximately 10 vertical sections through the hair follicles were examined for fluorescence. In 362 hair follicles of skin treated with FA-PLGA$_{256}$, fluorescence was detected at an average depth of 630.16 (± 135.75) µm. In 414 hair follicles treated with FA-PLGA$_{430}$, it was detected at an average depth of 604.79 (± 132.42) µm (Tab. 2). These mean penetration depths differed significantly ($p \leq 0.05$), as was determined using an unpaired T-test. The null hypothesis of equal variance could not be rejected and is therefore supported on the basis of Levene's test ($p \geq 0.05$). Comparisons between the mean follicular penetration depths of FA-PLGA$_{256}$ and FA-PLGA$_{430}$ within individual specimens were made (Fig. 13), and paired T-tests were applied. Statistically significant differences were only found for Specimens 4 and 6 ($p \leq 0.05$). In all other specimens, statistically significant differences were not found ($p \geq 0.05$). FA-PLGA$_{256}$ penetrated deeper into the hair follicles than FA-PLGA$_{430}$, with the exceptions of Specimens 5, 6 and 10. The frequency distributions, showing observations centered around the mean, and the course of the theoretical normal distribution of the follicular penetration depths found for FA-PLGA$_{256}$ and FA-PLGA$_{430}$ are illustrated in Figs. 14 and 15.

Tab. 2: Mean penetration depths of FA-PLGA$_{256}$ and FA-PLGA$_{430}$ into the hair follicles of dog skin

Specimen	Mean follicular penetration depth (µm) of FA-PLGA$_{256}$ (± SD)	Mean follicular penetration depth (µm) of FA-PLGA$_{430}$ (± SD)
1	674.40 (± 193.93)	606.67 (± 124.98)
2	582.42 (± 90.43)	571.15 (± 134.34)
3	521.90 (± 114.00)	494.85 (± 104.23)
4	695.13 (± 128.00)	614.15 (± 132.70)
5	648.61 (± 121.79)	661.06 (± 189.94)
6	547.94 (± 67.42)	609.81 (± 89.09)
7	647.47 (± 126.78)	603.88 (± 87.31)
8	743.57 (± 110.44)	717.02 (± 125.54)
9	686.40 (± 108.18)	637.77 (± 117.42)
10	593.58 (± 104.68)	598.91 (± 112.15)
$\overline{x}$	630.16 (± 135.75)	604.79 (± 132.42)
	N = 362	N = 414

± SD: Plus-minus standard deviation
$\overline{x}$: Total mean follicular penetration depth
N: Sample size

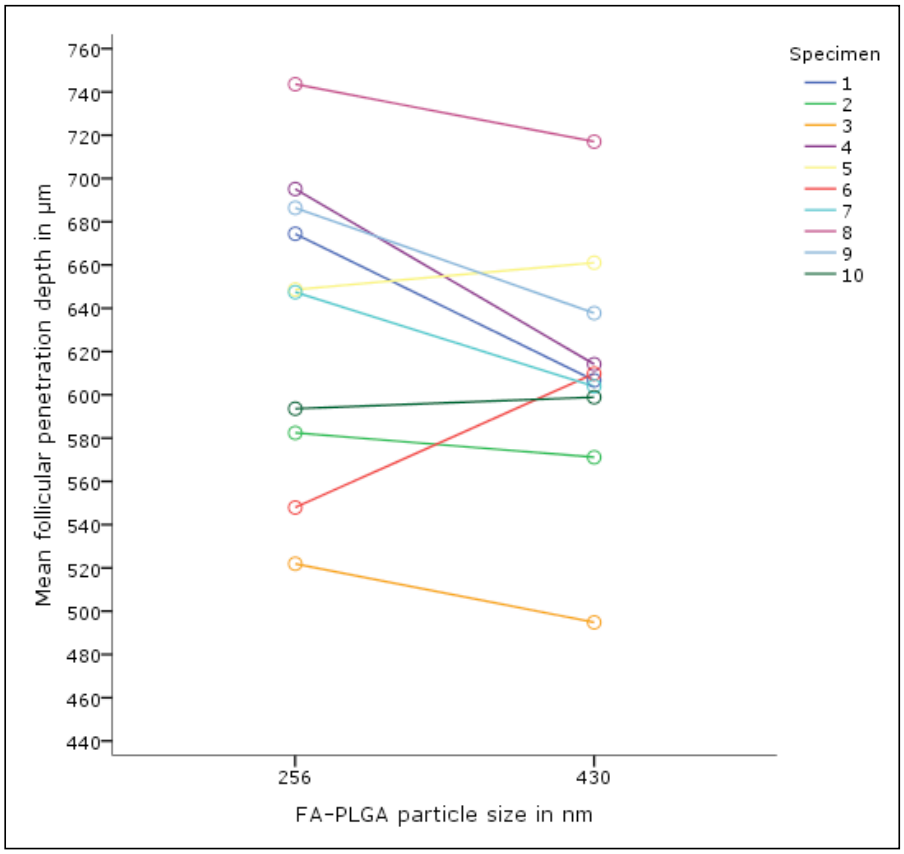

Fig. 12: Comparison between the mean follicular penetration depths of FA-PLGA$_{256}$ and FA-PLGA$_{430}$ within each dog specimen

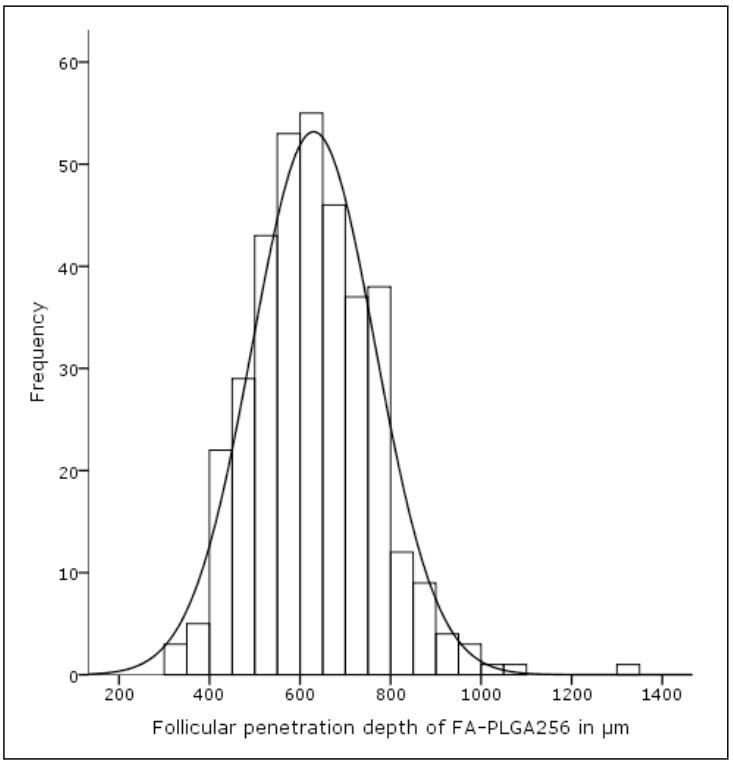

Fig. 13: Frequency distribution and theoretical normal distribution of follicular penetration depths of FA-PLGA$_{256}$ in dog skin

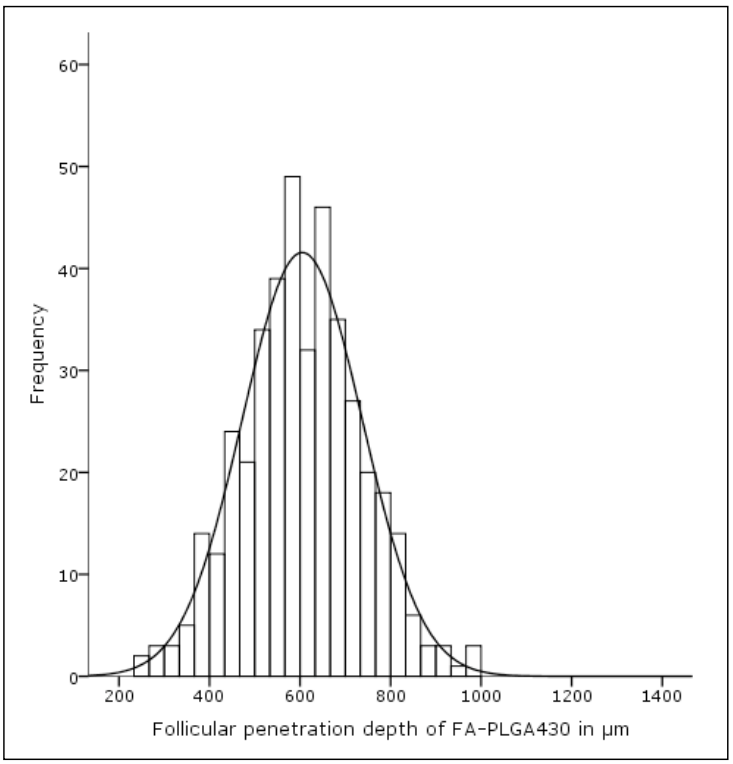

Fig. 14: Frequency distribution and theoretical normal distribution of follicular penetration depths of FA-PLGA$_{430}$ in dog skin

4.1.2. Follicular penetration of FA-PLGA$_{256}$ and FA-PLGA$_{430}$ in rat skin

Due to the small size of the skin samples excised from the dorsum of the animals, only one test area per specimen could be treated with formulation. FA-PLGA$_{256}$ was applied to 8 specimens, while FA-PLGA$_{430}$ was applied to 6. Approximately 8 cross-sections were examined per specimen. Fluorescence was detected at an average depth of 253.55 (± 47.36) µm in 188 hair follicles of skin treated with FA-PLGA$_{256}$, and at an average depth of 262.87 (± 55.25) µm in 155 hair follicles of skin treated with FA-PLGA$_{430}$ (Tab. 3). A modified T-test for independent variables, which does not assume equality of variances, was implemented to compare these mean follicular penetration depths, which are illustrated in Fig. 16. A statistically significant difference could not be determined ($p \geq 0.05$). In Figs. 17 and 18, the frequency distributions and the course of the theoretical normal distribution of the follicular penetration depths of FA-PLGA$_{256}$ and FA-PLGA$_{430}$ are shown. The frequency distributions depict observations centering around the mean.

Tab. 3: Mean penetration depths of FA-PLGA$_{256}$ and FA-PLGA$_{430}$ into the hair follicles of rat skin

Specimen	Mean follicular penetration depth (µm) of FA-PLGA$_{256}$ (± SD)	Mean follicular penetration depth (µm) of FA-PLGA$_{430}$ (± SD)
1	303.15 (± 58.71)	
2	223.10 (± 39.20)	
3	234.44 (± 26.07)	
4		260.35 (± 55.64)
5		293.75 (± 39.60)
6		285.06 (± 59.75)
7	248.59 (± 31.58)	
8	251.32 (± 53.64)	
9	254.77 (± 32.07)	
10		288.95 (± 38.93)
11		236.92 (± 51.46)
12		213.06 (± 32.75)
13	268.81 (± 52.00)	
14	242.26 (± 36.25)	
$\overline{x}$	253.55 (± 47.36)	262.87 (± 55.25)
	N = 188	N = 155

± SD: Plus-minus standard deviation
$\overline{x}$: Total mean follicular penetration depth
N: Sample size

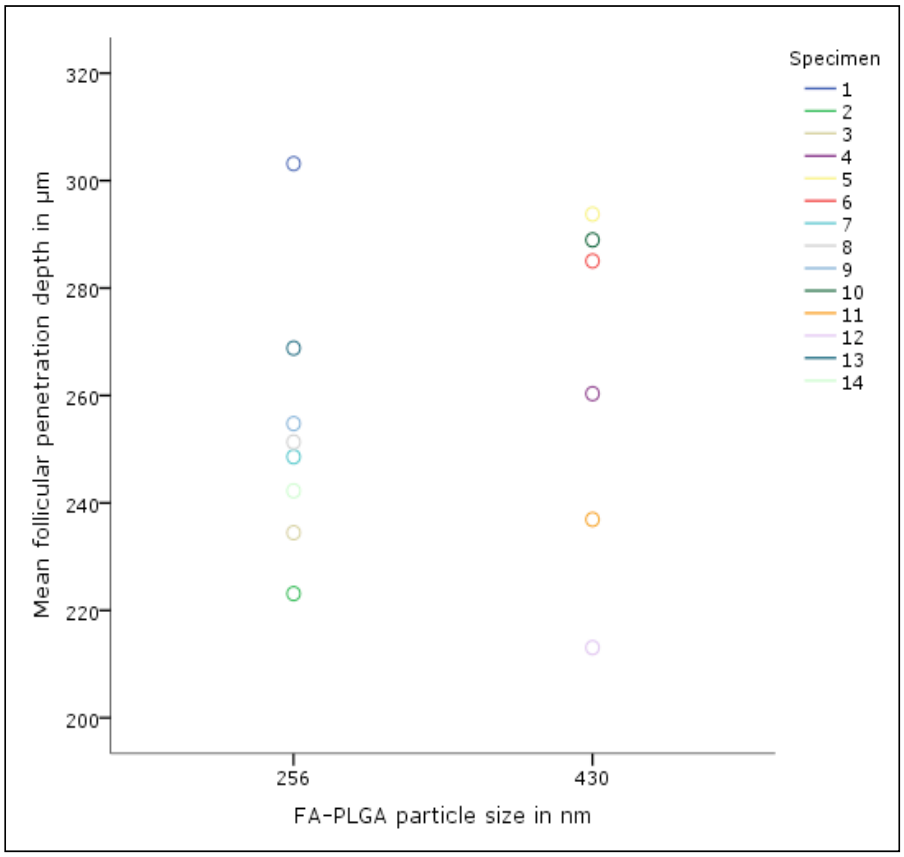

Fig. 15: Mean follicular penetration depths of FA-PLGA$_{256}$ and FA-PLGA$_{430}$ in rat specimens

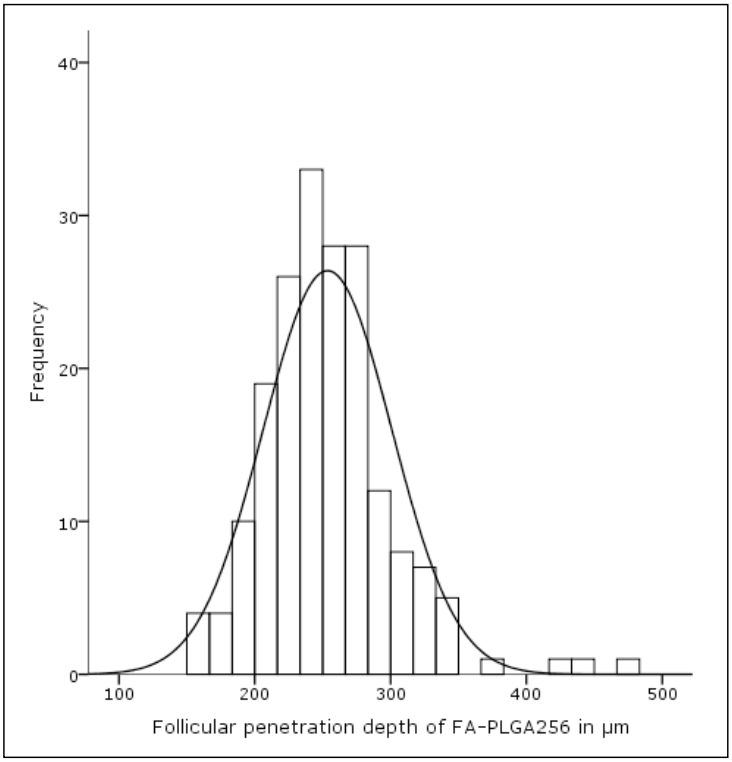

Fig. 16: Frequency distribution and theoretical normal distribution of follicular penetration depths of FA-PLGA$_{256}$ in rat skin

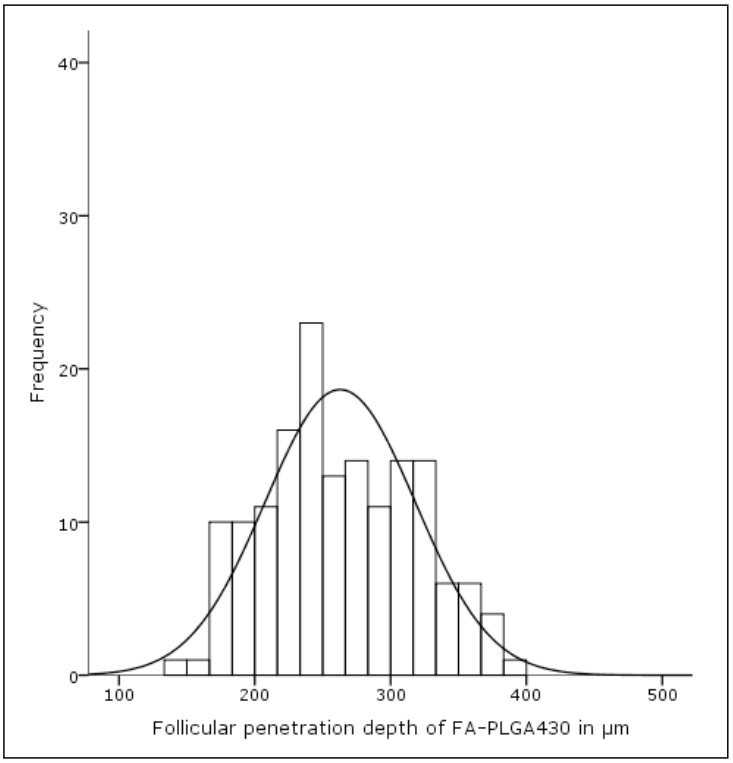

Fig. 17: Frequency distribution and theoretical normal distribution follicular penetration depths of FA-PLGA$_{430}$ in rat skin

4.1.3. Follicular penetration of FA-PLGA$_{256}$ and FA-PLGA$_{430}$ in porcine skin

As a result of the low follicular density in porcine ear skin, comparatively few hair follicles were found in the cross-sections which could be examined for particulate fluorescence. Approximately 29 sections were scrutinized for each test area. Fluorescence was detected at an average depth of 653.40 (± 94.71) µm in 62 hair follicles of skin treated with FA-PLGA$_{256}$. In samples treated with FA-PLGA$_{430}$, fluorescence was detected at an average depth of 786.81 (± 121.73) µm in 59 hair follicles (Tab. 4). In all specimens, FA-PLGA$_{430}$ penetrated to a greater mean follicular depth than FA-PLGA$_{256}$. Using an unpaired T-test, it was determined that the mean follicular penetration depths determined for FA-PLGA$_{256}$ and FA-PLGA$_{430}$ differed significantly ($p \leq 0.05$). The mean follicular penetration depths of the two formulations were compared in each individual specimen (Fig. 19), and paired T-tests were implemented. Statistically significant differences were found for all specimens with the exception of Specimen 2 ($p \leq 0.05$). Illustrations of the frequency distributions centering around the mean and the course of the theoretical normal distribution of the follicular penetration depths of FA-PLGA$_{256}$ and FA-PLGA$_{430}$ are shown in Figs. 20 and 21.

Tab. 4: Mean penetration depths of FA-PLGA$_{256}$ and FA-PLGA$_{430}$ into the hair follicles of porcine skin

Specimen	Mean follicular penetration depth (µm) of FA-PLGA$_{256}$ (± SD)	Mean follicular penetration depth (µm) of FA-PLGA$_{430}$ (± SD)
1	604.84 (± 63.60)	738.68 (± 136.40)
2	773.43 (± 68.16)	799.35 (± 131.79)
3	667.59 (± 96.06)	815.91 (± 83.11)
4	610.93 (± 57.89)	831.23 (± 92.78)
$\overline{x}$	653.40 (± 94.71)	786.81 (± 121.73)
	N = 62	N = 59

± SD: plus-minus standard deviation
$\overline{x}$: Total mean follicular penetration depth
N: sample size

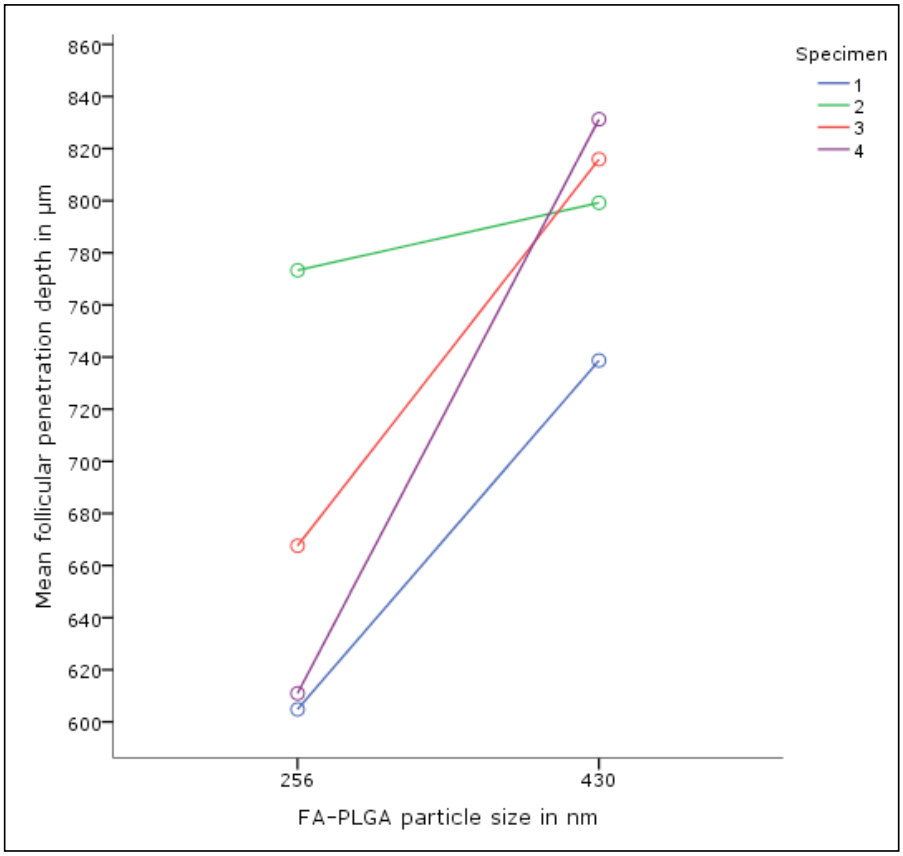

Fig. 18: Comparison between the mean follicular penetration depths of FA-PLGA$_{256}$ and FA-PLGA$_{430}$ within each porcine specimen

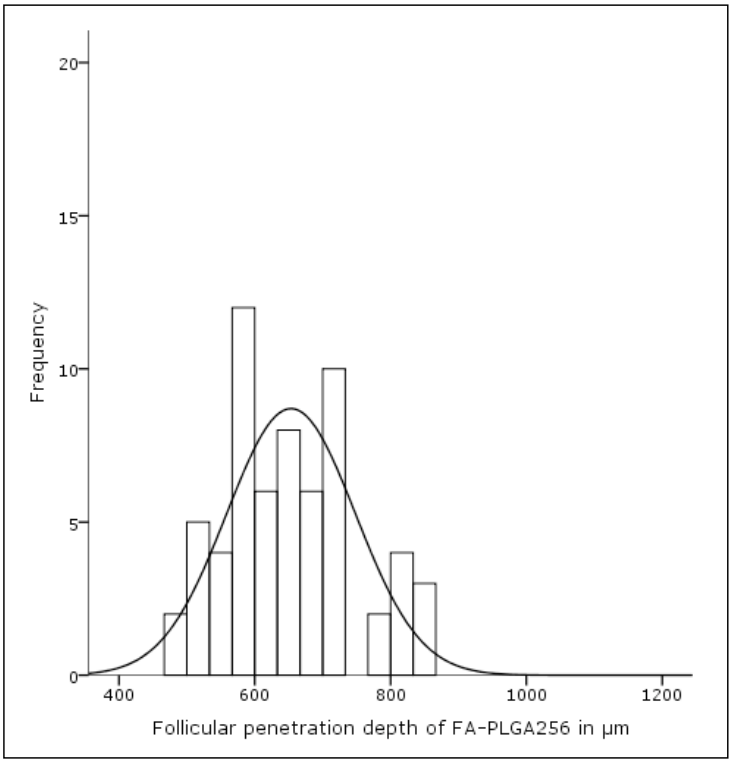

Fig. 19: Frequency distribution and theoretical normal distribution of follicular penetration depths of FA-PLGA$_{256}$ in porcine skin

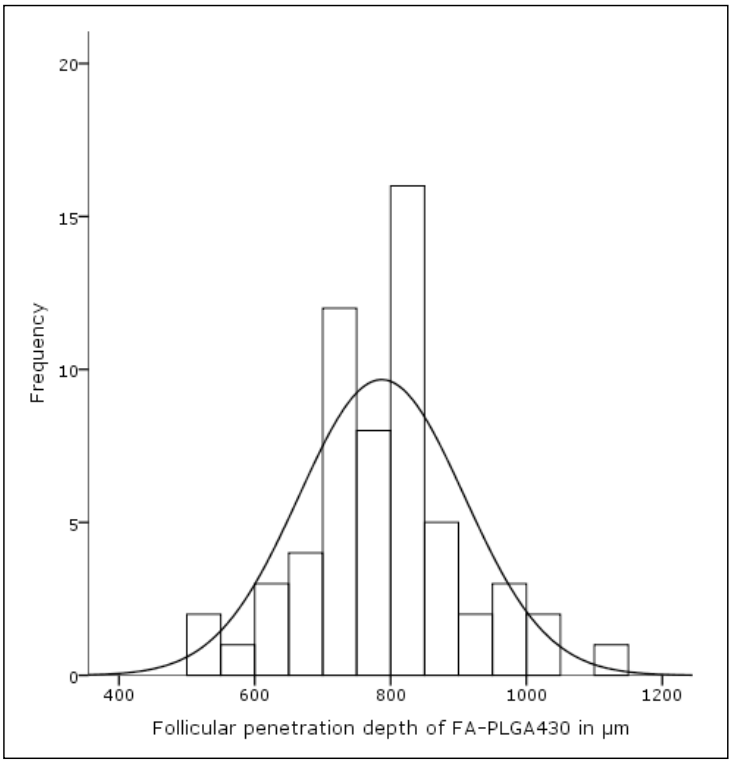

Fig. 20: Frequency distribution and theoretical normal distribution of follicular penetration depths of FA-PLGA$_{430}$ in porcine skin

4.1.4. Comparisons between the follicular penetration of FA-PLGA$_{256}$ and FA-PLGA$_{430}$ in dog, rat and porcine skin

FA-PLGA particles penetrated deepest into the hair follicles of porcine skin, followed by dog and rat skin. FA-PLGA$_{430}$ penetrated to a greater mean follicular depth than FA-PLGA$_{256}$ in porcine and rat skin. In contrast, the mean follicular penetration depth of FA-PLGA$_{256}$ was greater than that of FA-PLGA$_{430}$ in dog skin. FA-PLGA$_{256}$ penetrated to mean follicular depths of 653.40 µm and 630.16 µm in porcine and dog skin, respectively. In contrast, FA-PLGA$_{256}$ penetrated to a mean depth of 253.55 µm in the hair follicles of rat skin. Differences between the mean follicular penetration depths were statistically significant between dog and rat as well as porcine and rat skin ($p \leq 0.05$), but were not statistically significant between dog and porcine skin ($p \geq 0.05$). In porcine skin, FA-PLGA$_{430}$ penetrated to a mean depth of 786.81 µm. This was followed by dog skin, in which FA-PLGA$_{430}$ was found at a mean depth of 604.79 µm. In the rat, FA-PLGA$_{430}$ penetrated to a mean follicular depth of 262.87 µm. Differences between the mean follicular penetration depths of FA-PLGA$_{430}$ were statistically significant between all species ($p \leq 0.05$).

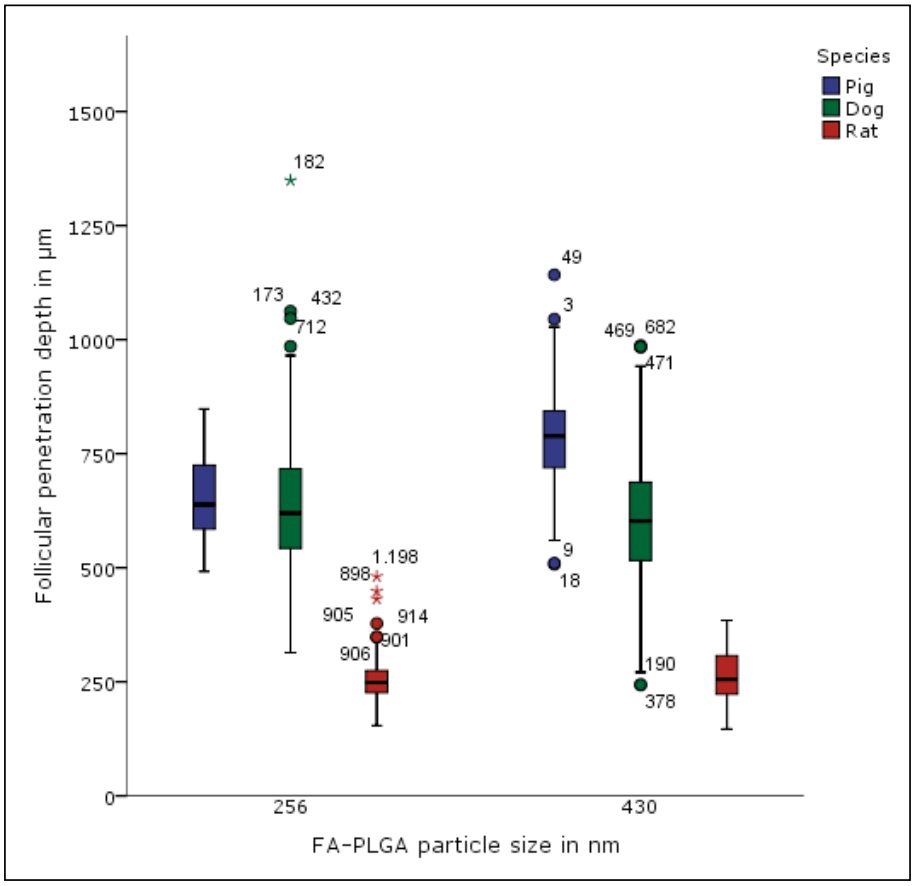

Fig. 21: Boxplot of follicular penetration of FA-PLGA$_{256}$ and FA-PLGA$_{430}$ in dog, rat and porcine skin
Circles: Outliers
Stars: Extreme outliers
Numbers: Observation numbers

4.2. The selective quantification of follicular RhBITC in porcine skin

The amount of topically applied RhBITC found in the hair follicles of porcine ear skin was determined by removing the stratum corneum, and extracting follicular RhBITC from biopsies using ethanol. The fluorescence emitted by the extraction solutions was measured with a fluorescence spectrometer, and quantified on the basis of reference values established with a calibration curve for the intensity of fluorescence emitted by RhBITC. The extraction solutions of the experimental controls were examined for autofluorescence emitted by the skin biopsies at the wavelengths used for excitation of RhBITC.

4.2.1. Fluorescence microscopy

The RhBITC formulation produced a dark red color on the skin samples, which became lighter as tape stripping progressed (Figs. 9-11). After the removal of 80 strips, the dye was visible only in the follicular pores of the stripped regions. Using the transmission mode, cellular components of the horny layer that had attached to the strips could be visualized. The amount of corneocytes on the strips decreased as tape stripping progressed. On the 1st, 10th and 25th strips, large numbers of corneocyte aggregates were present. On the last strips, only individual cells and scattered cell debris could be observed (Figs. 23-25). The fluorescence mode of the BX 60 enabled viewing of the intense red fluorescence emitted by RhBITC. The dye was dispersed throughout the corneocyte matrix that was attached to the first tape strips. Fluorescence decreased significantly by the 25th strips (Figs. 26-28). Isolated spots of fluorescence found on the last strips corresponded to RhBITC located in the follicular orifices, which was verified macroscopically (Fig. 12). These results were consistent for all porcine ear samples treated with the RhBITC formulation. They verified the complete removal of all layers of the stratum corneum as well as the formulation interspersed between its cells.

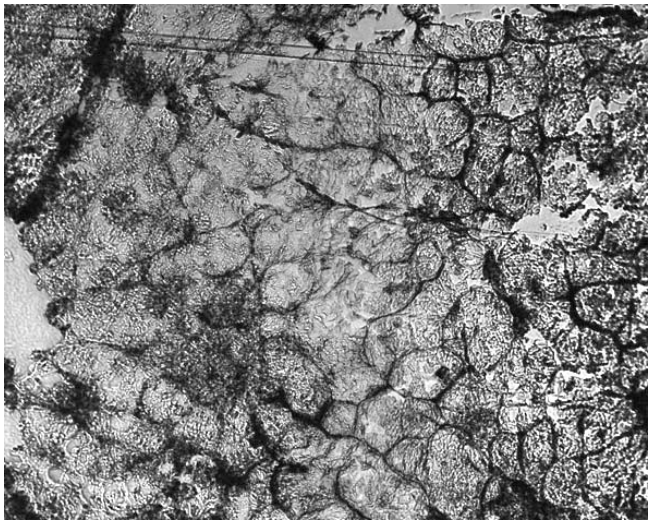

Fig. 22: 1st tape strip of Specimen 1 in the transmission mode (4x)

Fig. 23: 25th tape strip of Specimen 1 in the transmission mode (4x)

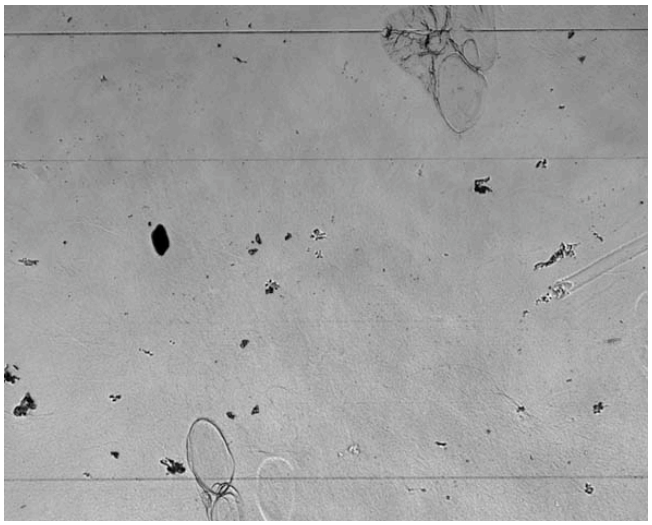

Fig. 24: 80th tape strip of Specimen 1 in the transmission mode (4x)

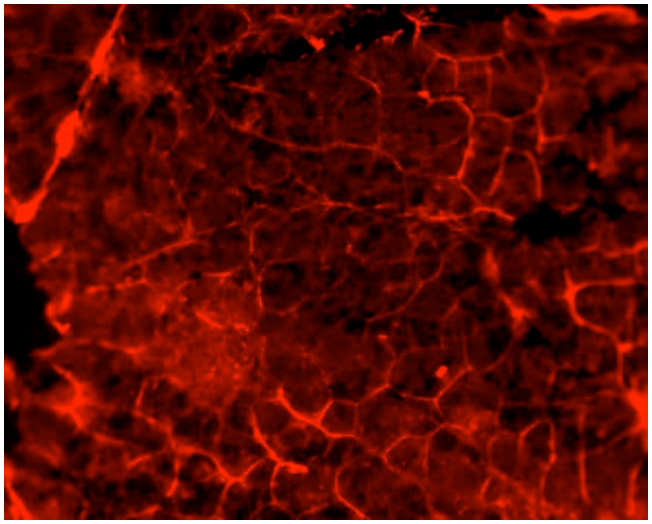

Fig. 25: 1st tape strip of Specimen 1 in the fluorescence mode (4x)

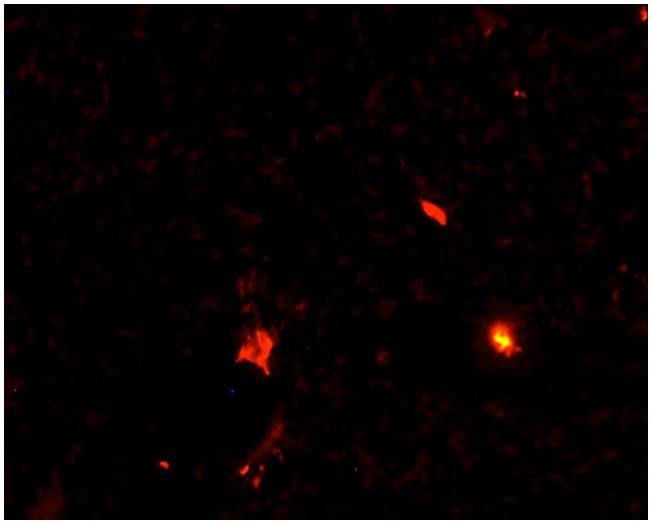

Fig. 26: 25th tape strip of Specimen 1 in the fluorescence mode (4x)

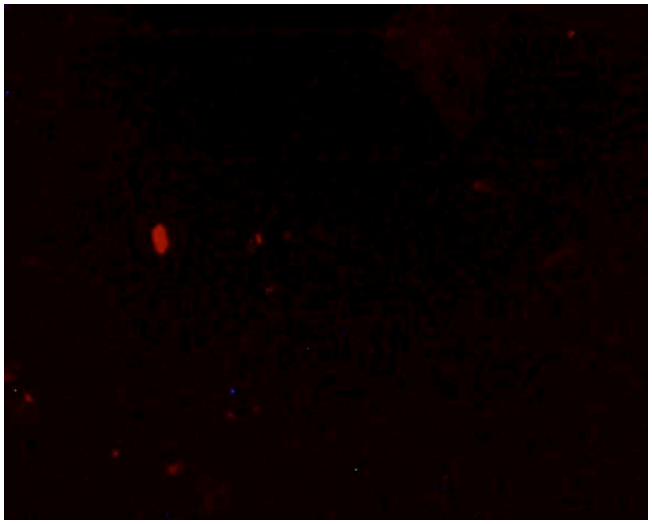

Fig. 27: 80th tape strip of Specimen 1 in the fluorescence mode (4x)

4.2.2. Fluorescence spectroscopy

Known dilution concentrations of RhBITC were plotted against the corresponding fluorescence emissions to produce a calibration curve (Fig. 28), with which to determine the absolute concentrations of RhBITC found in the extraction solutions of the treated and untreated biopsies on the basis of their emitted fluorescence. Using linear regression analysis, the slope of the line was calculated to have a value of 3104. By substituting the variable y with the emission, and solving the equation for x, absolute concentrations of RhBITC in µg were determined, which corresponded to specific relative fluorescence values. The coefficient of determination for the calibration curve was 0.97, indicating that 97% of the variability in the measured fluorescence emissions could be attributed to the concentrations of RhBITC in the extraction solutions.

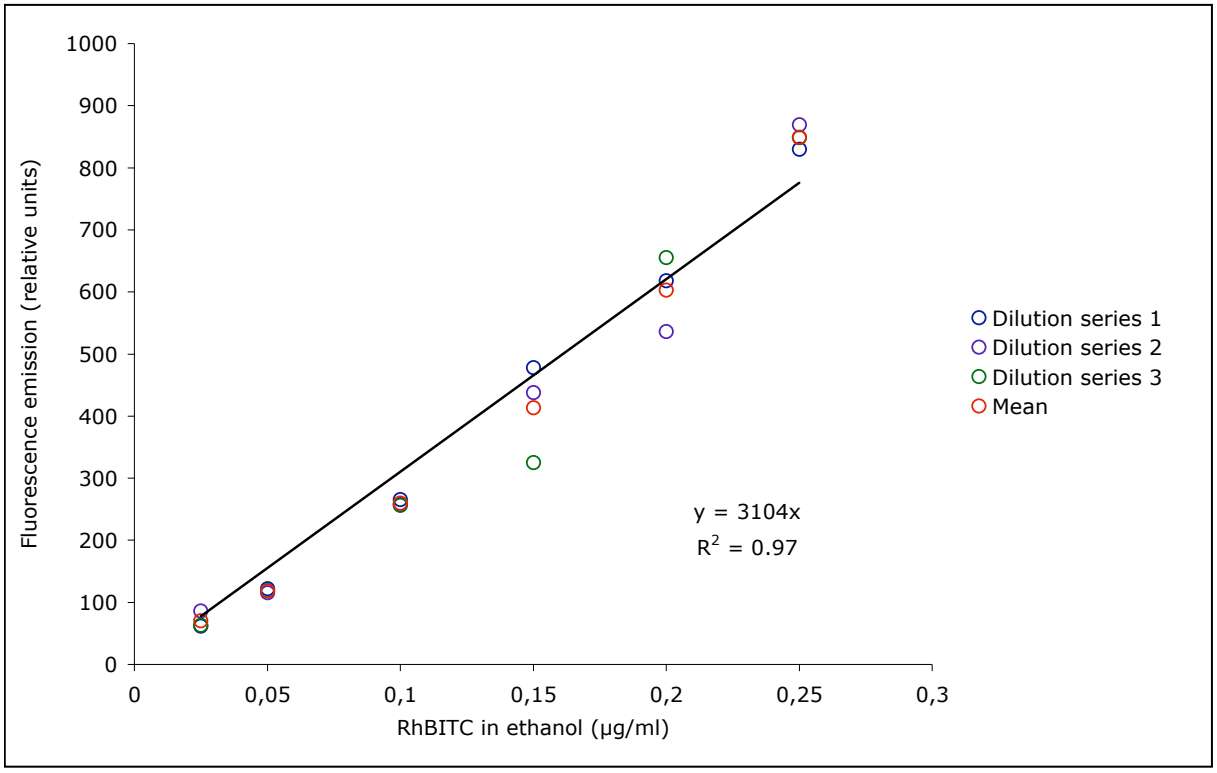

Fig. 28: Calibration curve for RhBITC dilutions in ethanol

Spectroscopic measurements of the extraction solutions yielded graphs for each sample, where fluorescence emissions were plotted against emission wavelengths (Appendix b). The results pertaining to the experimental controls indicated the presence of small amounts of fluorescence in the extraction solutions, which were ascribed to skin fluorophores. Imperfections in the cuvettes and traces of contaminants in the ethanol presumably produced fluorescence in negligible amounts. Subtraction of the fluorescence emissions of the experimental controls ($F_{control}$) from the fluorescence emissions of the experimental samples

(F_{exp}) enabled the determination of the fluorescence emissions which were attributable only to follicular RhBITC ($F_{correct}$) extracted from the skin samples (Tab. 5).

Tab. 5: Corrected fluorescence emission by the experimental samples

Specimen	F_{exp} (relative unit)	$F_{control}$ (relative unit)	$F_{correct}$ (relative unit)
1	366.90	2.93	363.97
2	190.70	2.66	188.04
3	459.00	2.46	456.54
4	462.30	3.04	459.26
5	462.90	4.70	458.20
6	362.40	3.52	358.88
7	221.80	2.61	219.19
8	188.70	2.24	186.46
9	458.80	1.46	457.34
10	518.40	13.00	505.40

F_{exp}: Fluorescence emission of the experimental samples
$F_{control}$: Fluorescence emission of the experimental controls
$F_{correct}$: Corrected fluorescence emission

For each porcine ear, the regression equation was solved for x by substituting the variable y with $F_{correct}$, giving the absolute concentrations of follicular RhBITC in ethanol extracted from the samples in the concentration µg per ml. The cumulative area of the biopsies of each sample (2.95 cm^2) was analogous to the amount of ethanol in which the biopsies were immersed (2.95 ml). The percentage of RhBITC applied to the biopsies, which was subsequently extracted from the hair follicles and detected in the extraction solutions, could therefore be determined using the formula:

$$(Rh_{extract} / Rh_{applied}) \cdot 2.95 \cdot 100 = Rh_{follicular}$$

For all specimens, an average of 5.01 (± 1.86)% of $Rh_{applied}$ was found in the extraction solutions. The values found for all specimens are listed in Tab. 6.

Tab. 6: Overview of RhBITC extracted from the hair follicles of porcine skin

Specimen	$Rh_{applied}$ (µg)	$F_{correct}$ (relative unit)	$Rh_{extract}$ (µg)	$Rh_{follicular}$ (%)
1	7.16	363.97	0.12	4.82
2	7.09	188.04	0.06	2.52
3	6.39	456.54	0.15	6.78
4	8.91	459.26	0.15	4.89
5	8.08	458.20	0.15	5.38
6	5.34	358.88	0.12	6.38
7	8.52	219.19	0.07	2.44
8	6.15	186.46	0.06	2.88
9	6.70	457.34	0.15	6.48
10	6.33	505.40	0.16	7.57

$Rh_{applied}$: RhBITC applied to 2.95 cm^2
$F_{correct}$: Corrected fluorescence emission
$Rh_{extract}$: RhBITC extracted per ml ethanol
$Rh_{follicular}$: $Rh_{applied}$ extracted from the hair follicles

5. Discussion

5.1. Considerations on the follicular penetration of nano-sized particulate FA-PLGA in dog, rat and porcine skin

In this study, the presence of nano-sized FA-PLGA particles in the hair follicles of dog, rat and porcine skin were verified subsequent to topical application using confocal laser scanning microscopy. Statistically significant differences were found between the mean follicular penetration depths of FA-PLGA$_{256}$ and FA-PLGA$_{430}$ in dog and porcine skin. The differences were most pronounced in porcine skin, where the larger particles penetrated to distinctly deeper follicular depths than the smaller particles. However, the small sample size used for this species may limit the validity of this result. In the dog, FA-PLGA$_{256}$ penetrated slightly deeper into the hair follicles than FA-PLGA$_{430}$ on average. Statistically significant differences were not found between the mean follicular penetration depths of FA-PLGA$_{256}$ and FA-PLGA$_{430}$ in the rat. Within individual skin samples, statistically significant differences between the follicular penetration depths of the two particle sizes were found in three of the four porcine specimens, while in the majority of the dog samples, no statistically significant differences were found. The mean follicular penetration depths of FA-PLGA$_{256}$ and FA-PLGA$_{430}$ differed significantly between all examined species, with the exception of values obtained for FA-PLGA$_{256}$ between dog and porcine specimens.

5.1.1. Follicular morphometries and skin constitutions

The relatively high intra- and interindividual standard deviations and the varying values between species can be ascribed to variations in the morphometries of the hair follicles as well as in the skin compositions. These are influenced by the breed, age, sex and housing conditions of the animals from which the skin samples were taken, as well as the body regions from which the skin was sampled (Holbrook & Odland, 1974; Lauer et al., 1995; Lowe & Stoughton, 1977; Meyer, 1986; Meyer, 2009; Nieminen et al., 1967). Prior to their use, all specimens were thoroughly examined, and damaged or visibly diseased skin samples were discarded. For the purposes of this study, variations in the constitutions of the individual samples of a species, pertaining to the dryness of the skin, the hair and hair follicle densities and the hair follicle morphometries, were accepted as within the limits of interindividual variations. In the pig, these variations were most pronounced, as a result of the sparse hairs and large follicles. The breed, age and housing conditions of the animals remained the same for all individuals of one species. Their gender was unknown.

Discussion

Hair coat

The thick and dense fur coat found in some animals represents the first barrier against topically applied substances, as some drugs may physically bind to hair and prevent absorption into the skin (Rivière & Papich, 2001). This is of special interest for patients with dermatological disorders in which the hair coat is damaged (Walters & Roberts, 1993). Jung et al. (2006) for example observed that topically applied liposomes adhered to hair shafts, slowing penetration, and simultaneously decelerating the flushing out of the particles from the follicular canal by sebum. Marzulli et al. (1969) and Tregear (1966) however reported high follicular densities to correlate positively with overall skin penetration. This may be explained by the attenuated interfollicular epidermis found in densely haired skin (Rivière & Papich, 2001). In the skin of dogs, hair follicles are commonly arranged in groups, with a total of 1500 to 4000 hairs per cm^2 skin (Mangelsdorf, 2007). The central primary hair follicles are often flanked by several lateral primary or secondary hair follicles (Meyer, 2009). Hair thickness averages at 75 µm across breeds, although individual values vary significantly (Sato et al., 2006). As the skin is relatively thin in dogs, their primary hair follicles often project into the hypodermal fat reservoir, with an insertion depth varying between 400 and 1200 µm (Meyer, 2009). Rats are more densely haired with 5000 to 8000 hairs in individual follicles per cm^2 (Mangelsdorf, 2007), reaching lengths of 550 µm (Stahl, 2007). Reports on hair thickness range from 45 to 150 µm (Meyer et al., 2002a). Strong bristles with a mean diameter of 95 µm dominate in primary follicles in the pig, with a density between 10 to 40 per cm^2 skin (Mangelsdorf, 2007), while short secondary hairs are inconspicuous and not found in modern breeds. The primary hair follicles are fixated at depths ranging between 3000 and 5300 µm below the skin surface, with hair roots crossing the entire dermis and bulbs anchoring the hypodermis between fat cells (Meyer, 2009). To minimize substance loss, the hairs and bristles of the skin samples used in this study were shortened to a length of 1 to 2 mm with scissors. They were not shaved with a razor so as to avoid damage to the skin surface. In spite of the shortening of the hairs, small amounts of the formulation presumably remained bound to them, particularly in the densely haired dog and rat specimens.

'Active' and 'inactive' hair follicles

Lademann et al. (2001) proposed the concept of 'active' and 'inactive' hair follicles. While 'active' hair follicles receptive to penetration demonstrate hair growth and sebum production, 'inactive' follicles are in the telogen phase of their hair cycle, and thus unreceptive to penetration. The 'inactive' hair follicles are covered by a crust of desquamated corneocytes, dry sebum and other cell detritus, that further impedes penetration (Otberg et al., 2004). This is consistent with results found in this study, where 30 to 40% of the hair follicles did not show fluorescence.

Follicular orifices and infundibula

Reflective of the known morphometries of dog, rat and porcine hair follicles, it can be reasoned that the dimensions of the follicular openings and infundibula are critical for predicting the follicular penetration depths of particulate formulations. The FA-PLGA particles submerged in cellulose gel entered and traversed the hair follicles by the mechanical effect of the massage during application of the formulations to the skin. The external, standardized pressure combined with the vibrational action of the massage applicator presumably pressed the fluorescing particles into the follicular orifices, filling the follicular infundibula. The amount of particulate gel able to enter into the follicular canal and to fill the infundibulum at a given time seemed to correspond to the diameter of the hair follicle openings, as well as the length of the infundibula. The orifices of the hair follicles in the dog have a mean diameter of 155 µm and cover more than 7% of the skin surface. The follicular infundibula, which range from the follicular openings to the orifices of the sebaceous glands, have a length of 225 µm. The follicular orifices of the rat constitute about 2% of the skin surface and have a mean diameter of 38 µm. The infundibula extend 113 µm into the skin. In pigs, approximately 1% of the skin surface is comprised of hair follicles. Their openings are 200 µm in diameter, from which the infundibula reach a length of more than 500 µm (Mangelsdorf, 2007). Based on these measurements, the follicular orifices are widest in porcine skin, followed by dog and rat skin, respectively. The hair follicle infundibula extend deepest into the skin of the pig. In the dog, they reach approximately half, and in the rat, about one-fourth the length of the infundibula found in porcine hair follicles. This corresponds to the results of this study which evidenced that FA-PLGA$_{256}$ and FA-PLGA$_{430}$ penetrated deepest into porcine hair follicles, and least deep into the hair follicles of the rat. By fully saturating the infundibula with test formulation during massage application, the likelihood is increased that particles will be pushed further down into the follicular canal. In all examined species, the FA-PLGA particles penetrated below the follicular infundibula. Relative to the species-specific lengths of the infundibula, they penetrated deepest in the dog, and least far in the pig. As a continuous stream of sebum reaches the follicular infundibulum from the outlet of the sebaceous glands and protrudes to the follicular openings on the skin surface, particles that penetrate below this confluence are presumably no longer flushed out by sebum. Penetration beyond the infundibulum is especially desirable for nano-sized particles intended to act systemically by delivering drugs to immune cells surrounding the hair follicles or to their capillary networks. Considering the chemical environment of the sebum-filled follicular canal, such particles situated deeply in the hair follicles are soon likely to be subjected to degradation, releasing their drugs upon breakdown (Lauer et al., 1995).

On account of the comparatively large dimensions, it can be assumed that the nano-sizes of the FA-PLGA particles do not have a significant effect on follicular penetration in the

infundibular region. Below the infundibulum, however, the follicular canal becomes greatly attenuated and their nano-sizes may become relevant to the follicular penetration process. The follicular sheath is lined with overlapping, cuticular cells that interlock with the cuticles on the hair shaft, fixating the hair in the epidermis. This is confirmed by the fact that forcible plucking of an intact terminal anagen hair reveals the outer root sheath coating the pigmented shaft and the inner root sheath, that is closely apposed to the shaft and lying just within the outer root sheath, and not merely the naked hair shaft (Sperling, 1991). Lademann et al. (2007) proposed that nano-sized particles pushed into the follicular canal by massage action move along the cleft between the cuticular lock, the efficacy of which is believed to correspond to the size of the particles as well as the dimensions of the cuticular cells.

Tab. 7: Overview of the skin and hair follicle parameters in dog, rat and porcine skin (Mangelsdorf, 2007; Meyer et al., 2002a; Sato, et al., 2006; Stahl, 2007)

Skin and hair follicle parameters	Dog	Rat	Pig
Number of hairs per cm^2 of skin	1500-4000	5000-8000	10-40
Follicular openings in % of skin	~ 7%	~ 2%	~ 1%
Diameter of hair follicle openings	155 µm	38 µm	200 µm
Mean diameter of the hair shaft	75 µm	45-150 µm	95 µm
Length of hair follicle infundibula	225 µm	113 µm	> 500 µm
Insertion depth of hair follicles in skin	400-1200 µm	550 µm	3000-5300 µm

Sebaceous glands

The sebaceous glands are implicated in the etiology of acne (Thiboutot, 2004) and androgenetic alopecia (Meidan & Touitou, 2001), as well as other sebaceous gland dysfunctions in humans, and thus represent obvious sites for follicular targeting. Considerable effort has been directed towards maximizing the accumulation of various molecules into these glands, including adapalene (Rolland et al., 1993), an erythromycin-zinc complex (Morgan et al., 1993), isotretinoin (Tschan et al., 1997) and anti-androgen RU58841 (Bernard et al., 1997; Münster et al., 2005). Liposomes carrying entrapped compounds accumulated preferentially in the sebaceous glands (Bernard et al., 1997). Although the process of sebum synthesis and secretion on the skin surface is slow (Downing et al., 1975), the upward flowing sebum may

pose a physical as well as a chemical barrier for drug penetration (Lauer et al., 1996; Singh et al., 2000). At the same time, sebum may serve as a vehicle for drugs which are soluble in it (Illel, 1997; Rivière & Papich, 2001). Interspecial variations in the sebum composition must be considered in this context (Mangelsdorf, 2007).

Bulge region

The bulge region in the outer root sheath near the insertion of the M. arrector pili is known to be a reservoir for keratinocyte stem cells in humans and rodents (Claudinot et al., 2005; Cotsarelis et al., 1990; Lyle, et al., 1998; Morris & Potten, 1999; Ohyama et al., 2006; Oshima et al., 2001; Taylor et al., 2000), responsible for the reconstitution of the hair follicles during hair regeneration (Ohyama, 2007). Cultured and individually cloned bulge cells from adult mice were shown to form hair follicles in skin reconstitution assays (Blanpain et al., 2004). Hair follicle stem cells from adult mice formed hair follicles after injection into immunodeficient mice, when combined with neonatal dermal cells (Blanpain et al., 2004; Morris et al., 2004). Results from Taylor et al. (2000) indicate that hair follicle stem cells can give rise not only to hair follicle cells, but also to epidermal cells. Oshima et al. (2001) suggested that the upper outer root sheath of whisker follicles of adult mice contain multipotent stem cells, which can differentiate into hair follicle matrix cells, sebaceous gland basal cells and epidermis. Ito et al. (2005) and Levy et al. (2005) recently elucidated that they contribute to wound repair but do not contribute to the normal epidermis homeostasis in non-wounded skin. Toma et al. (2001) demonstrated that multipotent adult stem cells isolated from the mammalian dermis can proliferate and differentiate into neurons, glia, smooth muscle cells and adipocytes in culture. Hoffman (2007) similarly showed that hair follicle stem cells differentiated into neurons, glia, keratinocytes, smooth muscle cells and melanocytes in vitro. In vivo studies indicated that hair follicle stem cells can differentiate into blood vessels and neural tissue after transplantation into the subcutis of nude mice. Furthermore, it was found that hair follicle stem cells implanted into the gap region of a severed or sciatic tibial nerve greatly enhanced the rate of nerve regeneration and the restoration of nerve function. The follicle cells predominantly transdifferentiated into Schwann cells, which support neuron regrowth. Nishimura et al. (2005) proclaimed that the exhaustion or incomplete maintenance of the melanocyte stem cell supply from the bulge region results in the loss of hair shaft pigmentation, as well as in grey hairs. Other cells such as Merkel cells (Narisawa et al., 1993) and Langerhans cells (Moresi & Horn, 1997) can also be found in the bulge region, signifying the importance of the bulge in the homeostasis of the skin (Ohyama, 2007). In light of these results, bulge cells have attracted attention as a stem cell source for cutaneous regenerative medicine. One goal is to treat alopecia with new hair follicles bioengineered from the bulge cells of patients (Stenn & Cotsarelis, 2005). Gene delivery to specific bulge stem cells may possibly facilitate long-term gene correction of congenital hair diseases (Ohyama & Vogel,

2003). In addition, as the bulge cells are able to repopulate the interfollicular epidermis, targeting of cells by gene transfer is considered to be a promising approach for the treatment of genetic skin disorders (Ohyama & Vogel, 2003; Sugiyama-Nakagiri et al., 2006). Additional desirable targets include the follicular papilla and the hair matrix cells, which are situated at the base of the follicle (Meidan et al., 2005).

Tight junctions

Tight junctions are regions of intimate contacts between the plasma membranes of two neighboring cells without any intermembranous material or intercellular gaps, which functionally provide hydrophobic barriers and prevent paracellular diffusion of water and solutes. Brandner et al. (2003) found evidence for their presence in the cell layers facing the hair shaft and the stratum corneum as well as the border between the outer and inner root sheaths in the hair follicles of human scalp skin. The junctional system in the hair follicles has been suggested to provide architectural stability to mechanically challenged skin and to contribute to the maintenance the skin barrier. The cell layers strongly positive for tight junction proteins represent the border with the environment and the first viable cells contacted by substances penetrating via the hair follicles, and may therefore be selective in substances they allow to penetrate. Furuse et al. (2002) for example demonstrated a tremendous increase in transepidermal water loss in claudin-1 knockout mice, a tight junction-associated protein, resulting in the death of the mice on their first day after birth.

Capillary network

The interface between the site of topical application and the systemic circulation is approximately 100 µm in humans. A perifollicular network of capillaries associated with the upper dermal vasculature supplies the upper region of the hair follicles with blood. The blood vessels of the deep dermis and the subcutaneous tissue nourish the lower region of the hair follicles (Ryan, 1983). A dense network of capillaries also surrounds the sweat glands (Schäfer & Redelmeier, 1996). Depending on the thermoregulatory status, dermal perfusion has been estimated to change by a factor of 100 (Rivière & Papich, 2001). Noteworthy differences exist in the morphology of the capillary networks between species. In dogs, for example, the vascularization of the hair follicles is much more pronounced than in the pig (Kristensen, 1975). Topically applied substances that reach the cutaneous vasculature generally permeate into the central circulatory system. This results in rapid dilution (Schäfer & Redelmeier, 1996) and dispersion of the applied substances within the entire circulatory system (Lauer et al., 1996). For certain substances, modulation of the dermal perfusion has been reported to alter drug delivery. Vasoconstriction decreased dermal perfusion and trapped drugs that had penetrated the epidermal barrier, thus decreasing the systemic absorption but

enhancing the local activity. Vasodilatation in contrast promoted systemic delivery but minimized local accumulation of the substances (Rivière & Papich, 2001).

5.1.2. Characteristics of the particulates

Size

While it has been established that nano-sized particles permeate the skin by penetrating into the follicular canals, their specific mechanisms of action are speculative at best, and remain to be elucidated. FA-PLGA$_{256}$ and FA-PLGA$_{430}$ used in this study differed solely in the size of their FA-PLGA particles. Therefore, on the basis of the obtained results, no clear trends can be substantiated which suggest that the size of the FA-PLGA particles markedly influenced their penetration into the hair follicles of the examined species.

Aggregation

Due to the high energetic adhesive forces close to their surface, nano-sized particles bear the potential risk of agglomerating to their neighbors, adhering to surfaces or adsorbing to other molecules (Borm et al., 2006), leading to altered penetration behavior. Using confocal microscopy, De and Robinson (2004) showed that after storage at 37° C for 6 days, nano-sized PLGA particles marked with the fluorescent dye Biodipy had aggregated significantly. No aggregation however was observed after the particles were stored at 4° C for 6 days, indicating that it is crucial to maintain this temperature during storage to avoid irreversible aggregation. Furthermore, the extent of aggregation of PLGA particles stored at 37° C decreased as the particle size of the delivery system increased from 300 to 2000 nm. To ensure that aggregation of the FA-PLGA particles used in this study was minimized, the particulate formulations were kept at a temperature of 4° C at all times prior to the experiments.

Degradation

Nano-sized PLGA particles have been reported to have a shelf-life of more than 3 months (Feng & Huang, 2001). Weiss et al. (2006) studied the degradation of nano-sized particulate FA-PLGA by incubating the nanoparticles in PBS at 37° C over a course of 15 weeks. Immediately after their preparation, the particles were of a spherical shape and had a smooth surface without any visible pores. After 1 week, first pittings could be seen on the surface of the particles. This effect progressed until week 3, during which the particles were observed to develop a porous outer appearance. The depth of these indentations increased until week 7, although their number did not rise. In week 15, the particles did not appear as porous as

before, possibly due to a swelling process which resulted in a smoothening of the surface. During this process, the mean particle size did not change notably. Specifically in the lipid-rich environment of the follicular ducts, Borm et al. (2006) reported nano-sized PLGA particles to be stable over the course of several days. The FA-PLGA particles used in this study were applied to the skin samples within 10 days of their preparation.

Leakage of fluoresceinamine

Nano-sized FA-PLGA particles demonstrate a stable association between the particles and the marker. After an initial burst effect resulting in the loss of approximately 12% of the fluorescent marker, more than 60% of the fluoresceinamine was still bound to particles sized 270 nm after 8 days of incubation in PBS at 37° C (Weiss et al., 2006). As the particles implemented in this study were applied to the skin samples within 10 days of their preparation, it is surmised that detectable amounts of fluoresceinamine remained bound to the particles at the time of the experiments.

Risks and toxicity

In companion and farm animals, the topical application of particulate formulations to the skin bears the specific risk of unintentional uptake by ingestion or contact with the mucous membranes of the eyes as a result of licking, biting or itching of the treated skin, as well as to a lesser extent by inhalation through sniffing. Ingestion can result in systemic uptake via the lymph. Once in the blood circulation, nano-sized particles can be distributed throughout the organism, and be taken up by the liver, spleen, bone marrow, heart and other organs. Access to the central nervous system and ganglia via translocation along axons and dendrites of neurons has been observed (Oberdörster et al., 2005). Recently, specific concerns have been raised about the potential of topically applied nano-sized particles to penetrate the skin (Hoet et al., 2004; Oberdörster et al., 2005). Some evidence exists that particles smaller than 10 nm can be taken up by lymphatic nodes at the skin level, and translocate to the circulatory system via lymphatic pathways (Kim et al., 2004). There is, however, no conclusive evidence that intact nano-sized particles 20 nm and larger can permeate into viable tissue (Alvarez-Román et al., 2004b; Lekki et al., 2007). In damaged or diseased skin, the stratum corneum is often ruptured, reducing its barrier function and thereby leading to increased skin penetration (Nohynek et al., 2008). Here, particular concerns must be raised. Tinkle et al. (2003) demonstrated that in conjunction with flexed skin, fine beryllium particles penetrated the stratum corneum and lodged in the epidermis, which led to a murine beryllium-specific, cell-mediated immune response. Podoconiosis has been ascribed to soil particles sized 400 to 500 nm, which are driven through the soles of the feet of individuals who walk barefoot. The particles were observed in the femoral and inguinal lymph nodes of patients (Blundell et al.,

1989). In psoriatic skin, the stratum corneum thickness increases to about 100 µm, and comprises corneocytes as well as vital keratinocytes, such that TiO_2 particles were found to come into direct contact with living cells. Systemic uptake was not observed (NANODERM, 2007).

The toxicity of insoluble and inert nano-sized particles corresponds to their cellular uptake through the phagocytotic capacity of the treated cells. Phagocytosis of non-degradable particles results in oxidative cell damage, inhibition of cell proliferation, cytotoxicity, and the release of inflammatory factors into the surroundings of the cell (Nohynek et al., 2008). Biodegradable particulates such as PLGA generally decompose into their individual constituents once the pharmacologically active agent is released from their core or surface soon after application. Toxicologically harmful effects to patients are therefore not expected to differ from particles of the same substance but of a larger size (Greßler et al., 2009). For the specific use of particulate FA-PLGA in biological systems, it is pivotal to obtain sufficient fluorescence signals at particle concentrations well below the level that causes any cytotoxic effects. Weiss et al. (2006) assayed nano-sized FA-PLGA on human intestinal epithelial cells for the specific risk assessment of their potential cytotoxic effects. The half maximal inhibitory concentration was in the same order as found for pure nano-sized PLGA, which is known for its excellent biocompatibility. With respect to possible absorption of FA-PLGA particles from the lumen of the intestine, results indicated that only the degradation products were transported across the intestinal epithelial barrier.

5.1.3. Future outlook on the follicular penetration of nano-sized particulates in animals relevant for veterinary practitioners

Clinical concerns in veterinary practice are becoming increasingly similar to those of human medicine (Rathbone & Martinez, 2002). The number and diversity of animals being cared for and the corresponding anatomical and physiological differences have created a vast market for innovative treatment options and veterinary spin-offs from human pharmaceuticals. Therapy regimens which are painless, simple to carry out and cost-effective are of key importance in the successful treatment of veterinary patients. Cremes, gels and spot-on treatments which are applied topically are therefore widespread in veterinary practices (Mills & Cross, 2006). The implementation of particulate drug delivery systems in such formulations is still insubstantial however. Only few particulates are commercially available for veterinary use, most of which are based on the injection of microparticles smaller than 200 µm into subcutaneous or muscle tissue (Johnson & Thompson, 1999; Miller et al., 1998; Rock et al., 2000). In spite of the abundance of follicular target structures and the comparatively large follicular reservoir in most companion and farm animals (Mangelsdorf, 2007), follicular

targeting using nano-sized particles smaller than 1 µm has thus far only been studied in a number of animal models and in humans. The fundamental research on the follicular penetration of particulates conducted in this work illustrates the potential for follicular targeting in animals, which in the future may include the treatment of skin diseases, hair follicle-associated disorders and the stimulation of systemic effects such as by targeting of follicular immune cells or blood vessels. It remains the subject of future research to further elucidate variances in follicular morphometries and skin compositions between individuals as well as the factors influencing them. This in consequence will enable the customized production of nano-sized particulates for follicular drug delivery in the diversity of veterinary patients.

5.2. Considerations on the selective quantification of follicular RhBITC in porcine skin

In this study, the established procedure of differential stripping was modified to enable the selective quantification of the dye RhBITC located in the follicular canals of porcine skin subsequent to topical application. RhBITC was implemented as a model drug. On average, 5% of the dye administered to the skin was detected in the follicular extraction solutions of the skin samples. This is in accordance with a study by Teichmann et al. (2005), in which 5% of topically applied sodium fluorescein was extracted from the follicular casts of human subjects by differential stripping.

5.2.1. Porcine skin as an in vitro model for the human integument

Porcine skin, which can be easily obtained as waste from slaughtered animals (Barbero & Frasch, 2009), has histological and physiological features that are analogous to human skin (Dick & Scott, 1992; Hawkins & Reifenrath, 1986; Jacobi et al., 2007; Meyer, 1996; Meyer et al., 2007) and similar permeability properties (Frum et al., 2008). It is is often utilised to replace human skin in studies on transdermal drug transport (Bronaugh, 1989), as excised human skin of sufficient quality and size is not readily accessible and only available in limited amounts (Schmook et al., 2001). Furthermore, considerable variety exists among human samples due to differences in gender, race, age and the anatomical site of sample excision (Barbero & Frasch, 2009). In humans, approximately 500 to 1000 hairs per cm^2 are found on the scalp and face with each follicular opening exhibiting a diameter of 50 to 100 µm. The combined areas of their follicular openings constitute as much as 10% of the skin surface (Meidan et al., 2005). In other parts of the body, such as the calf, an average of 14 hairs per

cm^2 can be found. Here the hair follicles represent only 0.1% of the skin surface (Schäfer & Redelmeier, 1996). Hair shaft diameters vary between 16 and 42 µm (Wosicka & Cal, 2010).

5.2.2. Methodology

The porcine ears used in this study belonged to animals of the same cross-breed, age and keeping conditions. The gender corresponding to the specimens was unknown. Visibly diseased, injured or scarred skin samples were discarded prior to the experiments, to avoid falsification of the results. Variations in their skin surface compositions, follicular densities, morphometries and sebum contents, as well as in the dryness of the skin samples were accepted as within the limits of interindividual variations for the purposes of this study. To maintain its stability, RhBITC was stored at conditions excluding light throughout the duration of the experiments, with the exception of the preparation of the dilution series and the application procedure. The homogenous distributions of RhBITC within the hydroxyethylcellulose gel and of the RhBITC formulation on the test areas were ensured by the slow stirring of RhBITC into the gel for a period of 3 minutes, as well as by the standardized massage application, respectively. To avoid contaminations of the skin with excess RhBITC, each strip was covered with a piece of paper before being pressed onto the skin. Using a roller to press the tape strips onto the skin with standardized pressure ensured the removal of the dye from the furrows and wrinkles of the skin as well as of dye adhering to the bristles. Three dilution series were prepared for RhBITC to increase the accuracy of the calculations performed on the basis of the calibration curve to quantify RhBITC in the extraction solutions. Separation of the skin biopsies from the extraction solutions containing follicular RhBITC subsequent to the ultrasonic treatments was achieved by centrifugation.

5.2.3. Future outlook on the selective quantification of drugs located in the follicular canals of porcine skin

For follicular penetration experiments, excised porcine ear skin is a particularly suitable alternative to human skin, as its follicular reservoir capacity corresponds to that of living human skin. In human ex vivo skin, the follicular reservoir is diminished to 9.5% of the in vivo hair follicle reservoir as a result of the contraction of the elastic fibers surrounding the hair follicles during excision from the donor, as well as the sudden absence of blood flow and loss of hydration (Patzelt et al., 2008). Porcine ear skin maintains a constant follicular reservoir as the skin is fixed on an underlying cartilage, and does not contract upon removal of the ears from the carcass (Lademann et al., 2009). Thus far, its implementation in follicular penetration studies as a model for human skin has been limited however. The method of

differential stripping, commonly implemented in follicular penetration studies, is not applicable to porcine skin as the removal of cyanoacrylate follicular biopsies produces tears in the cyanoacrylate, falsifying results. The quantification of follicular contents is crucial for questions pertaining to drug administration, concentrations and dosages, and alternative, drug-specific procedures are therefore necessary for the quantification of follicular contents in porcine skin. In this study, the dye RhBITC was implemented as a model drug and extracted from the hair follicles of porcine skin on the preconditions of its solubility in ethanol as well as the detection of its fluorescence emission using fluorescence spectrometry. Additional research aimed at methodological optimizations and modifications is needed to ensure the successful applicability of this procedure for a wide range of topical drugs.

6. Appendix

6.1. Appendix a: Descriptive statistics

6.1.1. Dog skin

Tab. 8: Descriptive statistics of the follicular penetration of nano-sized particulate FA-PLGA in dog skin

Specimen	Particles	N	Mean follicular penetration depth (µm) (± SD)	Min	Median	Max
1	FA-PLGA$_{256}$	31	674.40 (± 193.93)	400.10	679.00	1349.00
	FA-PLGA$_{430}$	30	606.67 (± 124.98)	361.00	612.60	846.00
2	FA-PLGA$_{256}$	31	582.42 (± 90.43)	370.50	589.00	728.80
	FA-PLGA$_{430}$	71	571.15 (± 134.34)	243.10	592.50	795.70
3	FA-PLGA$_{256}$	43	521.90 (± 114.00)	313.80	526.40	781.80
	FA-PLGA$_{430}$	43	494.85 (± 104.23)	300.90	467.60	695.60
4	FA-PLGA$_{256}$	37	695.13 (± 128.00)	421.70	709.10	1046.70
	FA-PLGA$_{430}$	37	614.15 (± 132.70)	243.90	641.10	866.60
5	FA-PLGA$_{256}$	23	648.61 (± 121.79)	445.80	690.50	860.10
	FA-PLGA$_{430}$	29	661.06 (± 189.94)	369.60	657.70	987.20
6	FA-PLGA$_{256}$	39	547.94 (± 67.42)	400.80	557.60	696.00
	FA-PLGA$_{430}$	43	609.81 (± 89.09)	442.70	594.90	783.10
7	FA-PLGA$_{256}$	43	647.47 (± 126.78)	400.70	633.90	948.50
	FA-PLGA$_{430}$	41	603.88 (± 87.31)	437.70	597.50	792.50
8	FA-PLGA$_{256}$	32	743.57 (± 110.44)	569.30	744.20	985.10
	FA-PLGA$_{430}$	33	717.02 (± 125.54)	389.40	730.30	984.40
9	FA-PLGA$_{256}$	41	686.40 (± 108.18)	496.00	698.20	965.00
	FA-PLGA$_{430}$	44	637.77 (± 117.42)	429.60	616.00	887.00
10	FA-PLGA$_{256}$	42	593.58 (± 104.68)	411.60	609.90	823.90
	FA-PLGA$_{430}$	43	598.91 (± 112.15)	408.80	580.20	850.50
$\overline{x}$	FA-PLGA$_{256}$	362	630.16 (± 135.75)	313.80	619.40	1349.00
	FA-PLGA$_{430}$	414	604.79 (± 132.42)	243.10	602.50	987.20

N: Sample size
(± SD): Plus-minus standard deviation
Min: Minimum
Max: Maximum
$\overline{x}$: Total mean follicular penetration depth

6.1.2. Rat skin

Tab. 9: Descriptive statistics of the follicular penetration of nano-sized particulate FA-PLGA in rat skin

Specimen	Particles	N	Mean follicular penetration depth (µm) (± SD)	Min	Median	Max
1	FA-PLGA$_{256}$	22	303.15 (± 58.71)	228.20	293.00	448.50
2	FA-PLGA$_{256}$	22	223.1 (± 39.20)	166.10	220.10	305.60
3	FA-PLGA$_{256}$	20	234.44 (± 26.07)	195.60	235.90	295.30
4	FA-PLGA$_{430}$	26	260.35 (± 55.64)	173.10	253.80	374.70
5	FA-PLGA$_{430}$	26	293.75 (± 39.60)	240.80	291.70	368.60
6	FA-PLGA$_{430}$	25	285.06 (± 59.75)	173.00	299.40	384.70
7	FA-PLGA$_{256}$	23	248.59 (± 31.58)	199.70	251.90	321.80
8	FA-PLGA$_{256}$	22	251.32 (± 53.64)	160.40	239.30	341.50
9	FA-PLGA$_{256}$	26	254.77 (± 32.07)	198.50	254.30	331.90
10	FA-PLGA$_{430}$	26	288.95 (± 38.93)	229.00	294.50	366.70
11	FA-PLGA$_{430}$	26	236.92 (± 51.46)	166.70	227.10	355.70
12	FA-PLGA$_{430}$	26	213.06 (± 32.75)	146.40	217.80	280.60
13	FA-PLGA$_{256}$	26	268.81 (± 52.00)	200.80	267.70	481.00
14	FA-PLGA$_{256}$	27	242.26 (± 36.25)	154.00	247.50	311.00
$\overline{x}$	FA-PLGA$_{256}$	188	253.55 (± 47.36)	154.00	248.60	481.00
	FA-PLGA$_{430}$	155	262.87 (± 55.25)	146.40	255.40	384.70

N: Sample size
(± SD): Plus-minus standard deviation
Min: Minimum
Max: Maximum
$\overline{x}$: Total mean follicular penetration depth

6.1.3. Porcine skin

Tab. 10: Descriptive statistics of the follicular penetration of nano-sized particulate FA-PLGA in porcine skin

Specimen	Particles	N	Mean follicular penetration depth (µm) (± SD)	Min	Median	Max
1	FA-PLGA$_{256}$	19	604.84 (± 63.60)	492.00	589.00	726.00
	FA-PLGA$_{430}$	22	738.68 (± 136.40)	508.00	733.50	1045.00
2	FA-PLGA$_{256}$	11	773.27 (± 68.14)	640.00	770.00	848.00
	FA-PLGA$_{430}$	13	799.23 (± 131.81)	619.00	782.00	1142.00
3	FA-PLGA$_{256}$	17	667.59 (± 96.06)	515.00	696.00	813.00
	FA-PLGA$_{430}$	11	815.91 (± 83.11)	716.00	836.00	990.00
4	FA-PLGA$_{256}$	15	610.93 (± 57.89)	527.00	600.00	708.00
	FA-PLGA$_{430}$	13	831.23 (± 92.78)	700.00	814.00	1028.00
$\overline{x}$	FA-PLGA$_{256}$	62	653.40 (± 94.71)	492.00	638.50	848.00
	FA-PLGA$_{430}$	59	786.81 (± 121.73)	508.00	789.00	1142.00

N: Sample size
(± SD): Plus-minus standard deviation
Min: Minimum
Max: Maximum
$\overline{x}$: Total mean follicular penetration depth

6.2. Appendix b : Fluorescence emission of follicular RhBITC

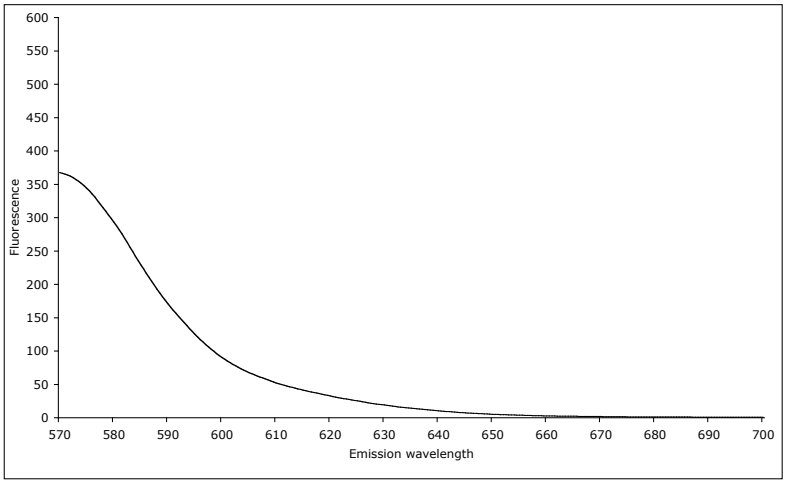

Fig. 29: Fluorescence emission of follicular RhBITC in Specimen 1

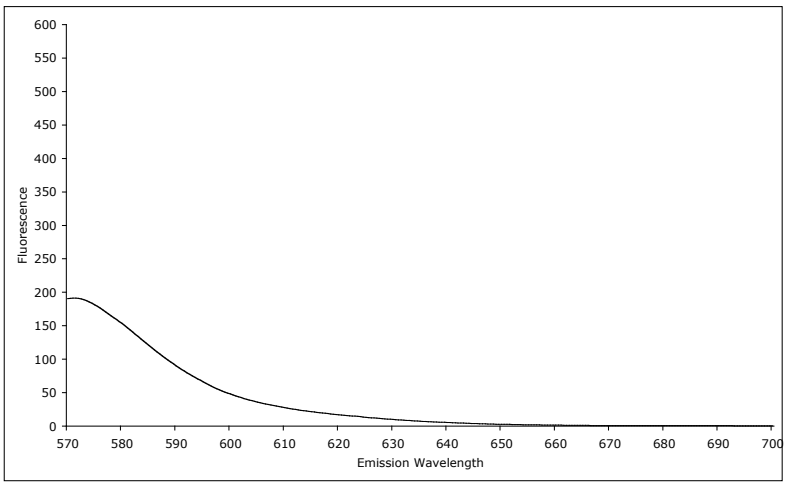

Fig. 30: Fluorescence emission of follicular RhBITC in Specimen 2

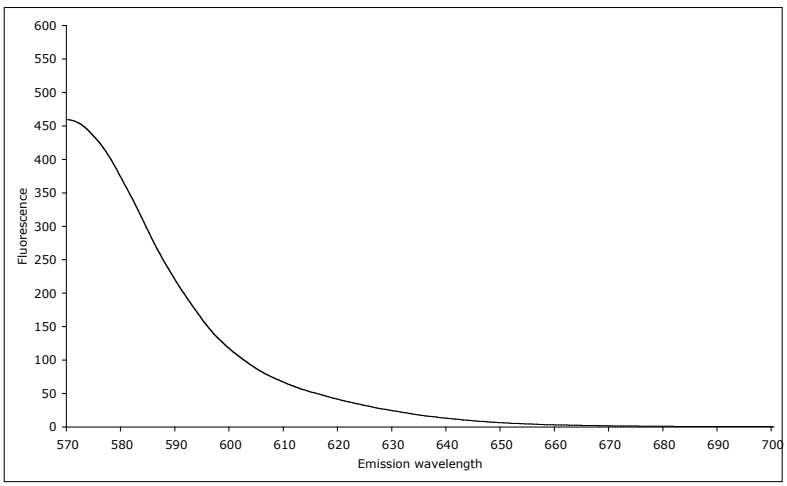

Fig. 31: Fluorescence emission of follicular RhBITC in Specimen 3

Appendix

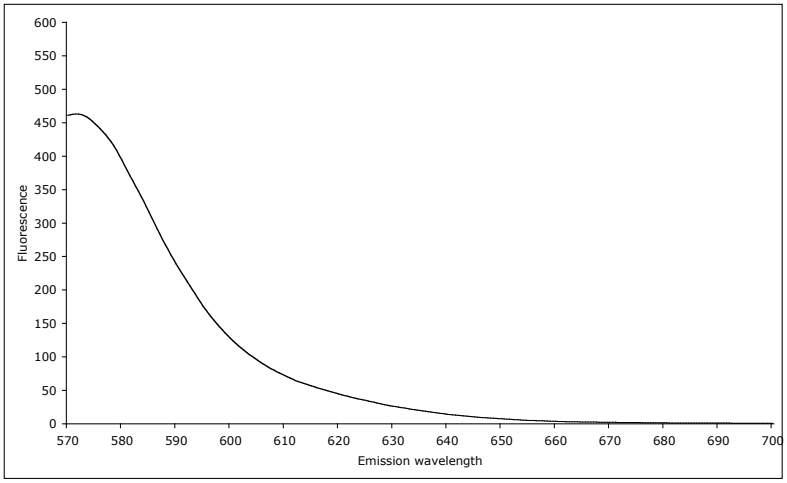

Fig. 32: Fluorescence emission of follicular RhBITC in Specimen 4

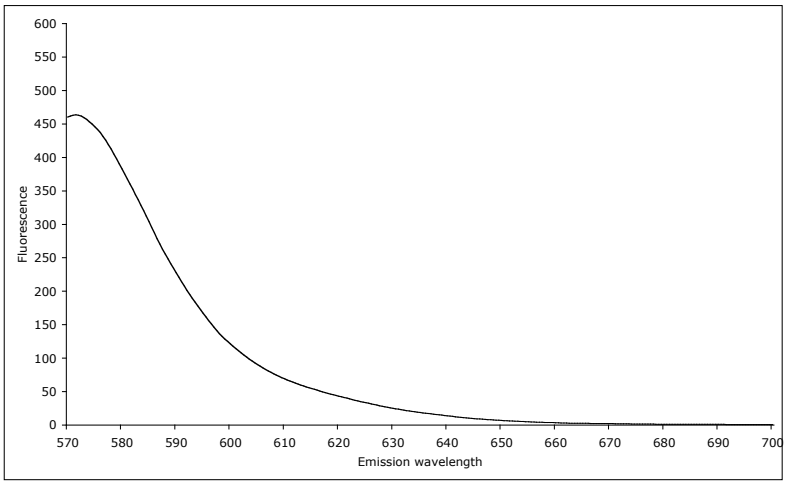

Fig. 33: Fluorescence emission of follicular RhBITC in Specimen 5

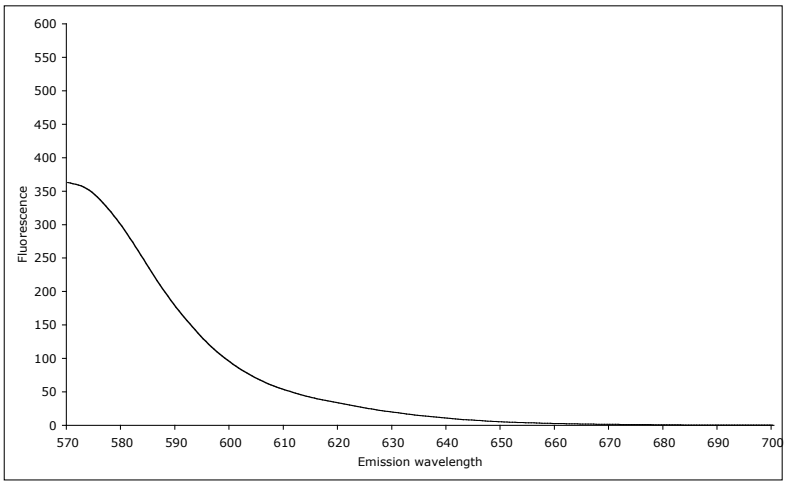

Fig. 34: Fluorescence emission of follicular RhBITC in Specimen 6

Appendix

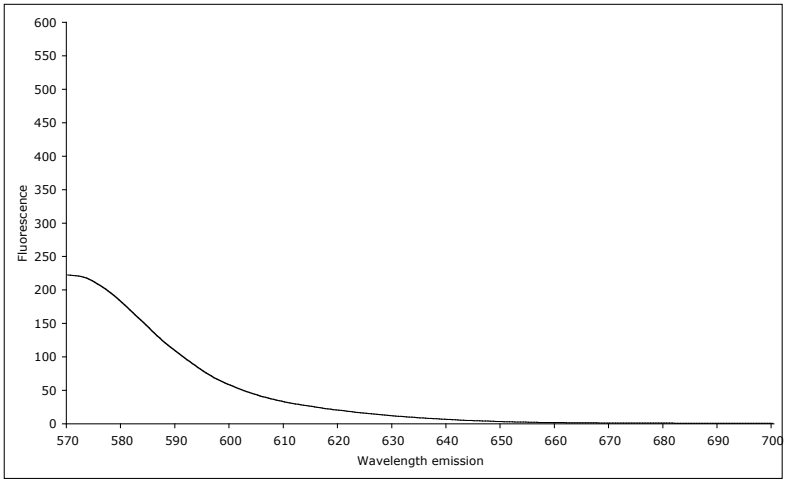

Fig. 35: Fluorescence emission of follicular RhBITC in Specimen 7

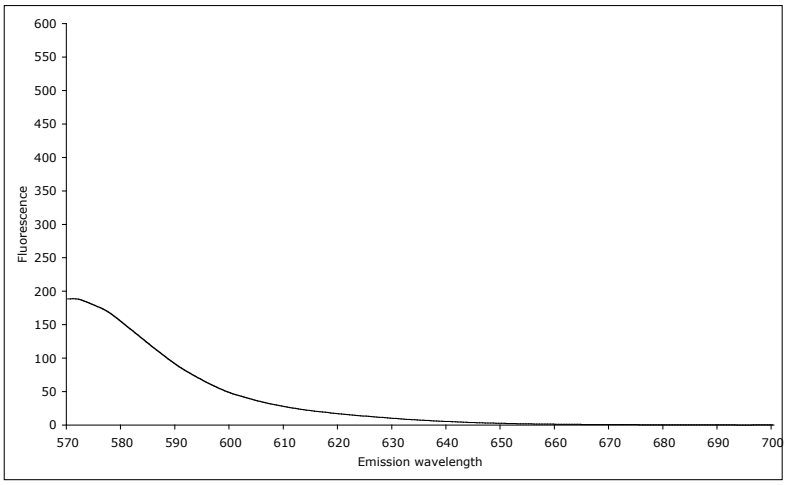

Fig. 36: Fluorescence emission of follicular RhBITC in Specimen 8

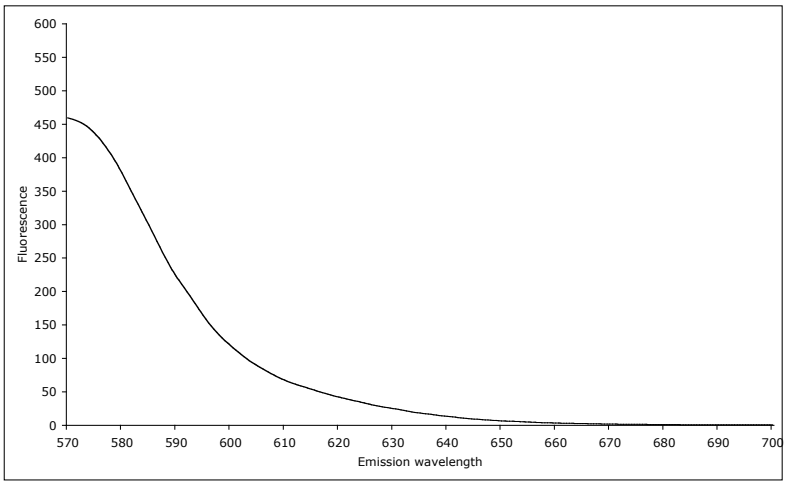

Fig. 37: Fluorescence emission of follicular RhBITC in Specimen 9

Appendix

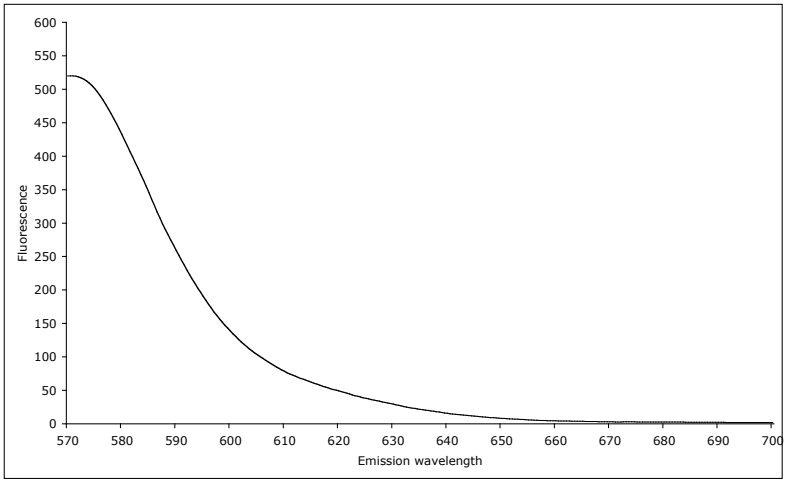

Fig. 38: Fluorescence emission of follicular RhBITC in Specimen 10

7. Summary

Summary

The skin as the outermost covering of the body provides a compliant and painless interface for topical drug administration. It is well established that pharmaceutical agents applied to its surface spread throughout the upper corneocyte layers by diffusing into the lipid matrix of the stratum corneum. Recent studies have evidenced the hair follicles to be effective shunt routes for the transportation of topically applied substances to deeper skin layers and long-term storage reservoirs for drugs in a number of laboratory animals and humans. Interest in the hair follicles as target structures is aimed at their use as depots for localized treatments of disorders including skin diseases and follicle-related disorders, as well as for systemic drug delivery by targeting of the capillary networks and immune and stem cells found in the vicinity of the skin appendages. Research is increasingly focussed on the development of nano-sized particulate drug delivery systems loaded with therapeutic agents customized to target the hair follicles. In the follicular canal, particulates are shielded from abrasion, enabling drug retention and long-term drug release. The success and efficacy of follicular penetration is largely determined by the numbers, distributions, morphometries and activities of the hair follicles found in the treated skin, as well as the skin constitution, the agent itself and the mode of application.

In spite of the obvious abundance of follicular target structures and the comparatively large follicular reservoir, only very few studies have been conducted on the follicular penetration of nano-sized drug delivery systems in companion and farm animals. In the first part of this work, the penetration of topically applied, nano-sized particulates into the hair follicles of excised dog, rat and porcine skin was investigated. The formulations used consisted of FA-PLGA particles sized 256 nm and 430 nm suspended in hydrocellulose gels. Subsequent to application of the formulations to the skin samples using massage, the particles were visualized in cross-sections of the treated skin using a laser scanning microscope, and the follicular penetration depth was determined digitally. FA-PLGA particles were found to penetrate into 60 to 70% of the hair follicles of all skin samples investigated, corresponding to ‘active’ hair follicles receptive to penetration. The results indicated that the follicular penetration depths of the particulate formulations correlated positively with the sizes of the follicular orifices and the lengths of the infundibula in the examined skin samples. Studies have shown that the follicular openings are widest in porcine skin, followed by dog and rat skin, respectively. The hair follicle infundibula extend deepest into the skin of the pig, while in the dog they reach about half, and in the rat, about one-fourth the length of the infundibula found in porcine hair follicles. This is consistent with results of this study in which the particulates penetrated deepest into porcine hair follicles, and least deep into the hair follicles of the rat. While the two FA-PLGA formulations used in this study differed solely in the size of the FA-PLGA particles, no clear trends could be substantiated suggesting that the size significantly influenced follicular penetration. The hair coat, sebaceous glands, tight junctions and capillary networks of the skin samples, as well as the aggregation, degradation and

marker leakage properties of the particulates were discussed as additional potential factors influencing follicular penetration of particulate FA-PLGA.

The quantification of topically applied agents located in the follicular canals is crucial for questions pertaining to administration, concentrations and dosages for follicular penetration experiments. To date, no procedure exists by which follicular contents can be quantified in porcine skin commonly used as a model for the human integument. Excised porcine skin is a particularly suitable alternative to human skin, as its follicular reservoir capacity corresponds to that of living human skin. In the second part of this study, the established method of differential stripping was modified using tape stripping and an extraction technique. This enabled the selective quantification of the dye RhBITC, which was implemented as a model drug and located in the hair follicles of porcine skin subsequent to topical administration. An average of 5% of the dye applied to the skin was extracted from the follicular canals with ethanol and detected using a fluorescence spectrometer, which was in accordance with results from previous studies, substantiating the efficacy of the developed method.

8. Zusammenfassung

Follikuläre Penetration von nanogroßen FA-PLGA Partikeln und dem Farbstoff RhBITC in die Rückenhaut von Hunden und Ratten, sowie in die Ohrenhaut von Schweinen als in vitro Modell für die menschliche Haut

Die Haut als äußerste Schutzschicht des Körpers stellt eine breite Kontaktfläche für topisch applizierte Substanzen dar. Es ist bekannt, dass pharmazeutische Agenzien, die auf die Hautoberfläche aufgetragen werden, sich in den oberen Korneozytenschichten verteilen, indem sie in die Lipidmatrix des Stratum corneums diffundieren. Neueste Studien haben gezeigt, dass Haarfollikel effektive Transportrouten von oberflächlich aufgetragenen Wirkstoffen zu tiefer gelegenen Hautschichten und Langzeitreservoire für phamazeutisch aktive Substanzen in einigen Versuchstieren und im Menschen darstellen. Das Interesse an den Haarfollikeln als Zielstrukturen orientiert sich an ihrer Verwendung als Depots für lokalisierte Behandlungen von Störungen wie Hauterkrankungen und haarfollikelassoziierte Krankheiten, und an der zielgerichteten systemischen Anreicherung von Wirkstoffen in den follikulären Blutkapillaren und den Immun- und Stammzellen in der Umgebung der Hautanhangsdrüsen. Forschungsaktivitäten konzentrieren sich vorwiegend auf die Entwicklung von Systemen zur zielgerichteten Medikamentenabgabe mit maßgeschneiderten Partikeln im Nanobereich, die mit für Haarfollikel therapeutischen Agenzien angereichert sind. Im follikulären Kanal sind die Partikel vor Abschilferung geschützt, wodurch eine Wirkstoffretention und eine langfristige, kontrollierte Wirkstoffabgabe gewährleistet wird. Der Erfolg und die Wirksamkeit der Follikelpenetration wird weitgehend durch die Anzahl, Verteilung, morphometrischen Eigenschaften und Aktivität der Haarfollikel, die in der behandelten Haut vorhanden sind, sowie durch die Konstitution der Haut, den Wirkstoff selbst und die Anwendungsform bestimmt.

Trotz der offensichtlichen Fülle von follikulären Zielstrukturen und des vergleichbar großen follikulären Reservoirs wurde bisher die Penetration von Partikeln im Nanobereich in die Haarfollikel von Haus- und Nutztieren nur in wenigen Studien bearbeitet. Im ersten Teil dieser Arbeit wurde daher die Penetration topisch applizierter Partikel im Nanobereich in die Haarfollikel von exzidierter Hunde- und Rattenhaut sowie im Schweineohr untersucht. Die verwendeten Formulierungen bestanden aus in Hydrozellulosegelen suspendierten FA-PLGA Partikeln der Größen 256 nm beziehungsweise 430 nm. Nach Aufbringen der Formulierungen auf die Hautproben durch Massage wurden die Partikel in Querschnitten der behandelten Haut mit einem Laserscanningmikroskop erfasst, und die follikulären Penetrationstiefen digital bestimmt. Die FA-PLGA Partikel penetrierten in 60 bis 70% aller untersuchten Haarfollikel, die mit der Anzahl der ‚aktiven' Haarfollikel, die für die Penetration zugänglich sind, in Zusammenhang stehen. Studien haben gezeigt, dass die follikulären Penetrationstiefen der partikulären Formulierungen mit den Größen der Haarfollikelöffnungen und der Längen der

Infundibula in den untersuchten Hautproben positiv korrelieren. Die Haarfollikelöffnungen sind beim Schwein am größten, und bei der Ratte am kleinsten. Die Infundibula sind in der Haut des Schweins am längsten. Im Hund erreichen sie ungefähr die Hälfte, und in der Ratte ungefähr ein Viertel der Länge der Infundibula des Schweins. Diese Erkenntnisse stimmen mit den Ergebnissen der vorliegenden Studie überein, in der die Partikel am tiefsten in die Schweinehaarfollikel penetriert und am geringsten in die Rattenhaarfollikel eingedrungen sind. Obwohl die zwei Formulierungen, die in der Studie verwendet wurden, sich ausschließlich in der Größe der FA-PLGA Partikel unterschieden haben, konnten keine klaren Trends identifiziert werden, die auf einen signifikanten Einfluss der Größe auf die follikuläre Penetration hinweisen. Das Haarkleid, die Talgdrüsen, die Tight Junctions und die Kapillarnetzwerke der Hautproben, sowie die Aggregation, der Abbau und der Markerverlust der Partikel wurden in dieser Arbeit als zusätzliche Faktoren, die die follikuläre Penetration der FA-PLGA Partikel beeinflussen, diskutiert.

Die Quantifizierung oberflächlich angewandter Wirkstoffe, die in den follikulären Kanälen lokalisiert sind, ist essentiell für Fragen zu Anwendungen, Konzentrationen und Dosierungen für follikuläre Penetrationsversuche. Zurzeit existieren keine Methoden, bei denen die follikulären Inhalte der Schweinehaut, die üblicherweise als Modell für die menschliche Haut dient, quantifiziert werden können. Exzidierte Schweinehaut ist eine besonders geeignete Alternative zur menschlichen Haut da die Kapazität des follikulären Reservoirs mit dem der lebenden Humanhaut vergleichbar ist. Im zweiten Teil dieser Arbeit wurde die etablierte Methode des Differential Strippings unter Verwendung der Abrißmethode und einem Extraktionsverfahren modifiziert. Dies erlaubte die selektive Quantifizierung des Farbstoffes RhBITC, der als Modellsubstanz implementiert wurde, und nach topischer Applikation in den Haarfollikeln der Schweinehaut lokalisiert war. Durchschnittlich 5% des Farbstoffes, der auf die Haut aufgebracht wurde, konnte von den follikulären Kanälen mittels Ethanol extrahiert und unter Verwendung eines Fluoreszenzspektrometers bestimmt werden. Diese Daten waren in Übereinstimmung mit früheren Studien, womit die Wirksamkeit der entwickelten Methode belegt wurde.

9. References

References

Abrams, K., Harvell, J. D., Shriner, D., Wertz, P. W., Maibach, H., Maibach, H. I., Rehfeld, S. J., 1993. Effect of organic solvents on in vitro human skin water barrier function. *Journal of Investigative Dermatology*, 101 (4): 609-613.

Alvarez-Román, R., Barré, G., Guy, R. H., Fessi, H., 2001. Biodegradable polymer nanocapsules containing a sunscreen agent: Preparation and photoprotection. *European Journal of Pharmaceutics and Biopharmaceutics*, 52: 191-195.

Alvarez-Román, R., Merina, G., Kalia, Y. N., Naik, A., Guy, R. H., 2003. Skin permeability enhancement by low frequency sonophoresis: Lipid extraction and transport pathways. *Journal of Pharmaceutical Sciences*, 92 (6): 1138-1146.

Alvarez-Román, R., Naik, A., Kalia, Y., N., Guy, R. H., Fessi, H., 2004a. Enhancement of topical delivery from biodegradable nanoparticles. *Pharmaceutical Research*, 21: 1818-1825.

Alvarez-Román, R., Naik, A., Kalia, Y., N., Guy, R. H., Fessi, H., 2004b. Skin penetration and distribution of polymeric nanoparticles. *Journal of Controlled Release*, 99: 53-62.

Anderson, J. M., Shive, M. S., 1997. Biodegradation and biocompatibility of PLA and PLGA microspheres. *Advanced Drug Delivery Reviews*, 28: 5-24.

Bala, I., Hariharan, S., Kumar, M. N., 2004. PLGA nanoparticles in drug delivery: The state of the art. *Critical Reviews in Therapeutic Drug Carrier Systems*, 21: 387-422.

Barbero, A. M., Frasch, H. F., 2009. Pig and guinea pig skin as surrogates for human in vitro penetration studies: A quantitative review. *Toxicology in Vitro*, 23: 1-13.

Baroli, B., Ennas, M. G., Loffredo, F., Isola, M., Pinna, R., Lopez-Quintela, M. A., 2007. Penetration of metallic nanoparticles in human full-thickness skin. *Journal of Investigative Dermatology*, 127: 1701-1712.

Barry, B. W., 1983. Structure, function, diseases and topical treatment of human skin. In: *Dermatological Preparations: Percutaneous Absorption*. New York: Marcel Dekker.

Bashir, S. J., Chew, A.-L., Anigbogu, A., Dreher, F., Maibach, H. I., 2001. Physical and physiological effects of stratum corneum tape stripping. *Skin Research and Technology*, 7 (1): 40-48.

References

Bernard, E., Dubois, J., Wepierre, J., 1997. Importance of sebaceous glands in cutaneous penetration of an antiandrogen: Target effect of liposomes. *Journal of Pharmaceutical Sciences*, 86: 573-578.

Bidmon, H. J., Pitts, J. D., Solomon, H. F., Bondi, J. V., Stumpf, W. E., 1990. Estradiol distribution and penetration in rat skin after topical application, studied by high resolution autoradiography. *Histochemistry and Cell Biology*, 95 (1): 43-54.

Blanpain, C., Lowry, W. E., Geoghegan, A., Polak, L., Fuchs, E., 2004. Self-renewal, multipotency and the existence of two cell populations within an epithelial stem cell niche. *Cell*, 118: 635-648.

Blume, U., Ferracin, J., Verschoore, M., Czernielewski, J. M., Schäfer, H., 1991. Physiology of the vellus hair follicle: Hair growth and sebum excretion. *British Journal of Dermatology*, 124 (1): 21-28.

Blundell, G., Henderson, W. J., Price, E. W., 1989. Soil particles in the tissues of the foot in endemic elephantiasis of the lower legs. *Annals of Tropical Medicine and Parasitology*, 83 (4): 381-385.

Borelli, S., Metzger, M., 1957. Fluoreszenzmikroskopische Untersuchungen über die perkutane Penetration fluoreszierender Stoffe. *Hautarzt*, 8 (6): 261-266.

Bouwstra, J., Pilgram, G., Gooris, G., Koerten, H., Ponec, M., 2001. New aspects of the skin barrier organization. *Skin Pharmacology and Applied Skin Physiology*, 14 (Suppl. 1): 52-62.

Brandner, J. M., McIntyre, M. Kief, S., Wladykowski, E., Moll, I., 2003. Expression and localization of tight junction-associated proteins in human hair follicles. *Archives of Dermatological Research*, 295: 211–221.

Braverman, I. M., 1989. Ultrastructure and organization of the cutaneous microvasculature in normal and pathological states. *Journal of Investigative Dermatology*, 93: 2s-9s.

Brigger, I., Dubernet, C., Couvreur, P., 2002. Nanoparticles in cancer therapy and diagnosis. *Advanced Drug Delivery Reviews*, 54: 631-651.

Bronaugh, R. L., 1989. Determination of percutaneous absorption by in vitro techniques. In: Bronaugh, R. L., Maibach, H. I., eds. *Percutaneous Absorption: Mechanisms, Methodology, Drug Delivery*. 2nd edition. New York: Marcel Dekker.

References

von Burkersroda, F., Schedl, L., Göpferich, A., 2002. Why degradable polymers undergo surface erosion or bulk erosion. *Biomaterials*, 23 (21): 4221-4231.

Caputo, R., Peluchette, D., 1976. The junctions of normal human epidermis: A freeze-fracture study. *Journal of Ultrastructure Research*, 61: 44-61.

Calvo, P., Thomas, C., Alonso, M. J., Vila-Jato, J. L., Robinson, J. R., 1994. Study of the mechanism of interaction of poly(epsilon-caprolactone) nanocapsules with the cornea by confocal laser scanning microscopy. *International Journal of Pharmaceutics*, 103: 283-291.

Cavalli, R., Gasco, M. R., Chetoni, P., Burgalassi, S., Saettone, M. F., 2002. Solid lipid nanoparticles (SLN) as ocular delivery system for tobramycin. *International Journal of Pharmaceutics*, 238 (1-2): 241-245.

Cevc, G., 2004. Lipid vesicles and other colloids as drug carriers on the skin. *Advanced Drug Delivery Reviews*, 56: 675-711.

Cheng, Y., Dovichi, N. J., 1988. Subatomole amino acid analysis by capillary zone electrophoresis and laser-induced fluorescence. *Science*, 242 (4878): 562-564.

Choi, E. H., Lee, S. H., Ahn, S. K., Hwang, S. M., 1999. The pretreatment effect of chemical skin penetration enhancers in transdermal drug delivery using iontophoresis. *Skin Pharmacology and Applied Skin Physiology*, 12 (6): 326-355.

Claudinot, S., Nicolas, M., Oshima, H., Rochat, A., Barrandon, Y., 2005. Long-term renewal of hair follicles from clonogenic multipotent stem cells. *Proceedings of the National Academy of Sciences*, 102: 14677-14682.

Claxton, N. S., Fellers, T. J., Davidson, M. W., 200-. Laser Scanning Confocal Microscopy [Online]. Available at http://www.olympusconfocal.com/theory/LSCMIntro.pdf [Accessed on July 10, 2009].

Clarys, P., Barel, A., 1995. Quantitative evaluation of skin surface lipids. *Clinics in Dermatology*, 13 (4): 307-321.

Colton, S. W., Downing, D. T., 1985. The time-course of lipid biosynthesis in horse skin. *Biochimica et Biophysica Acta*, 836 (3): 306-311.

References

Cotsarelis, G., 2006. Epithelial stem cells: A folliculocentric view. *Journal of Investigative Dermatology*, 126: 1459-1468.

Cotsarelis, G., Sun, T. T., Lavker, R. M., 1990. Label-retaining cells reside in the bulge are of pilosebaceous unit: Implications for follicular stem cells, hair cycle and skin carcinogenesis. *Cell*, 61: 1329-1337.

Cutts, J., Lee, G., Berarducci, M., Thomas, C., Dempsey, P. K., Kadish, S. P., 2002. Goosebumps. *The Lancet*, 360 (9334): 690.

Daniels J., 2006. How polymeric microspheres deliver the goods. *Pharmaceutical Technology Europe*, 18:30-32.

De, S., Robinson, D. H., 2004. Particle size and temperature effect on the physical stability of PLGA nanospheres and microspheres containing Biodipy [Online]. *AAPS PharmSciTech*, 5 (4): Article 53. Available at http://www.aapspharmscitech.org [Accessed August 14, 2009].

Degim, I. T., 2006. New tools and approaches for predicting skin permeability. *Drug Discovery Today*, 11 (11/12): 517-523.

Dick, I. P., Scott, R.C., 1992. Pig ear skin as an in-vitro model for human skin permeability. *Journal of Pharmacy and Pharmacology*, 44 (8): 640-645.

Dinauer, N., von Briesen, H., Balthasar, S., Weber, C., Kreuter, J., Langer, K., 2005. Selective targeting of antibody-conjugated nanoparticles to leukemic cells and primary T-lymphocytes. *Biomaterials*, 26: 5898-5906.

Dokka, S., Cooper, S. R., Kelly, S., Hardee, G. E., Karras, J. G., 2005. Dermal delivery of topically applied oligonulceotides via follicular transport in mouse skin. *Journal of Investigative Dermatology*, 124: 971-975.

Downing, D. T., Stewart, M. E., Strauss, J. S., 1981. Estimation of sebum production rates in man by measurement of the squalene content of skin biopsies. *Journal of Investigative Dermatology*, 77: 358-360.

Downing, D. T., Strauss, J. S., Ramasastry, P., Abel, M., Lees, C. W., Pochi, P. E., 1975. Measurement of the time between synthesis and surface excretion of sebaceous lipids in sheep and man. *Journal of Investigative Dermatology*, 64: 215-219.

References

Dreher, F., Arens, A., Hostýnek, J. J., Mudumba, S., Ademola, J., Maibach, H. I., 1998. Colorimetric method for quantifying human stratum corneum removed by adhesive tape stripping. *Acta Dermato-Venereologica*, 78: 186-189.

Ebling, F. J., 1974. Hormonal control and methods of measuring sebaceous gland activity. *Journal of Investigative Dermatology*, 62: 161-171.

Ebling, F., Eady, R., Leigh, I., 1992. Anatomy and organisation of human skin. In: Champion, R. H., Burrington, J. L., Ebling, F., J., G., eds. *Textbook of Dermatology*. 5th edition. New York: Blackwell Scientific Publications.

Eckert, R. L., 1989. Structure, function and differentiation of the keratinocyte. *Physiological Reviews*, 69 (4): 1316-1346.

Elias, P. M., 1983. Epidermal lipids, barrier function and desquamation. *Journal of Investigative Dermatology*, 80: 44-49.

Essa, E. A., Bonner, M. C., Barry, B. W., 2002. Human skin sandwich for assessing shunt route penetration during passive and iontophoretic drug and liposome delivery. *Journal of Pharmacy and Pharmacology*, 54: 1-10.

Fan, H., Lin, Q., Morrissey, G. R., Khavari, P. A., 1999. Immunization via hair follicles by topical application of naked DNA to normal skin. *Nature Biotechnology*, 17: 870-872.

Feldmann, R. J., Maibach, H. I., 1967. Regional variations in percutaneous penetration of ^{14}C-cortisol in man. *Journal of Investigative Dermatology*, 48: 181-183.

Feng, S. S., Huang, G., 2001. Effects of emulsifiers on the controlled release of paclitaxel (Taxol) from nanospheres of biodegradable polymers. *Journal of Controlled Release*, 71: 53-69.

Fessi, H., Puisieux, F., Devissaguet, J. P., Ammoury, N., Benita, S., 1989. Nanocapsule formation by interfacial polymer deposition following solvent displacement. *International Journal of Pharmaceutics*, 55: R1-R4.

Fernández-Urrusuno, R., Calvo, P., Remuñán-López, C., Vila-Jato, J. L., Alonso, M. J., 1999. Enhancement of nasal absorption of insulin using chitosan nanoparticles. *Pharmaceutical Research*, 16 (10): 1576-1581.

References

Finlay, B., 1969. Scanning electron microscopy of the human dermis under uni-axial strain. *Biomedical Engineering*, 4: 322-327.

Flynn, G. L., 1990. Physicochemical determinants of skin absorption. In: Gerrity, T. R., Henry, C. J., eds. *Principles of route-to-route extrapolation for risk assessment*. New York: Elsevier.

Fritsch, P., 1998. Aufbau und Funktionen der Haut. In: Fritsch, P., ed. *Dermatologie und Venerologie*. *Lehrbuch und Atlas*. Berlin: Springer Verlag.

Frum, Y., Eccleston, G. M., Meidan, V. M., 2008. In vitro permeation of drugs into porcine hair follicles: Is it quantitatively equivalent to permeation into human hair follicles? *Journal of Pharmacy and Pharmacology*, 60: 145-151.

Fuchs, E., 2007. Scratching the surface of skin development. *Nature*, 445: 834-842.

Furuse, M., Hata, M., Furuse, K., Yoshida, Y., Haratake, A., Sugitani, Y., Noda, T., Kubo, A., Tsukita, S., 2002. Claudin-based tight junctions are crucial for the mammalian epidermal barrier: A lesson from claudin-1-deficient mice. *Journal of Cell Biology*, 156: 1099-1111.

Genina, E. A., Bashkatov, A. N., Sinichkin, Y. P., Kochubey, V. I., Lakodina, N. A., Altshuler, G. B., Tuchin, V. V., 2002. In vitro and in vivo study of dye diffusion into the human skin and hair follicles. *Journal of Biomedical Optics*, 7: 471-477.

Ghirardelli, R., Bonasoro, F., Porta, C., Cremaschi, D., 1999. Identification of particular epithelial areas and cells that transport polypeptide-coated nanoparticles in the nasal respiratory mucosa of the rabbit. *Biochimica et Biophysica Acta*, 1416: 39-47.

Grayson, S., Johnson-Winegar, A. G., Wintraub, B. U., Isserhof, R. R., Epstein, E. H., Elias, P. M., 1985. Lamellar body-enriched fractions from neonatal mice: Preparative techniques and partial characterization. *Journal of Investigative Dermatology*, 85: 285-289.

Göpferich, A., 1996. Mechanism of polymer degradation and erosion. *Biomaterials*, 17: 103-114.

Gupta, P. N., Mishra, V., Rawat, A., Dubey, P., Mahor, S., Jain, S., Chatterji, D. P., Vyas, S. P., 2005. Non-invasive vaccine delivery in transfersomes, niosomes and liposomes: A comparative study. *International Journal of Pharmaceutics*, 293 (1-2): 73-82.

References

Habermehl, K. H., 1996. Haut und Hautorgane. In: Nickel, R., Schummer, A., Seiferle, E., eds. *Lehrbuch der Anatomie der Haussäugetiere. Band III: Kreislaufsystem, Haut und Hautorgane*. 3rd edition. Berlin: Blackwell Wissenschaftsverlag.

Hadgraft, J., 2001. Skin, the final frontier. *International Journal of Pharmaceutics*, 224: 1-18.

Hadgraft, J., 2004. Skin deep. *European Journal of Pharmaceutics and Biopharmaceutics*, 58 (2): 291-299.

Hadgraft, J., Walters, K. A., Guy, R. H., 1992. Epidermal lipids and topical delivery. *Seminars in Dermatology*, 11 (2): 139-144.

Harkey, M. R., 1993. Anatomy and physiology of hair. *Forensic Science International*, 63: 9-18.

Hawkins, G. S., Reifenrath, W. G., 1986. Influence of skin source, penetration cell fluid and partition coefficient on in vitro skin penetration. *Journal of Pharmaceutical Science*, 75: 378-381.

Hendriks, F. M., 2005. *Mechanical behavior of human epidermal and dermal layers in vivo*. Ph.D.: Technische Universiteit Eindhoven.

Hisoire, G., Bucks, D., 1997. An unexpected finding in percutaneous absorption observed between haired and hairless guinea pig skin. *Journal of Pharmaceutical Sciences*, 86 (3): 398-400.

Hoffman, R. M., 2007. The potential of nestin-expressing hair follicle stem cells in regenerative medicine. *Expert Opinion on Biological Therapy*, 7 (3): 289-291.

Holbrook, K. A., Odland, G. F., 1974. Regional differences in the thickness (cell layers) of the human stratum corneum: An ultrastructural analysis. *Journal of Investigative Dermatology*, 62: 415-422.

Holbrook, K. A., Wolff, K., 1993. The structure and development of skin. In: Fitzpatrick, T. B., Eisen, A. Z., Wolff, K., Freedberg, I. M., Austen, K. F., eds. *Dermatology in general medicine*. New York: McGraw-Hill.

Holland, K. T., Roberts, C. D., Cunliffe, W. J., 1974. A technique for sampling microorganisms from the pilosebaceous ducts. *Journal of Applied Bacteriology*, 37: 289-296.

References

Horisawa, E., Kubota, K., Tuboi, I., Sato, K., Yamamoto, H., Takeuchi, H., Kawashima, Y., 2002. Size-dependency of DL-lactide/glycolide copolymer particulates for intra-articular delivery system on phagocytosis in rat synovium. *Pharmaceutical Research*, 19:132-139.

Houben, E., De Paepe, K., Rogiers, V., 2007. A keratinocyte's course of life. *Skin Pharmacology and Physiology*, 20: 122-132.

Hueber, F., Wepierre, J., Schäfer, H., 1992. Role of Transepidermal and Transfollicular Routes in Percutaneous Absorption of Hydrocortisone and Testosterone: In vivo Study in the Hairless Rat. *Skin Pharmacology and Physiology*, 5 (2): 99-107.

Iizuka, H., 1994. Epidermial turnover time. *Journal of Dermatological Science*, 8 (3): 215-217.

Illel, B., Schäfer, H., Wepierre, J., Doucet, O., 1991. Follicles play an important role in percutaneous absorption. *Journal of Pharmaceutical Sciences*, 80: 424-427.

Imokawa, G., Akasaki, S., Minematsu, Y., Kawai, M. 1989. Importance of intercellular lipids in water retention properties of stratum corneum: Induction and recovery study of surfactant dry skin. *Archives of Dermatological Research,* 281: 45-51.

Ito, M., Liu, Y., Yang, Z., Nguyen, J., Liang, F., Morris, R., Cotsarelis, G., 2005. Stem cells in the hair follicle bulge contribute to wound repair but not to homeostasis of the epidermis. *Nature Medicine*, 11: 1351-1354.

Jacobi, U., Kaiser, M., Toll, R., Mangelsdorf, S., Audring, H., Otberg, N., Sterry, W., Lademann, J., 2007. Porcine ear skin: An in vitro model for human skin. *Skin Research and Technology*, 13: 19-24.

Jacobi, U., Meykadeh, N., Sterry, W., Lademann, J., 2003. Einfluß der Salbengrundlage auf die mittels der Abrißmethode entnommene Menge an Stratum corneum. *Journal der Deutschen Dermatologischen Gesellschaft*, 1 (11): 884-889.

Jain, R. A., 2000. The manufacturing techniques of various drug loaded biodegradable poly(lactide-co-glycolide) devices. *Biomaterials*, 21: 2475-2490.

Jenning, V., Schäfer-Korting, M., Gohla, S., 2000. Vitamin A-loaded solid lipid nanoparticles for topical use: drug release properties. *Journal of Controlled Release*, 66: 115-126.

References

Jimbow, K., Quevedo, W. C., Fitzpatrick, Jr. T. B., Szabo, G., 1993. Biology of melanocytes. In: Fitzpatrick, T. B., Eisen, A. Z., Wolff, K., Freedberg, I. M., Austen, K. F., eds. *Dermatology in general medicine*. New York: McGraw-Hill.

Johnson, C. A., Thompson, D. L., 1999. Biodegradable delivery systems for estradiol: Comparison between poly(D,L-lactide) microspheres and the SABER delivery system. *Proceedings of the International Symposium on the Controlled Release of Biooactive Materials*, 147-148.

Jung, S., Otberg, N., Thiede, G., Richter, H., Sterry, W., Schanzer, S., Lademann, J., 2006. Innovative liposomes as a transfollicular drug delivery system: Penetration into porcine hair follicles. *Journal of Investigative Dermatology*, 126: 1728-1732.

Kahn, C. M., Line, S., eds., 2005. *The Merck Veterinary Manual*. 9th edition. Whitehouse Station: Merck & Co., Inc. & Merial Limited.

Kao, J., Hall, J., Helman, G., 1988. In vitro percutaneous absorption in mouse skin: Influence of skin appendages. *Toxicology and Applied Pharmacology*, 94: 93-103.

Kerscher, M., Korting, H. C., 1991. Skin ceramides: Structure and function. *European Journal of Dermatology*, 39-43.

Kim, D.-K., Holbrook, K. A., 1995. The appearance, density and distribution of Merkel cells in human embryonic and fetal skin: Their relationship to sweat gland and hair follicle development. *Journal of Investigative Dermatology*, 104: 411-416.

Kim, S., Lim, Y. T., Soltesz, E. G., de Grand, A. M., Lee, J., Nakayama, A., Parker, J. A., Mihaljevic, T., Laurence, R. G., Dor, D. M., Cohn, L. H., Bawendi, M. G., Frangioni, J. V., 2004. Near-infrared fluorescent type II quantum dots for sentinel lymph node mapping. *Nature Biotechnology*, 22 (1): 93-97.

Kligman, A. M., 1961. Pathological dynamics of human hair loss. 1. Telogen effluvium. *Archives of Dermatology*, 83: 175-198.

Kligman, A. M., Shelley, W. B., 1958. An investigation of the biology of the human sebaceous gland. *Journal of Investigative Dermatology*, 30 (3): 99-125.

References

Kotrotsiou, O., Kotti, K., Dini, E., Kammona, O., Kiparissides, C., 2005. Nanostructured materials for selective recognition and targeted drug delivery. *Journal of Physics: Conference Series*, 10: 281-284.

Koziara, J. M., Lockman, P. R., Allen, D. D., Mumper, R. J., 2004. Paclitaxel nanoparticles for the potential treatment of brain tumors. *Journal of Controlled Release*, 99: 259-269.

Kreuter, J., 2004. Nanoparticles as drug delivery systems. In: Nalwa, H. S., ed. *Encyclopedia of Nanoscience and Nanotechnology*. Vol. 7. Stevenson Ranch: American Scientific Publishers.

Kristensen, S., 1975. A study of skin diseases in dogs and cats. I. Histology of the hairy skin of dogs and cats. *Nordisk Veterinaermedicin*, 27: 593-603.

Künzel, E., 1990. Haut (Integumentum commune). In: Mosimann, W., Kohler, T., eds. *Zytologie, Histologie und mikroskopische Anatomie der Haussäugetiere*. Berlin: Verlag Paul Parey.

Labhasetwar, V., 1997. Nanoparticles for drug delivery. *Pharmaceutical News*, 4: 28-31.

Lademann, J., Otberg, N., Richter, H., Lindemann, U., Weigmann, H.-J., Schäfer, H., Sterry, W., 2001. Investigation of follicular penetration of topically applied substances. *Skin Pharmacology and Applied Skin Physiology*, 14 (Suppl. 1): 17-22.

Lademann, J., Richter, H., Schäfer, U. F., Blume-Peytavi, U., Teichmann, A., Otberg, N., Sterry, W., 2006. Hair follicles - a long-term reservoir for drug delivery. *Skin Pharmacology and Physiology*, 19: 232-236.

Lademann, J., Richter, H., Teichmann, A., Otberg, N., Blume-Peytavi, U., Luengo, J., Weiß, B., Schäfer, U. F., Lehr, C.-M., Wepf, R., Sterry, W., 2007. Nanoparticles - an efficient carrier for drug delivery into the hair follicles. *European Journal of Pharmaceutics and Biopharmaceutics*, 66 (2): 159-164.

Lademann, J., Weigmann, H.-J., Lindemann, U., Audring, H., Antoniou, C., Tsikrikas, G., Schaefer, H., Sterry, W., 2002. Investigations on the influences of furrows and wrinkles when quantifying penetration of drugs and cosmetics by tape stripping. In: Brain, K. R., Walters, K. A., eds. *Perspectives in Percutaneous Penetration*. Volume 8a: 49. Cardiff: STS.

References

Lakowicz, J. R., 2006. *Principles of fluorescence spectroscopy*. 3rd edition. Berlin: Springer Verlag.

Lamprecht, A., Schäfer, U. F., Lehr, C. M., 2001. Size-dependent bioadhesion of micro- and nanoparticulate carriers to the inflamed colonic mucosa. *Pharmaceutical Research*, 18: 788-793.

Landmann, L., 1986. Epidermal permeability barrier: Transformation of lamellar granule-disks into intercellular sheets by a membrane fusion process, a freeze-fracture study. *Journal of Investigative Dermatology*, 87: 202-209.

Langer, R., 1990. New methods of drug delivery. *Science*, 249 (4976): 1527-1533.

Langer, R., 1997. Tissue engineering: A new field and its challenges. *Pharmaceutical Research*, 14 (7): 840-841.

Langer, R., 1998. Drug delivery and targeting. *Nature*, 392 (Suppl. 1): 5-10.

Lauer, A. C., Lieb, L. M., Ramachandran, C., Flynn, G. L., Weiner, N. D., 1995. Transfollicular drug delivery. *Pharmaceutical Research*, 12 (2): 179-186.

Lauer, A. C., Ramachandran, C., Lieb, L. M., Niemiec, S., Weiner, N. D., 1996. Targeted delivery to the pilosebaceous unit via liposomes. *Advanced Drug Delivery Reviews*, 18: 311-324.

Lavker, R. M., Leyden, J. J., Thorne, E. G., 1992. An ultrastructural study of the effects of topical tretinoin on microcomedones. *Clinical Therapeutics*, 14 (6): 773-780.

Lekki, J., Stachura, Z., Dąbroś, W., Stachura, J., Menzel, F., Reinert, T., Butz, T., Pallon, J., Gontier, E., Ynsa, M. D., Moretto, P., Kertesz, Z., Szikszai, Z., Kiss, A. Z., 2007. On the follicular pathway of percutaneous uptake of nanoparticles: Ion microscopy and autoradiography studies. *Nuclear Instruments and Methods in Physics Research. Section B: Beam Interactions with Materials and Atoms*, 260 (1): 174-177.

Leonhardt, H., 1990. *Histologie, Zytologie und Mikroanatomie des Menschen*. 8th edition. Stuttgart: Thieme Verlag.

Levy, V., Lindon, C., Harfe, B. D., Morgan, B. A., 2005. Distinct stem cell populations regenerate the follicle and interfollicular epidermis. *Developmental Cell*, 9: 855-61.

References

Lichtman, J. W., Conchello, J.-A., 2005. Fluorescence microscopy. *Nature Methods*, 2 (12): 910-919.

Liebich, H.-G., 1993. *Funktionelle Histologie*. *Farbatlas und Kurzlehrbuch der mikroskopischen Anatomie der Haussäugetiere*. 2nd edition. Stuttgart: Schattauer.

Liebich, H.-G., 2004. *Funktionelle Histologie der Haussäugetiere. Lehrbuch und Farbatlas für Studium und Praxis.* 4th edition. Stuttgart: Schattauer.

Liebich, H.-G., Reese, S., Budras, K. H., 1999. *Funktionelle Histologie der Haussäugetiere*. *Lehrbuch für Studium und Praxis*. 4th edition. Stuttgart: Schattauer.

Löffler, H., Dreher, F., Maibach, H. I., 2004. Stratum corneum adhesive tape stripping: Influence of anatomical site, application pressure, duration and removal. *British Journal of Dermatology*, 151 (4): 746-752.

Loth, H., 1987. Grundlagen des intra- und transdermalen Transports von Arzneistoffen. *Acta Pharmaceutica Technologica*, 33: 3-14.

Lowe, N. J., Stoughton, R. B., 1977. Essential fatty acid deficient hairless mouse: a model of chronic epidermal hyperproliferation. *British Journal of Dermatology*, 96: 155-162.

Lyle, S., Christofidou-Solomidou, M., Liu, Y., Elder, D. E., Albelda, S., Cotsarelis, G., 1998. The C8/144B monoclonal antibody recognizes cytokeratin 15 and defines the location of human hair follicle stem cells. *Journal of Cell Science*, 111 (Pt. 21): 3179-3188.

MacKee, G. M., Sulzberger, M. B., Herrmann, F., Baer, R. L., 1945. Histologic studies on percutaneous penetration with special reference to the effect of vehicles. *Journal of Investigative Dermatology*, 6: 43-61.

Maibach, H. I., Feldman, R. J., Milby, T. H., Serat, W. F., 1971. Regional variation in percutaneous penetration in man. Pesticides. *Archives of Environmental Health*, 23 (3): 208-211.

Mangelsdorf, S., 2007. V*ergleichende Untersuchung hautphysiologischer Parameter mit Einfluss auf die perkutane Penetration bei verschiedenen Spezies*. Ph.D.: Freie Universität Berlin.

References

Marks, R., Dawber, R. P. R., 1971. Skin surface biopsy: An improved technique for the examination of the horny layer. *British Journal of Dermatology*, 84 (2): 117-123.

Marttin, E., Neelissen-Subnel, M. T., De Haan, F. H., Boddé, H. E., 1996. A critical comparison of methods to quantify stratum corneum removed by tape stripping. *Skin Pharmacology*, 9 (1): 69-77.

Marzulli, F. N., Brown, D. W. C., Maibach, H. I., 1969. Techniques for studying skin penetration. *Toxicology and Applied Pharmacology*, Suppl. 3: 79-83.

Meidan, V. M., Bonner, M. C., Michniak, B. B., 2005. Transfollicular drug delivery - is it a reality? *International Journal of Pharmaceutics*, 306 (1-2): 1-14.

Meidan, V. M., Docker, M., Walmsley, A. D., Irwin, W. J., 1998. Low intensity ultrasound as a probe to elucidate the relative follicular contribution to total transdermal absorption. *Pharmaceutical Research*, 15 (1): 85-92.

Meidan, V. M., Touitou, E., 2001. Treatment for androgenetic alopecia and alopecia areata: Current opinions and future prospects. *Drugs*, 61: 53-69.

Menon, G. K., Feingold, K. R., Elias, P. M., 1992. The lamellar secretory response to barrier disruption. *Journal of Investigative Dermatology*, 98: 279-289.

Meyer, W., 1986. *Die Haut des Schweines*. Hannover: Schlütersche Verlagsanstalt und Druckerei.

Meyer, W., 1996. Bemerkungen zur Eignung der Schweinehaut als biologisches Modell für die Haut des Menschen. *Hautarzt*, 47: 178-182.

Meyer, W., 2009. Hair follicles in domesticated mammals with comparison to laboratory animals and humans. In: Mecklenburg, L., Linek, M., Tobin, D. J., eds. *Hair Loss Disorders in Domestic Animals*. Ames: Wiley-Blackwell.

Meyer, W., Hülmann, G., Seger, H., 2002a. *REM-Atlas on the hair cuticle structure of central european mammals*. Alfeld - Hannover: Verlag M. & H. Schaper.

Meyer, W., Schnapper, A., Hülmann, G., 2002b. The hair cuticle of mammals and its relationship to functions of the hair coat. *Journal of Zoology*, 256: 489-494.

References

Meyer, W., Kaczab, J., Zschemisch, N.-H., Godynicki, S., Seeger, J., 2007. Observations on the actual structural conditions in the stratum superficiale dermidis of porcine ear skin, with special reference to its use as model for human skin. *Annals of Anatomy*, 189 (2): 143-156.

Michel, M., L'Heureux, N., Pouliot, R., Xu, W., Auger, F. A., Germain, L., 1999. Characterization of a new tissue engineered human skin equivalent with hair. *In Vitro Cellular & Developmental Biology - Animal*, 35 (6): 318-326.

Millar, S. E., 2002. Molecular mechanisms regulating hair follicle development. *Journal of Investigative Dermatology*, 118: 216-225.

Miller, J. A., Oehler, D. D., Pound, J., 1998. Delivery of ivermectin by injectable microspheres. *Journal of Economic Entomology*, 91: 655-659.

Mills, P. C., Cross, S. E., 2006. Transdermal drug delivery: Basic principles for the veterinarian. *The Veterinary Journal*, 172: 218-233.

Mills, O. H., Kligman, A. M., 1983. The follicular biopsy. *Dermatologica*, 167: 57-63.

Milner, Y., Sudnik, J., Filippi, M., Kizoulis, M., Kashgarian, M., Stenn, K., 2002. Exogen, shedding phase of the hair growth cycle: Characterization of a mouse model. *Journal of Investigative Dermatology*, 119: 639-644.

Moghimi, S. M., Hunter, A. C., Murray, J. C., 2001. Long-circulating and target specific nanoparticles: Theory to practice. *Pharmacological Reviews*, 53: 283-318.

van der Molen, R. G., Spies, F., van 't Noordende, J. M., Boelsma, E., Mommaas, A. M., Koerten, H. K., 1997. Tape stripping of human stratum corneum yields cell layers that originate from various depths because of furrows in the skin. *Archives of Dermatological Research*, 289 (9): 514-518.

Montagna, W., 1954. Penetration and local effect of vitamin A on the skin of the guinea pig. *Proceedings of the Society for Experimental Biology and Medicine*, 86 (4): 668-672.

Moresi, J. M., Horn, T. D., 1997. Distribution of Langerhans cells in human hair follicle. *Journal of Cutaneous Pathology*, 24: 636-640.

Morgan, A. J., Lewis, G., van den Hoven, W. E., Akkerboom, P. J., 1993. The effect of zinc in the form of erythromycin-zinc complex (Zineryt® lotion) and zinc acetate on metallothionein

expression and distribution in hamster skin. *British Journal of Dermatology*, 129 (5): 563-570.

Morris, R. J., Potten, C. S., 1999. Highly persistent label-retaining cells in the hair follicles of mice and their fate following introduction of anagen. *Journal of Investigative Dermatology*, 112: 470-475.

Morris, R. J., Liu, Y., Marles, L., Yang, Z., Trempus, C., Li, S., Lin, J. S., Sawicki, J. A., Cotsarelis, G., 2004. Capturing and profiling adult hair follicle stem cells. *Nature Biotechnology*, 22: 411-417.

Morris, R. J., Fischer, S. M., Slaga, T. J., 1986. Evidence that a slowly cycling subpopulation of adult murine epidermal cells retains carcinogen. *Cancer Research*, 46: 3061-3066.

Müller, R. H., Dingler, A., 1998. Feste Lipid-Nanopartikel (Lipopearls™) als neuartiger Carrier für kosmetische und dermatologische Wirkstoffe. *PZ Wissenschaft*, 49: 11-15.

Münster, U., Nakamura, C., Haberland, A., Jores, K., Mehnert, W., Rummel, S., Schaller, M., Korting, H. C., Zouboulis, Ch. C., Blume-Peytavi, U., Schäfer-Korting, M., 2005. RU 58841-myristate-prodrug development for topical treatment of acne and androgenetic alopecia. *Pharmazie*, 60 (1): 8-12.

Na, R., Stender, I.-M., Ma, L., Wulf, H. C., 2000. Autofluorescence spectrum of skin: Component bands and body site variations. *Skin Research and Technology*, 6: 112-117.

NANODERM, 2007. *Quality of skin as a barrier to ultra-fine particles. Final Report* [Online]. Available at http://www.uni-leipzig.de/~nanoderm/Downloads/Nanoderm_Final_Report.pdf [Accessed on November 11, 2009].

Narisawa, Y., Hashimoto, K., Kohda, H., 1993. Epithelial skirt and bulge of human facial vellus hair follicles and associated Merkel cell-nerve complex. *Archives for Dermatological Research*, 285: 269-277.

Nicolaides, N., Hwei, C. F., Rice, G. R., 1968. The skin surface lipids of man compared with those of eighteen species of animals. *Journal of Investigative Dermatology*, 51: 83-89.

Nickel, R., Schummer, A., Seiferele, E., 1996. *Lehrbuch der Anatomie der Haustiere. III. Kreislauf, Haut und Hautorgane*. Berlin: Verlag Parey.

References

Nieminen, E., Leikola, E., Koljonen, M., Kiistala, U., Mustakallio, K. K., 1967. Quantitative analysis of epidermal lipids by thin layer chromatography with special reference to seasonal and age variation. *Acta Dermato-venereologica* 47: 327-338.

Nishimura, E. K., Granter, S. R., Fischer, D. E., 2005. Mechanisms of hair greying: Incomplete melanocyte stem cell maintenance in the niche. *Science*, 307: 720-724.

Noga, E. J., Udomkusonsri, P., 2002. Fluorescein: A rapid, sensitive, nonlethal method for detecting skin ulceration in fish. *Veterinary Pathology*, 39: 726-731.

Nohynek, G. J., Dufour, E. K., Roberts, M. S., 2008. Nanotechnology, cosmetics and skin: Is there a health risk? *Skin Pharmacology and Physiology*, 21: 136-149.

Oberdörster, G., Oberdörster, E., Oberdörster, J., 2005. Nanotoxicology: An emerging discipline evolving from studies of ultrafine particles. *Environmental Health Perspectives*, 113 (7): 823-839.

Odland, G., 1991. Structure of the skin. In: Goldsmith, L.A., ed. *Physiology, biochemistry, and molecular biology of the skin*. Oxford: Oxford University Press.

Ogiso, T., Shiraki, T., Okajima, K., Tanino, T., Iwaki, M., Wada, T., 2002. Transfollicular drug delivery: Penetration of drugs through human scalp skin and comparison of penetration between scalp and abdominal skins in vitro. *Journal of Drug Targeting*, 10: 369-378.

Ohyama, M., 2007. Hair follicle bulge. A fascinating reservoir of epithelial stem cells. *Journal of Dermatological Science*, 46: 81-89.

Ohyama, M., Terunuma, A., Tock, C. L., Radonovich, M. F., Pise-Masison, C. A., Hopping, S. B., Brady, J. N., Udey, M. C., Vogel, J. C., 2006. Characterization and isolation of stem cell-enriched human hair follicle bulge cells. *Journal of Clinical Investigation*, 116: 249-260.

Ohyama, M., Vogel, J. C., 2003. Gene delivery to the hair follicle. *Journal of Investigative Dermatology. Symposium Proceedings*, 8: 204-206.

Oshima, H., Rochat, A., Kedzia, C., Kobayashi, K., Barrandon, Y., 2001. Morphogenesis and renewal of hair follicles from adult multipotent stem cells. *Cell*, 104: 233-245.

References

Ossadnik, M., Czaika, V., Teichmann, A., Sterry, W., Tietz, H.-J., Lademann, J., Koch, S., 2007. Differential stripping: Introduction of a method to show the penetration of topically applied antifungal substances into the hair follicles. *Mycoses*, 50 (6): 457-462.

Ossadnik, M., Richter, H., Teichmann, A., Kock, S., Schäfer, U., Wepf, R., Sterry, W., Lademann, J., 2006. Investigation of differences in follicular penetration of particle- and nanoparticle-containing emulsions by laser scanning microscopy. *Laser Physics*, 16 (5): 747-750.

Otberg, N., Patzelt, A., Rasulev, U., Hagemeister, T., Linscheid, M., Sinkgraven, R., Sterry, W., Lademann, J., 2008. The role of hair follicles in the percutaneous absorption of caffeine. *British Journal of Clinical Pharmacology*, 65 (4): 488-492.

Otberg, N., Richter, H., Knuttel, A., Schäfer, H., Sterry, W., Lademann, J., 2004. Laser spectroscopic methods for the characterization of open and closed follicles. *Laser Physics Letters*, 1 (1): 46-49.

Otberg, N., Teichmann, A., Rasuljev, U., Sinkgraven, R., Sterry, W., Lademann, J., 2007. Follicular penetration of topically applied caffeine via a shampoo formulation. *Skin Pharmacology and Skin Physiology*, 20 (4): 195-198.

Oxlund, H., Manschot, J., Viidik, A., 1988. The role of elastin in the mechanical properties of skin. *Journal of Biomechanics*, 21 (3): 213-218.

Pagnoni, A., Kligman, A. M., El Gammal, S., Stoudemayer, T., 1994. Determination of density of follicles on various regions of the face by cyanoacrylate biopsy: Correlation with sebum output. *British Journal of Dermatology*, 131: 862-865.

Pan, Y., Li, Y., Zhao, H., Zheng, J., Xu, H., Wie, G., Hao, J., Cui, F., 2002. Bioadhesive polysaccharide in protein delivery system: Chitosan nanoparticles improve the intestinal absorption of insulin in vivo. *International Journal of Pharmaceuticals*, 249: 139-147.

Panyam, J., Dali, M. M., Sahoo, S. K., Ma, W., Chakravarthi, S. S., Amidon, G. L., Levy, R. J., 2003. Polymer degradation and in vitro release of a model protein from poly(D,L-lactide-co-glycolide) nano- and microparticles. *Journal of Controlled Release*, 92: 173-187.

Panyam, J., Labhasetwar, V., 2003. Biodegradable nanoparticles for drug and gene delivery to cells and tissue. *Advanced Drug Delivery Reviews*, 55: 329-347.

References

Patzelt, A., Richter, H., Büttemeyer, R., Hubera, H. J. R., Blume-Peytavi, U., Sterry, W., Lademann, J., 2008. Differential stripping demonstrates a significant reduction of the hair follicle reservoir in vitro compared to in vivo. *European Journal of Pharmaceutics and Biopharmaceutics*, 70 (1): 234-238.

Paus, R., Cotsarelis, G., 1999. The biology of hair follicles. *New England Journal of Medicine*, 341 (7): 491-497.

Pawley, J. B., ed., 2006. *Handbook of Biological Confocal Microscopy*, 3rd edition., Berlin: Springer Verlag.

PerkinElmer Life and Analytical Sciences, 2006. *An introduction to fluorescence spectroscopy*.[Online]. Available at www.perkinelmer.com [Accessed August 10, 2009].

Piérard, G. E., Piérard-Franchimont, C., Lê, T., Lapière, C., 1987. Patterns of follicular sebum excretion rate during lifetime. *Archives of Dermatological Research*, 279 (Suppl. 1): S104-107.

Pinkus, H., 1951. Examination of the epidermis by the strip method of removing horny layers. I. Observations on thickness of the horny layer, and on mitotic activity after stripping. *Journal of Investigative Dermatology*, 16 (6): 383-386.

Plewig, G., Scheuber, E., Reuter, B., Waidelich, W., 1983. Thickness of corneocytes. In: Marks, R., Plewig, G., eds. *Stratum corneum*. New York: Springer Verlag.

Pochi, P. E., Downing, D. T., Strauss, J. S., 1970. Sebaceous gland response in man to prolonged total caloric deprivation. *Journal of Investigative Dermatology*, 55: 303-309.

Potts, R. O., Francoeur, M. L., 1991. The influence of stratum corneum morphology on water permeability. *Journal of Investigative Dermatology*, 96: 495-499.

Prausnitz, M. R., Mitragotri, S., Langer, R., 2004. Current status and future potential of transdermal delivery. *Nature Reviews. Drug Discovery*, 3: 115-124.

Ramge, P., Unger, R. E., Oltrogge, J. B., Zenker, D., Begley, D., Kreuter, J., Von Briesen, H., 2000. Polysorbate-80 coating enhances uptake of polybutylcyanoacrylate (PBCA)-nanoparticles by human and bovine primary brain capillary endothelial cells. *European Journal of Neuroscience*, 12: 1931-1940.

References

Rathbone, M. J., Martinez, M. N., 2002. Modified release drug delivery in veterinary medicine. *Drug Discovery Today*, 7 (15): 823-829.

Raufast, V., Mavon, A., 2006. Transfollicular delivery of linoleic acid in human scalp skin: Permeation study and microautoradiographic analysis. *International Journal of Cosmetic Sciences*, 28 (2): 117-123.

Reichert, U., Michels, S. Schmidt, R., 1993. The cornified envelope: A key structure to terminally differentiating keratinocytes. In: Darmon, M., Blumenberg, M., eds. *The keratinocytes*. San Diego: Academic Press.

Rivière, J. E., Papich, M.G., 2001. Potential and problems of developing transdermal patches for veterinary applications. *Advanced Drug Delivery Reviews*, 50: 175-203.

Robbins, C. R., 2002. *Chemical and physical behavior of human hair*. New York: Springer Verlag.

Rock, D., Heaney, K., Peterson, D., Barton, W., Levy, S., Smith, L., Terhune, T., 2000. Field evaluation of a moxidectin sustained release injectable for the prevention of heartworm disease in dogs. *Proceedings of the American Association for Veterinary Parasitology*, 56.

Rogers, G. E., 2004. Hair follicle differentiation and regulation. *International Journal of Developmental Biology*, 48: 163-170.

Rolland, A., Wagner, N., Chatelus, A., Shroot, B., Schäfer, H., 1993. Site-specific drug delivery to pilosebaceous structures using polymeric microspheres. *Pharmaceutical Research*, 10 (12): 1738-1744.

Roze, E., Oubary, P., Chedru, F., 2000. Status-like recurrent pilomotor seizures: Case report and review of the literature. *Journal of Neurology, Neurosurgery, and Psychiatry*, 68: 647-649.

Rutherford, T., Black, J. G., 1969. The use of autoradiography to study the localization of germicides. *British Journal of Dermatology*, 81: 75-87.

Ryan, T. J., 1983. Cutaneous circulation. In: Goldsmith, L. A., ed. *Biochemistry and physiology of the skin*. London: Oxford University Press.

References

Salata, O., 2004. Applications of nanoparticles in biology and medicine. *Journal of Nanobiotechnology*, 2: 3-9.

Sato, H., Matsuda, H., Kubota, S., Kawano, K., 2006. Statistical comparison of dog and cat guard hairs using numerical morphology. *Forensic Science International*, 158: 94-103.

Schäfer, H., Lademann, J., 2001. The role of follicular penetration. *Skin Pharmacology and Applied Skin Physiology*, 14 (Suppl. 1): 23-27.

Schäfer, H., Redelmeier, T. E., 1996. *Principles of percutaneous absorption*. Freiburg: S. Karger Verlag.

Schätzlein, A., Cevc, G., 1998. Non-uniform cellular packing of the stratum corneum and permeability barrier function of intact skin: A high resolution confocal laser scanning microscopy study using highly deformable vesicles (Transfersomes). *British Journal of Dermatology*, 138 (4): 583-592.

Scheuplein, R. J., 1967. Mechanism of percutaneous absorption. *Journal of Investigative Dermatology*, 48 (1): 79-88.

Scheuplein, R. J., Blank, I. H., Brauner, G. J., MacFarlane, D. J., 1969. Percutaneous absorption of steroids. *Journal of Investigative Dermatology*, 52 (1): 63-70.

Scheuplein, R. J., Blank, I. H., 1971. Permeability of the skin. *Physiological Reviews*, 51: 702-747.

Schmook, F. P., Meingassner, J. G., Billich, A., 2001. Comparison of human skin or epidermis models with human and animal skin in vitro. *International Journal of Pharmaceutics*, 215 (1-2): 51-56.

Schütt, D. H., Kaiser, E., Stamm, I., Kubis, A., Müller, R. H., 1998. New generation of cosmetic products based on solid lipid nanoparticles (Lipoperls™). *Proceedings of the 2nd World Meeting APGI/APV*, 585-586.

Schurer, N. Y., Elias, P. M., 1991. The biochemistry and function of stratum corneum: Lipids. *Advances in Lipid Research*, 24: 27-55.

Seago, S. V., Ebling, F. J., 1985. The hair cycle on the human thigh and upper arm. *British Journal of Dermatology*, 135 (1): 9-16.

References

Shelley, W. B., Melton, F. M., 1949. Factors accelerating the penetration of histamine through normal intact human skin. *Journal of Investigative Dermatology*, 13: 61-71.

Shim, J., Kang, H. S., Park, W.-S., Han, S.-H., Kim, J., Chang, I.-S., 2004. Transdermal delivery of minoxidil with block copolymer nanoparticles. *Journal of Controlled Release*, 97 (3): 477-484.

Shimizu, H., 2007. *Shimizu's textbook of dermatology*. Sapporo, Japan: Hokkaido University Press/Nakayama Shoten.

Singh, P., Sihorkar, V., Jaitely, V., Kanaujia, P., Vyas, S. P., 2000. Pilosebaceous unit: Anatomical considerations and drug delivery opportunities. *Indian Journal of Pharmacology*, 32: 269-281.

Smith, K. R., 1977. The Haarscheibe. *Journal of Investigative Dermatology*, 69: 68-74.

Song, C., Labhasetwar, V., Cui, X., Underwood, T., Levy, R. J., 1998. Arterial uptake of biodegradable nanoparticles for intravascular local drug delivery: Results with an acute dog model. *Journal of Controlled Release*, 54: 201-211.

Sperling, L. C., 1991. Hair anatomy for the clinician. *Journal of the American Academy of Dermatology*, 25 (1, Pt 1): 1-17.

Spring, K. R., Davidson, M. W., 2009. *Introduction to Fluorescence Microscopy* [Online]. Available at www.microscopyu.com/articles/fluorescence/fluorescenceintro.html [Accessed October 27, 2009].

Stahl, J., 2007. *Einfluss des Lipidmusters und der Morphologie der Epidermis auf transdermale Permeationsraten im In-vitro-Versuch*. Ph. D.: Tierärztliche Hochschule Hannover.

Steinert, P. M., 1993. Structure, function and dynamics of keratin intermediate filaments. *Journal of Investigative Dermatology*, 100: 729-733.

Stenn, K. S., Cotsarelis, G., 2005. Bioengineering the hair follicle: Fringe benefits of stem cell technology. *Current Opinion in Biotechnology*, 16: 493-497.

Stevens, A., Lowe, J., 1992. *Histologie*. Weinheim: VCH Verlagsgesellschaft.

References

Steward, M. E., Downing, D. T., 1999. A new 6-hydroxy-4-sphingenine-cotaining ceramide in human skin. *Journal of Lipid Research*, 40: 1434-1439.

Stingl, G., Hauser, C., Wolff, K., 1993. The epidermis: An immunological environment. In: Fitzpatrick, T. B., Eisen, A. Z., Wolff, K., Freedberg, I. M., Austen, K. F., eds. *Dermatology in general medicine*. New York: McGraw Hill.

Straile, W. E., 1960. Sensory hair follicles in mammalian skin: The tylotrich follicle. *American Journal of Anatomy*, 106: 133-147.

Stüttgen, G., Forssmann, W. G., 1981. Pharmacology of the microvasculature of the skin. In: Stüttgen, G., Spier, H. W., Schwarz, E., eds. *Normal and pathologic physiology of the skin*. *III*. Berlin: Springer Verlag.

Sugiyama-Nakagiri, Y., Akiyama, M., Shimizu, H., 2006. Hair follicle stem cell-targeted gene transfer and reconstitution system. *Gene Therapy*, 13: 732-737.

Taylor, G., Lehrer, M. S., Jensen, P. J., Sun, T. T., Lavker, R. M., 2000. Involvement of follicular stem cells in forming not only the follicle but also the epidermis. *Cell*, 102: 451-461.

Teerink, B. J., 1991. *Hair of west european mammals*. *Atlas and identification key*. Cambridge: Cambridge University Press.

Teichmann, A., Jacobi, U., Ossadnik, M., Richter, H., Koch, S., Sterry, W., Lademann, J., 2005. Differential stripping: Determination of the amount of topically applied substances penetrated into the hair follicles. *Journal of Investigative Dermatology*, 125: 264-269.

Teichmann, A., Ossadnik. M., Richter, H., Sterry, W., Lademann, J., 2006. Semiquantitative determination of the penetration of a fluorescent hydrogel formulation into the hair follicle with and without follicular closure by microparticles by means of differential stripping. *Skin Pharmacology and Physiology*, 19: 101-105.

Tenjarla, S. N., Kasina, R., Puranajoti, P., Omar, M. S., Harris, W. T., 1999. Synthesis and evaluation of N-acetylprolinate esters - novel skin penetration enhancers. *International Journal of Pharmaceutics*, 192: 147-158.

References

Thiboutot, D., 2004. Regulation of human sebaceous glands. *Journal of Investigative Dermatology*, 123: 1-12.

Thielitz, A., Helmdach, M., Röpke, E.-M., Gollnick, H., 2001. Lipid analysis of follicular casts from cyanoacrylate strips as a new method for studying therapeutic effects of anti-acne agents. *British Journal of Dermatology*, 145 (1): 19-27.

Tinkle, S. S., Antonini, J. M., Rich, B. A., Roberts, J. R., Salmen, R. ,DePree, K., Adkins, E. J., 2003. Skin as a route of exposure and sensitization in chronic beryllium disease. *Environmental Health Perspectives*, 111: 1202–1208.

Toma, J. G., Akhavan, M., Fernandes, K. J. L., Barnabé-Heider, F., Sadikot, A., Kaplan, D. R., Miller, F. D., 2001. Isolation of multipotent adult stem cells from the dermis of mammalian skin. *Nature Cell Biology*, 3: 778-784.

Tregear, R. T., 1966. *Physical function of the skin*. London: Academic Press.

Tschan, T., Steffen, H., Supersaxo, A., 1997. Sebaceous gland deposition of isotretinoin after topical application: An in vitro study using human facial skin. *Skin Pharmacology and Physiology*, 10 (3): 126-134.

Turner, N. G., Guy, R. H., 1998. Visualisation and quantitation of iontophoretic pathways using confocal microscopy. *Journal of Investigative Dermatology. Symposium Proceedings*, 3 (2): 136-142.

Vinagradov, S. V., Bronich, T. K., Kabanov, A. V., 2002. Nanosized cationic hydrogels for drug delivery: Preparation, properties and interactions with cells. *Advanced Drug Delivery Reviews*. 54: 223-233.

Vogt, A., Blume-Peytavi, U., 2003. Die Biologie des menschlichen Haarfollikels. Neue Erkenntnisse und ihre klinische Bedeutung. *Hautarzt*, 54: 692-698.

Vogt, A., Mandt, N., Lademann, J., Schäfer, H., Blume-Peytavi, U., 2005. Follicular targeting - a promising tool in selective dermatotherapy. *Journal of Investigative Dermatology. Symposium Proceedings*, 10: 252-255.

Vogt, A., McElwee, K., Blume-Peytavi, U., 2008. Biology of the hair follicle. In: Blume-Peytavi, U., Tosti, A., Whiting, D. A., Trüb, R. M., eds. *Hair growth and disorders*. Berlin: Springer-Verlag.

References

Volodkin, D. V., Sukhorukov, G. B., Larionova, N. I., 2004. Protein encapsulation via porous CaCO3 microparticles templating. *Biomacromolecules*, 5:1962-1972.

Wahlberg, J. E., 1968. Transepidermal or transfollicular absorption? *Acta Dermato-venereologica*, 48: 336-344.

Walters, K. A., Roberts, M. S., 1993. Veterinary applications of skin penetration enhancers. In: Walters, K. A., Hadgraft, J., eds. *Pharmaceutical skin penetration enhancement*. New York: Marcel Dekker.

Wartlick, H., Michaelis, K., Balthasar, S., Kreuter, J., Langer, K., Strebhardt, K., 2004. Highly specific HER2-mediated cellular uptake of antibody-modified nanoparticles in tumor cells. J*ournal of Drug Targeting*, 12: 461-471.

Weigmann, H.-J., Lademann, J., Meffert, H., Schäfer, H., Sterry, W., 1999a. Determination of the horny layer profile by tape stripping in combination with optical spectroscopy in the visible range as a prerequisite to quantify percutaneous absorption. *Skin Pharmacology and Skin Physiology*, 12 (1-2): 34-45.

Weigmann, H.-J., Lademann, J., Pelchrzim, R. v., Sterry, W., Hagemeister, T., Molzahn, R., Schäfer, M., Lindscheid, M., Schäfer, H., Shah, V. P., 1999b. Bioavailability of clobetasol propionate - quantification of drug concentrations in the stratum corneum by dermato-pharmacokinetics using tape stripping. *Skin Pharmacology and Skin Physiology*, 12 (1-2): 46-53.

Weiss, B., 2007. *The potential of nanoscale carriers for drug delivery to intestinal mucosa and skin*. Ph.D.: Saarland University.

Weiss, B., Schäfer, U. F., Zapp, J., Lamprecht, A., Stallmach, A., Lehr, C. M., 2006. Nanoparticles made of fluorescence-labelled poly(L-lactide-co-glycolide): Preparation, stability, biocompatibility. *Journal of Nanoscience and Nanotechnology*, 6 (9-10): 3048-3056.

Wertz, P. W., Madison, K. C., Downing, D. T., 1989. Covalently bound lipids of human stratum corneum. *Journal of Investigative Dermatology*, 92: 109–111.

Wiechers, J. W., 1989. The barrier function of the skin in relation to percutaneous absorption of drugs. *Pharmacy World & Science*, 11 (6): 185-198.

References

Wosicka, H., Cal, K., 2010. Targeting to the hair follicles: Current status and potential. *Journal of Dermatological Science*, 57: 83-89.

Wu, X. S., 1995. Preparation, characterization, and drug delivery applications of microspheres based on biodegradable lactic/glycolic acid polymers. In: Wise, D. L., ed. *Encyclopedic handbook of biomaterials and bioengineering*. New York: Marcel Dekker.

Xu, P., Gullotti, E., Tong, L., Highley, C. B., Errabelli, D. R., Hasan, T., Cheng, J.-X., Kohane, D. S., Yeo, Y., 2009. Intracellular drug delivery by poly(lactic-*co*-glycolic acid) nanoparticles, revisited. *Molecular Pharmaceutics*, 6 (1): 190-201.

Yokoyama, M., 2005. Drug targeting with nano-sized carrier systems. *Journal of Artificial Organs*, 8: 77-84.

Zara, G. P., Bargoni, A., Cavalli, R., Fundaro, A., Vighetto, D., Gasco, M. R., 2002. Pharmacokinetics and tissue distribution of idarubicin-loaded solid lipid nanoparticles after duodenal administration to rats. *Journal of Pharmaceutical Sciences*, 91: 1324-1333.

Zirra, A.-M., 1976. The functional significance of the skin's stratum lucidum. *Revue Roumaine de Morphologie et d'Embryologie*, 26: 9-12.

10. Acknowledgements

First and foremost, my greatest appreciation goes to my doctoral advisor, Prof. Dr. Roland Rudolph, for kindly taking on the supervision of my thesis, and for his lectures on veterinary pathology, which were truly inspirational. Deep gratitude goes to Prof. Dr. Dr.-Ing. Jürgen Lademann, for his guidance, support and patience during the years of my research and the compilation of this manuscript. His faith in my work, enthusiasm and kindness were unfailing. Prof. Dr. Kerstin Müller is also most sincerely thanked for reviewing and evaluating this thesis.

Of my colleagues of the CCP, special thanks go to Heike Richter and Sabine Schanzer, whose assistance extended far beyond my experimental work, to Dr. Martina Meinke, who patiently provided insight into the statistical implications of my data, and to Bastiane Werner, for her smiling face and warm heart. I am grateful also for the academic support and input given by Dr. Gisela Thiede and Dr. Alexa Patzelt. Maxim Darvin and Stefan Haag, you made it fun.

Prof. Wolfram Sterry and the entire Clinic for Dermatology of the Charité Berlin, as well as the Department of Chemistry of the Humboldt University Berlin are sincerely thanked for providing the facilities and resources necessary for the completion of this work.

I thankfully acknowledge Dr. Martin Kock and his kind and cooperative staff of the Bayer Schering Pharma AG, as well as the Gut Hesterberg, for providing me with the skin samples. Prof. Claus-Michael Lehr, Dr. Ulrich Schäfer, and Peter Meiers of the Department of Biopharmaceutics and Pharmaceutical Technology, Saarland University are greatly thanked for providing me with the particulate formulations used in the first part of this work. I also thank Dr. Barbara Weiss for sharing her academic expertise.

Dr. Gisela Arndt of the Institute for Biometrics of the Free University Berlin and Henry Schäfer are appreciated for their help with the statistical analyses.

Tremendous gratitude goes to Andreas Trautwein, whose criticism, help (statistics!) and support have been of immeasurable value.

Sincerest thanks also go to my sisters Anna and Agnes, and my close friends, Alex Schaumann, Birgit Balke-Ihm and Taksi, Anne Bechtel, Tobias Albrecht and Nikki Suczek, whose personal cheering along the way has been greatly appreciated. To Max Wild, thank you for teaching me to take things more lightly, and for the many times you made me smile along the way.

Acknowledgements

Of course no acknowledgements would be complete without expressing my gratitude to my parents. They have taught me about hard work and persistence and how to be independent. Most of all, they have endured me when work was not forthcoming ("Are you done yet?"). Without their suggestions, inspirations, encouragement, money and love, the completion of this manuscript would not have been possible. I am grateful for them both and the "smart genes" they passed on to me.

To my stars, Max and Murmel, I miss you. Finally, warmest thanks go to my dog and most loyal supporter, Jorja.

Eidesstattliche Erklärung

Hiermit bestätige ich, daß ich die vorliegende Arbeit selbstständig angefertigt habe. Ich versichere, daß ich ausschließlich die angegebenen Quellen und Hilfen in Anspruch genommen habe.

Fanny Knorr
Berlin, den 15. Mai 2010